

SU(3) QUANTUM INTERFEROMETRY WITH BI-PHOTON INPUT PULSES

By
MUHAMMAD HABIB TAHIR




A dissertation submitted in partial fulfillment of the
DEGREE OF MASTER OF PHILOSOPHY
IN
PHYSICS

Supervised by
Dr. Aeysha Khalique

SCHOOL OF NATURAL SCIENCES
NATIONAL UNIVERSITY OF SCIENCES AND TECHNOLOGY
ISLAMABAD, PAKISTAN

National University of Sciences & Technology**MS THESIS WORK**

We hereby recommend that the dissertation prepared under our supervision by: MR. MUHAMMAD HABIB TAHIR, Regn No. 00000117043 Titled: SU(3) QUANTUM INTERFEROMETRY WITH BI-PHOTON INPUT PULSES be accepted in partial fulfillment of the requirements for the award of **MS** degree.

Examination Committee Members1. Name: DR. RIZWAN KHALIDSignature: 2. Name: DR. MUHAMMAD ALI PARACHASignature: External Examiner: DR. TASAWAR ABBASSignature: Supervisor's Name DR. AEYSHA KHALIQUESignature: 

 Head of Department

9-8-2019
 Date
COUNTERSIGNEDDate: 9/8/2019

 Dean/Principal

THESIS ACCEPTANCE CERTIFICATE

Certified that final copy of MS thesis written by Mr. Muhammad Habib Tahir (Registration No. 00000117043), of School of Natural Sciences has been vetted by undersigned, found complete in all respects as per NUST statutes/regulations, is free of plagiarism, errors, and mistakes and is accepted as partial fulfillment for award of MS/M.Phil degree. It is further certified that necessary amendments as pointed out by GEC members and external examiner of the scholar have also been incorporated in the said thesis.

Signature: Aeysha Khalique
Name of Supervisor: Dr. Aeysha Khalique
Date: 09-08-19

Signature (HoD): [Signature]
Date: 9-8-2019

Signature (Dean/Principal): [Signature]
Date: 9/8/2019

First of all, i would like dedicate my thesis to my religious mentor and teacher Late Mufti Muhammad Amin and i would also like to dedicate my thesis to my parents.

Acknowledgment

I am grateful to my supervisor, Dr. Aeysha Khalique, for her guidance throughout in my MS course work and during my research work under her supervision. Dr. Aeysha Khalique is not only my teacher and supervisor but I have always seen her as my educational mentor. Dr. Aeysha Khalique has been a great inspiration for me and Dr. Aeysha Khalique is the reason behind the development of my interest in the field of quantum optics and quantum information.

I would also like to thank, the members of guidance and examination committee (GEC), Dr. Rizwan Khalid and Dr. Ali Paracha, for the guidance throughout in my research work and I would also like to extend my gratitude to teachers of School of Natural Sciences (SNS), Who have taught me much about Physics and Mathematics.

I would like to thank my parents, who are my support system and they were always there, whenever I wanted any kind of help and support. Because of them, I have come this far in my life. I am also grateful to my siblings for their motivation and support.

I would also like to thank my class fellows, Umer, Sharoon, Waseem, Tahir, Jalal, Rizwan and Naveed for helping me in my course work and research work.

Muhammad Habib Tahir

Abstract

We have used the traditional $SU(3)$ group theoretical approach to study the quantum interferometry by using the bi-photon pulses. For this purpose, we have reviewed research articles focusing on the quantum interferometry of three photon by injecting single-photon in each of the input port of the six channel passive quantum optical interferometer (three input and three output channels) using $SU(3)$ group theoretical approach. The investigation of the symmetries in the different coincidence landscapes by using the $SU(3)$ plus the permutation group theory and the study of the relation between the immanants, Wigner D functions and distinguishability. Where these Wigner d functions also shows some properties like permutational symmetry partially. The observation of the permutational symmetries in the different kind of the output coincidence with multi-photon quantum interferometry (with the injection of combinations of bi-photon and single photon input pulses). These of all techniques are extensions of the general Hong-Ou-Mandel dip analysis of the two photon quantum interferometry to the multi-photon quantum interferometry.

We have used the same traditional $SU(3)$ group theoretical approach to study the quantum interferometry by the injecting bi-photon input pulses at input ports of the 6-channel passive quantum optical interferometer. We have also calculated the coincidence probabilities for all possible output coincidence patterns and then plotted these coincidence probabilities against the time-delay τ introduced between the arrivals of these photons at input ports to study different properties of the $SU(3)$ transission matrix and the scattering matrix. We have developed special condition to maximize the probability of getting desired output coincidence pattern to study different properties of the $SU(3)$ transition matrix and the scattering matrix. We have also observed the peaks and the dips for different coincidences with different occurrences of the photons at output ports.

Contents

1	Introduction	9
1.1	Quantum Interferometry	11
1.2	Hong-Ou-Mandel Effect	16
1.3	Group Theory	18
1.3.1	Special Unitary $SU(2)$ Group	20
1.3.2	Generator of $U(n)$ and $SU(n)$	22
1.3.3	Special Unitary $SU(3)$ Group	23
1.4	Outline of thesis	25
2	Quantum Interferometry with Single-Photon Input Pulses	27
2.1	$SU(2)$ Quantum Interferometry with Single-Photon Input Pulses . .	28
2.2	$SU(3)$ Quantum Interferometry with Single-Photon Input Pulses . .	30
3	Quantum Interferometry with Bi-Photon Input Pulses	34
3.1	Bi-Photon Input pulses at Input-1 and Input-2	35
3.1.1	Bi-Photon Clicks on Output-1 and Output-2	35
3.1.2	Bi-Photon Click on Output-1 and Single-Photon Click on Output-2 and Output-3	37
3.1.3	Tri-Photon Click on Output-1, Single-Photon Click on Output- 2 and no click on Output-3	40
3.1.4	Tetra-Photon Click on Output-1 and no Click on Output-2 and Output-3	42
3.2	Bi-Photon Input pulses at Input-1 and Input-3	43
3.2.1	Bi-Photon Click on Output-1 and Output-2 and no Click on Output-3	44
3.2.2	Bi-Photon Click on Output-1 and Single-Photon Click on Output-2 and Output-3	45
3.2.3	Tri-Photon Click on Output-1, Single-Photon Click on Output- 2 and no click on Output-3	48
3.2.4	Tetra-Photon Click on Output-1 and no Click on Output-2 and Output-3	50
3.3	Bi-Photon Input pulses at Input-2 and Input-3	52

3.3.1	Bi-Photon Click on Output-1 and Single-Photon Click on Output-2 and Output-3	54
3.3.2	Tri-Photon Click on Output-1, Single-Photon Click on Output-2 and no click on Output-3	57
3.3.3	Tetra-Photon Click on Output-1 and no Click on Output-2 and Output-3	59
3.4	Comparison between the Coincidence Probability Plots	61
3.5	Maximizing the Probabilities of the Outputs	63
3.6	Permanents and the Scattering Matrices	64
3.6.1	Permanents	64
3.6.2	Scattering Matrices	64
4	Conclusion	66
A	Appendix	68
Appendix		68
A	Rest of the Cases of Section 3.1	68
A.1	Bi-Photon Clicks on Output-1 and Output-3	68
A.2	Bi-Photon Clicks on Output-2 and Output-3	69
A.3	Bi-Photon Click on Output-2 and Single-Photon Click on Output-1 and Output-3	70
A.4	Bi-Photon Click on Output-3 and Single-Photon Click on Output-1 and Output-2	74
A.5	Tri-Photon Click on Output-1, Single-Photon Click on Output-3 and no click on Output-2	76
A.6	Tri-Photon Click on Output-2, Single-Photon Click on Output-1 and no click on Output-3	77
A.7	Tri-Photon Click on Output-2, Single-Photon Click on Output-3 and no click on Output-1	79
A.8	Tri-Photon Click on Output-3, Single-Photon Click on Output-1 and no click on Output-2	80
A.9	Tri-Photon Click on Output-3, Single-Photon Click on Output-2 and no click on Output-1	81
A.10	Tetra-Photon Click on Output-2 and no Click on Output-1 and Output-3	83
A.11	Tetra-Photon Click on Output-3 and no Click on Output-1 and Output-2	84
B	Rest of the Cases of Section 3.2	84
B.1	Bi-Photon Click on Output-1 and Output-3 and no Click on Output-2	84

B.2	Bi-Photon Click on Output-2 and Output-3 and no Click on Output-1	85
B.3	Bi-Photon Click on Output-2 and Single-Photon Click on Output-1 and Output-3	87
B.4	Bi-Photon Click on Output-3 and Single-Photon Click on Output-1 and Output-2	89
B.5	Tri-Photon Click on Output-1, Single-Photon Click on Output-3 and no click on Output-2	92
B.6	Tri-Photon Click on Output-2, Single-Photon Click on Output-1 and no click on Output-3	93
B.7	Tri-Photon Click on Output-2, Single-Photon Click on Output-3 and no click on Output-1	95
B.8	Tri-Photon Click on Output-3, Single-Photon Click on Output-1 and no click on Output-2	96
B.9	Tri-Photon Click on Output-3, Single-Photon Click on Output-2 and no click on Output-1	97
B.10	Tetra-Photon Click on Output-2 and no Click on Output-1 and Output-3	99
B.11	Tetra-Photon Click on Output-3 and no Click on Output-1 and Output-2	100
C	Rest of the Cases of Section 3.3	100
C.1	Bi-Photon Click on Output-1 and Output-3 and no Click on Output-2	101
C.2	Bi-Photon Click on Output-2 and Output-3 and no Click on Output-1	101
C.3	Bi-Photon Click on Output-2 and Single-Photon Click on Output-1 and Output-3	103
C.4	Bi-Photon Click on Output-3 and Single-Photon Click on Output-1 and Output-2	105
C.5	Tri-Photon Click on Output-1, Single-Photon Click on Output-3 and no click on Output-2	108
C.6	Tri-Photon Click on Output-2, Single-Photon Click on Output-1 and no click on Output-3	109
C.7	Tri-Photon Click on Output-2, Single-Photon Click on Output-3 and no click on Output-1	111
C.8	Tri-Photon Click on Output-3, Single-Photon Click on Output-1 and no click on Output-2	112
C.9	Tri-Photon Click on Output-3, Single-Photon Click on Output-2 and no click on Output-1	113

C.10	Tetra-Photon Click on Output-2 and no Click on Output-1 and Output-3	115
C.11	Tetra-Photon Click on Output-3 and no Click on Output-1 and Output-2	116

1

Introduction

Theory that laid the foundation of the quantum theory, was not the part of the main aspects or theories of the atomic physics. When any matter is being heated, it changes its color, first it turns red at comparatively low temperature and then turns white at comparatively high temperature. Material's surface was not really thing on which this change of the color depends and especially for the black bodies, the main reason behind is temperature. So the absorption and emission of the radiations at comparatively high temperature from black body became the hot topic for the researchers of that time. It should had been easy for the researcher to give an suitable explanation on the basis of the known laws of physics related to the heat and radiation. An attempt was made at the end of 19th century by Jeans and Rayleigh but they failed. They faced some serious difficulties. Those difficulties are not really relevant, so we move towards the actual explanation. It should be enough to say that the explanation in terms of the known laws of the physics, did not provide us with the required results.

In 1895, Plank was also researching in this field of the heat and radiation, so he tried to explain this phenomenon by shifting the focus from radiation prospective towards the radiating atom prospective. But this shift served him as he expected and failed to explain. He could not remove the difficulties present in previous explanation, but one thing productive happened was the simplification of the interpretation of the observed facts about the black body radiation. At the same time in beginning of the 19th century a very impressive work was done by Rubens and Curlbaum. They gave us almost perfect spectrum of the heat radiation. Plank started the development of the mathematical relation for this astonishing spectrum of the heat radiations as soon as he came to know about those spectrum. His result was quite similar with the results he got while developing his theory on the relation between radiations and heat. This relation afterward became the mild-stone of Plank's radiation law discovery.

Plank's suggested results for the spectrum was in complete agreement with

result that Rubens found recently, which they discussed with each other over a tea at Plank's house. This was the meeting that laid the foundation of the Plank's discovery of the radiation law. After the development of the Plank's formula, some very astonishing facts were come out. these results were going to astonish and stumble the world of known physics. It was very easy for the Plank to give his formula a suitable state-mental form on the basis of the theory he developed earlier. As he elaborated his formula for a radiating atom (Later known as the oscillator). He found something so unbelievable and astonishing that an oscillator (radiating atom) can only have discrete values of the energy (known as quanta). This was the fact that can not be comprehended by the known classical physics at that time. For a while Plank himself could not accept these results and refused to believe them to be true. It was the time when development in this field was happening intensively. In summer of same year 1900, he thought that there is no way of running away from these results and conclusions.

Plank thought that he had made the life-time discovery of so importance that his theory is somewhat of the same rank of the discoveries of the Newton. During a talk Plank's son reveled this and told that during a walk his father shared his new ideas about his discovery on the road of Grunewald. Grunewald is a German famous forest which is on the western-side of the Berlin. This shows that Plank was well aware of the consequences that his theory is going to touch the foundational description of the nature. And he also believed that due to his discovery the foundational description is going to discover new horizons of the knowledge that are unknown to human race. He made his publication in last month of the same year 1900 on his discovery, even though he was conservative in his nature and was well aware of the aftereffects of his discovery. When he received the criticism and contradiction, he ignored these things by saying that his interpretation is some thing that is mush ahead of his time.

Plank's interpretation of energy quantization, the emission and absorption of the energy from a material can only happen in discrete values of energy. This new theory can not be comprehended by all known laws physics at that time. When Plank himself tried to interpret his results in terms of the classical theory, he failed dramatically because he was missing all necessary points. It took almost five years to make any progress in this new direction. Plank's assumption influenced many new researchers to think out of the box. One of them was young dynamic genius Albert Einstein. He was the kind of researcher who was not afraid of rejecting old ways and accepting new ideas. When he read about Plank's interpretation, he had two problems in his mind in which he could use that. One problem he had in his mind was the emission of electrons from surface of metal when suitable light is thrown on it. It was the famous photoelectric effect. It had already be shown that this emission of electrons is independent of intensity of light and depends on

frequency of light by Lenard in experiments. It was almost impossible to explain this effect by using classical theory of radiations but can be explained by Plank's energy quantization theory. So this is what Einstein did, he said that light is a form of energy so light is also quantized and light is made-up small energy packets known as photons. And this photon can only have value given by the product of wavelength of the light and Plank's constant. The second thing Einstein had in his mind was the specific heat energy of solids, which is suitable to discuss here [1, 2].

Now we move forward towards interaction between this quantized light and matter which is known as quantum optics.

Along with development of the photon statistics theory, the researchers started their search for the coherence in the interaction between the light and the matter particles (Atoms and molecules) [3]. In the period of the Ramsey, Rabi and the other well known scientists were very active in this newly developed field of quantum optics, with their study spectroscopy (Radio-frequency) with atomic beam has already been begun. Brossel, series, Koestler, Dodd and well known scientists in the era of 1950s and 1960s developed the interaction of the light and atoms using the sensitive optical pumping probes [3].

Now we should move towards the main problem of this thesis, which is one of most important application of the quantum optics is quantum interferometry.

1.1 Quantum Interferometry

Passive optical interferometer is a device, which is comprised of elements like beam-splitter, phase-shifter and mirrors and is used for the scattering of light coherently. It works quantum mechanically and shows the quantum mechanical effects when we inject non-classical light at its input ports and observe the coincidence or count the number of photons on each of its output ports. From those outputs we can predict the results or do the post-selection for the rest of the output states. This post-selection of the output states is very important for the function of the quantum commutations and quantum-gates [4-6].

One of the most important application of the quantum passive optical interferometer is the Hong-Ou-Mandel-dip. The Hong-Ou-Mandel-dip is a phenomenon in which we shine two identical-photons at the two input ports of a 4-port (2-Inputs and 2-Output ports) passive quantum optical interferometer with adjustable time-delays between the arrival of the both of these photons. These two photons have two ways to leave the output ports either they can leave from the same output port or they can leave from the separate output ports. These two possibilities can be distinguished by the coincidence-dip measurement of these two photons. We can calculate the coincidence measurement by just taking the product of the number of the clicks, we are having on each the output-port. Such that if both

these photons leave the same output-port it yields the coincidence zero(0) because both photons are leaving from one output-port and nothing from the other output port so, according to defined rule for the coincidence measurement "2 * 0 = 0". On the other hand, if both these photons leave from the different output-ports yield the coincidence one(1) according to the same rule "1 * 1 = 1". Measurement of the coincidence of the two photon leaving the output-ports of a passive quantum optical interferometer covers most of the field of quantum interferometry. The word passive refers to that there are no active components like parametric or linear amplifiers involved in the operation of the quantum interferometry [4, 7, 8].

The Hong-Ou-Mandel dip actually deals with the decrease in the rate of the coincidence of the two photons at nearly zero time-delay between the arrival of the two identical single-photons at the ports of a 50/50 beam-splitter. The Hong-Ou-Mandel coincidence dip can be extended and generalized for the coincidence at more than two number of channels and we can extend it to the case where we inject single-photons and the vacuum states in different ports of the interferometer instead of entering the single-photons on each port of the passive quantum optical interferometer. One can also observe the Hong-Ou-Mandel coincidence dip for more than two number of photons at more than two number of the input ports. Suppose we have the 8-port quantum interferometer with 4-input ports and 4-output ports, with 'a', 'b', 'c' and 'd' be the 4-output ports and we shine 4 single-identical-photons on input ports and the detectors attached to each of the output ports click. Four photons B_a , B_b , B_c and B_d are detected at each of the output port for this the coincidence is defined as:

$$\prod_{i \in (a,b,c,d)} B_i$$

We can have the coincidence $\prod_{i \in (a,b,c,d)} B_i$, this shows that we shall get 1 only for the case where all the detectors click once and 0 for all rest of the cases, where more than one photon can be detected at any of the output ports and nothing on the other. Which means, we can only have the non-zero coincidence for the case where we get the click on each of the output detector. The total number of the photons detected at output detectors are $\sum_{i \in (a,b,c,d)} B_i \leq 4$, one can easily understand why this inequality sign is placed in the expression. In the process of the interferometry any of the photons can be lost in the system. Similarly, we can generalized the Hong-Ou-Mandel coincidence dip for the higher order cases, where multiple photons can be placed on multiple input ports [4].

The recent problem of boson-sampling (Boson-sampling is a simplified model for quantum computing that may hold the key to implementing the first ever post-classical quantum computer) is one of the important application of the quantum interferometry and Hong-Ou-Mandel effect. Boson-sampling is a non-universal quantum computer that is significantly more straightforward to build than any

universal quantum computer proposed so far [9]. The Hong-Ou-Mandel dip was the top priority of the researchers. This problem of the boson-sampling requires the case where we inject vacuum-states and single photon states at the different input-ports of the quantum interferometer. The computation of the such coincidence dip is very difficult to do classically but with the help of the optical quantum interferometer this can be done conveniently (with the some assumptions about the scalability and conjectures) [10]. The Boson-sampling problem made the theoretical and experimental verification of the Hong-Ou-Mandel dip, on the basis of which many successful experiment have been done [11–18].

In general the Hong-Ou-Mandel dip deals with the arrival of the single identical photons at the input ports simultaneously. When the arbitrary time-delays are introduced between the arrival of the single identical photons, the Hilbert-space become very large. Due to the introduction of the time delays between the arrival of the photons, the Hilbert-space deals with single-mode of each photon which gives us the continuum of infinite-many temporal-states for every input photon. In Hong-Ou-Mandel dip (generalized), there is another complication that is the number of the output ports (m) become much larger than the total number of the photons(n) arriving [4]. For this generalized case the dimension of the Hilbert-space can be written as $\dim\mathcal{H} = m^n$. When there are no time-delays between the arrival of the photons, there is no need to treat each of the photons separately every photon now can be treated in Hilbert-space within a single-mode framework and under any exchange, the collection of all photons remains symmetric. This forms a subspace within the complete Hilbert-space whose support (i.e. the largest subspace which gives non-zero value when the single photon subspace overlaps with the multi-photon subspace) is not zero. This is the only subspace within the Hilbert-space that remains completely symmetric when frequencies of the photons being permuted. This is also the largest subspace which gives non-zero value when the single photon subspace overlaps with the multi-photon subspace. Such Hilbert-space also has the much smaller dimensions,

$$\begin{bmatrix} m + n - 1 \\ n \end{bmatrix}.$$

From this one can observe that how different these types of the Hong-Ou-Mandel dips are, one with the adjustable delays between the arrival of the single identical photons and the other with the simultaneous arrival of the photons at the input ports. The adjustable time-delays(τ) between the arrival of the photons at the input-ports is very important for the verification of the dip that it is giving us the expected results and also for the calibration of the coincidence dips with the coincidence rates [4]. Recently this dip is also been observed for the bi-photons arrival at the input-ports of the beam-splitters. It has also been shown that at the input states the complete permutation symmetric can broken with non-simultaneity.

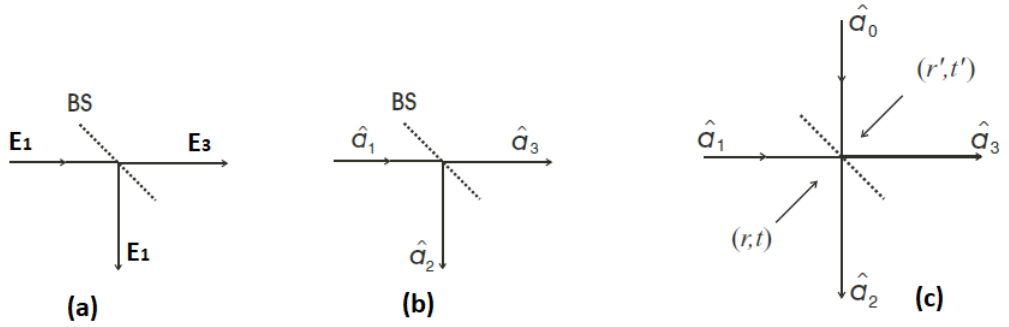


Figure 1.1:

It has also been observed that at output state the coincidence-rate depends on the immanants of the transition matrix, when there is no permutation symmetry present. We shall discuss that what these immanants are in this coming sections.

1.1.0.1 Beam Splitter

In this section, I shall discuss the quantum mechanical properties of the beam-splitter. If we use the classical approach of the beam-splitter for the level, where we are dealing with the single photon or a very few number of photons it will mislead us to the false results [3]. First of all, we shall try to explain how the classical approach mislead us to the false result. Consider a very simple example where a classical light is injected into the loss-less beam-splitter as shown in Fig.1.1(a) and the beam-splitter splits the beam into reflected beam and transmitted beam. Let's say E_1 , E_2 and E_3 be the complex amplitudes of the incident, reflected and transmitted beams respectively. The complex amplitudes of the reflected and transmitted beams can be written in terms of the complex amplitude of the incident beam as

$$E_2 = rE_1 \quad \text{and} \quad E_3 = tE_1. \quad (1.1)$$

where r and t be the coefficients of reflection and transmission respectively and for the balanced beam-splitter have the values $|r| = |t| = 1/\sqrt{2}$. The sum of the intensities of the reflected and the transmitted beams should be equal to the intensity of the incident beam, because we are using the lossless beam-splitter

$$|E_1|^2 = |E_2|^2 + |E_3|^2, \quad (1.2)$$

which can eventually be written as

$$1 = |r|^2 + |t|^2. \quad (1.3)$$

When we treat the beam quantum mechanically, the complex amplitudes should be replaced with the annihilation operators as shown in Fig.1.1(b). Let \hat{a}_1 be the annihilation operator of the incident beam, so \hat{a}_2 and \hat{a}_3 , are the annihilation operators for the reflected and the transmitted beam can be written as

$$\hat{a}_2 = r\hat{a}_1 \quad \text{and} \quad \hat{a}_3 = t\hat{a}_1. \quad (1.4)$$

These operators should satisfy the commutation relations

$$\begin{aligned} [\hat{a}_m, \hat{a}_n^\dagger] &= \delta_{mn}, \\ [\hat{a}_m, \hat{a}_n] &= 0 = [\hat{a}_m^\dagger, \hat{a}_n^\dagger], \end{aligned} \quad (1.5)$$

such that, ($m, n = 1, 2, 3$) The annihilation operators defined above do not satisfy the commutation relations:

$$[\hat{a}_2, \hat{a}_2^\dagger] = |r|^2[\hat{a}_1, \hat{a}_1^\dagger] = |r|^2, \quad [\hat{a}_3, \hat{a}_3^\dagger] = |t|^2[\hat{a}_1, \hat{a}_1^\dagger] = |t|^2, \quad \text{and} \quad [\hat{a}_2, \hat{a}_3^\dagger] = rt^* \neq 0. \quad (1.6)$$

So from this, one can easily see that the classical approach cannot give us the results for the quantum mechanical effects of the beam-splitter [3].

When we deal classically with beam-splitter and incident a photons state at one ports of the beam-splitter(say beam-splitter have two input ports) and nothing on the other port, then classically there will be no effect of the empty port on the output. But quantum mechanically this empty port is also containing a vacuum state. As we know the vacuum fluctuation gives birth to many quantum mechanical phenomena. The vacuum state effects are no exception for the beam-splitters. Now we inject another photon state at the empty port of the beam-splitter having, the annihilation operator \hat{a}_0 as shown in Fig.1.1(c). The transformation equations for the case can be written as

$$\hat{a}_2 = t'\hat{a}_0 + r\hat{a}_1 \quad \text{and} \quad \hat{a}_3 = r'\hat{a}_0 + t\hat{a}_1 \quad (1.7)$$

and in matrix form can be written as

$$\begin{pmatrix} \hat{a}_2 \\ \hat{a}_3 \end{pmatrix} = \begin{pmatrix} t' & r \\ r' & t \end{pmatrix} \begin{pmatrix} \hat{a}_0 \\ \hat{a}_1 \end{pmatrix}. \quad (1.8)$$

From this one can easily see under mentioned conditions these operators satisfy the commutation relations

$$|r| = |r'|, \quad |t'| = |t|, \quad |t|^2 + |r|^2 = 1, \quad t'r^* + t^*r' = 0, \quad \text{and} \quad t'^*r' + tr^* = 0. \quad (1.9)$$

These conditions are also known as the reciprocity relations [3].

We have used the passive quantum optical interferometer with 6-ports (3-input ports and 3-output ports) and injected two bi-photon input pulses on any of the two input ports. To distinguish the photons from each other, a frequency profile is given to them and introduced the time-delays between the arrivals of the photons. I shall discuss this how we achieved this purpose in the later sections. I have calculated the coincidence probabilities for different possible output for the given inputs and then plotted these coincidence probabilities against the time-delays introduced between the arrivals of the photons.

1.2 Hong-Ou-Mandel Effect

Hong -Ou-Mandel dip is a phenomenon, when two distinguishable photons enter the input ports of a four port 50 : 50 beam splitter (two input ports and two output ports), one photon in each input port. The photons can be detected at output ports in four ways such as shown in Fig.(1.2),

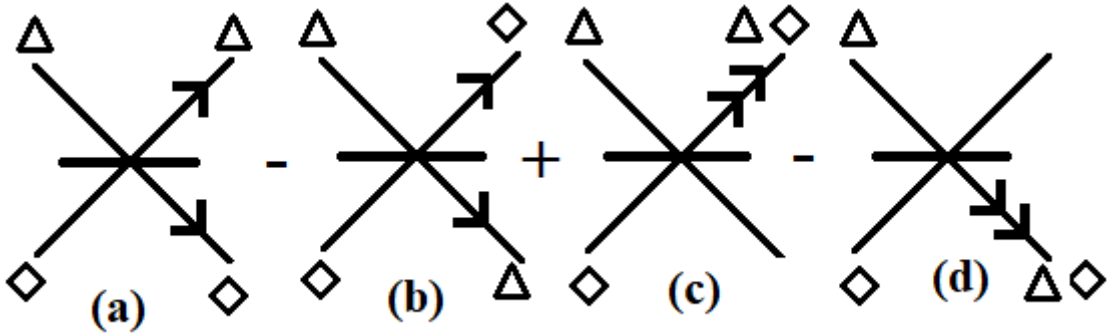


Figure 1.2: This diagram shows that if two distinguishable photons enter the input ports of a beam splitter, they can exit the output ports or detected at output ports in four different ways. (a) they can be detected on the same side as they entered, (b) they can be detected on the opposite sides as they entered, (c) both of them can be detected on one output port or (d) both of them can be detected on other output port.

This case represents the situation where photons are distinguishable as shown Fig.(1.2). So the final output will be superposition of the four types of the output patterns as mentioned above. As we know the photons are indistinguishable generally. Then for the case where the photons are indistinguishable, the first two output states will collapse and cancel each other because they have negative sign

between them as we can see in Fig.(1.2). So, we will be left with the patterns where both of the photons are detected at either of the output port Fig.(1.3).

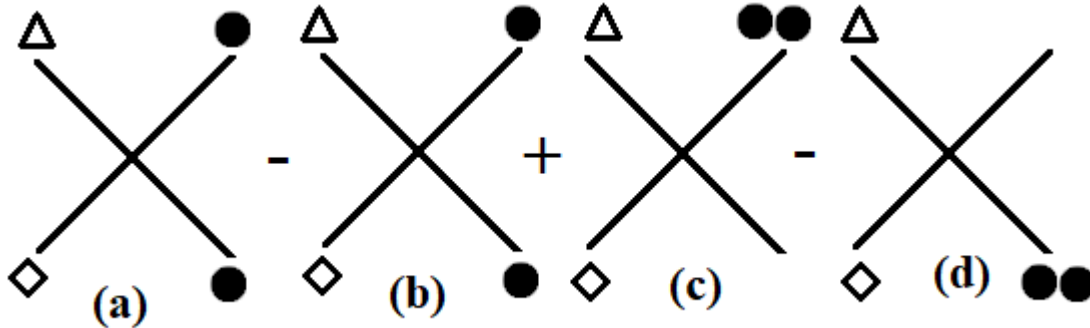


Figure 1.3: The diagram represents the situation where the photons are indistinguishable at output ports. As we can see in this diagram that first two patterns are the same under this situation. They will collapse and cancel each other out because they have a negative sign between them and we will be left with the last two patterns.

So when each photon leaves at different output ports, the states interfere destructively, that means each of the photon must be detected either on the one output port or the other. This effect is known as the Hong-Ou-Mandel effect. So when plot the coincidence probability of such case we get a dip for indistinguishable photons as shown in Fig.(2.2) [7].

We can analyze photon interferometry by using group theoretical approach. In the next section, I shall introduce this group theoretical approach.

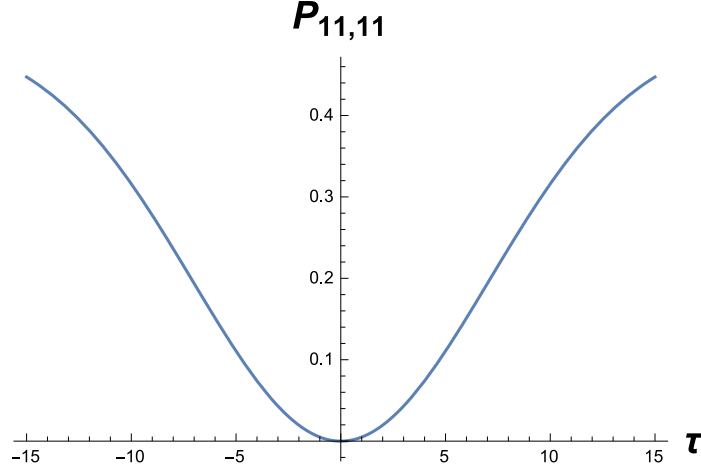


Figure 1.4: Coincidence probability plot against the time delay τ introduced between the arrival of the photons at input ports of the case where we have injected a single photon at each input port of the four passive quantum optical interferometer with two input ports and two output ports. Observed the coincidence probability of having single photon click at each of the output ports with time delay τ introduced between the arrival of these photons at input ports.

1.3 Group Theory

Here, I discuss the essentials of the group theory. Consider a group A , a set of the operations, a_i ,

$$A = (a_1, a_2, a_3, \dots, a_n).$$

Such that i varies from 1 to n . There are two type of groups, finite ones and infinite ones. For the finite groups, order of the group is the number of the elements n in the group. For better understanding, let us consider S_3 permutation group of three objects. Let these three objects be X , Y and Z . We can arrange these three objects in six ways. We can define different operations as the elements of the group by shuffling the arrangements of these three objects. Let us now write the elements of the S_3 permutation group A in the form of the operators from which one can easily understand how they will permute these three objects.

$$\begin{aligned} a_1 = I = [123], \quad a_2 = [231], \quad a_3 = [312], \\ a_4 = [132], \quad a_5 = [213] \quad \text{and} \quad a_6 = [321]. \end{aligned} \quad (1.10)$$

Now, we will explain how these elements(i.e. operations) will act on the arrangements of these three objects X , Y and Z .

$$a_1(XYZ) = [123](XYZ) = (XYZ), a_2(XYZ) = [231](XYZ) = (YZX),$$

$$\begin{aligned}
a_3(XYZ) &= [312](XYZ) = (ZXY), a_4(XYZ) = [132](XYZ) = (XZY), \\
a_5(XYZ) &= [213](XYZ) = (YXZ) \quad \text{and} \quad a_6(XYZ) = [321](XYZ) = ZYX,
\end{aligned}
\tag{1.11}$$

which shows, as a_1 is an identity element when there is no permutation of the objects, in a_2 operation second object changes its place with first object, third object with the second object and first with the third object, in a_3 operation third object changes its place with first object, first with second object and second with third object, in a_4 operation first remains at its place and other two objects interchange their places, in a_5 operation third object remains at its place and other two objects interchange their places and in a_6 operation second object remains at its position and other two objects interchange their places. This is how, these elements(operations) of the S_3 permutation group operate as defined in Eq.(1.11). Just the set of these operations does not constitute a group, but a group must satisfy a certain definition of the product, that is when more than one operation is applied on arrangements of the objects simultaneously. The resultant arrangement must be within the arrangements defined by any other element of this group A. Let us check this property of the group A by applying two operations simultaneously on the arrangement of the objects X, Y and Z i.e.

$$\begin{aligned}
a_2(a_3(XYZ)) &= [231]([312](XYZ)) = [231](ZXY) \\
&= (XYZ) = I(XYZ) = [123](XYZ) \\
&= a_1(XYZ).
\end{aligned}
\tag{1.12}$$

From this one can conclude that when we apply more than one operation simultaneously on an arrangement, we get an arrangement which is already defined by another operation within this group. So, one can write the product of the operations from the above Eq.(1.12) as,

$$a_2 o a_3(XYZ) = a_2 o a_3(XYZ) = a_1(XYZ), \tag{1.13}$$

$$a_2 o a_3 = a_1, \tag{1.14}$$

$$[231] o [312] = [123]. \tag{1.15}$$

We have used a symbol 'o' between the two elements in above Eq.(1.14) for the product, which just means that the product of the group elements must be defined in such a way that result of the such product must be an element of the group. In Table 1.1, we have defined all possible products of the group elements and this table is known as the multiplication table of the group A.

Table 1.1: Multiplication table of S_3 permutation group

o	[123]	[231]	[312]	[132]	[213]	[321]
[123]	[123]	[231]	[312]	[132]	[213]	[321]
[231]	[231]	[312]	[123]	[321]	[132]	[213]
[312]	[312]	[123]	[231]	[213]	[321]	[132]
[132]	[132]	[213]	[321]	[123]	[231]	[312]
[213]	[213]	[321]	[132]	[312]	[123]	[231]
[321]	[321]	[132]	[213]	[231]	[312]	[123]

A group under the defined product for its elements must satisfy the properties mentioned below:

1. Must satisfy the associative property under the defined product.

$$(a_i o a_j) o a_k = a_i o (a_j o a_k) \quad (1.16)$$

2. It must contain the identity element(operation) under the defined product.

$$a_1 = I = [123] \quad i.e. \quad a_1(XYZ) = [123](XYZ) = (XYZ) \quad (1.17)$$

3. There must exist the inverse elements for each of element of the group.

$$a o a^{-1} = a^{-1} o a = I, \quad (1.18)$$

such that $I = I^{-1}$,

$$a_2 o a_3 = a_3 o a_2 = I = [231][312] = [312][231] = [123]. \quad (1.19)$$

4. Closure property, that is if a_i and a_j are the elements of the set A, then $a_i o a_j$ must be the element of the set A.

One can find the inverse element for each element of the group A in the multiplication table(1.1). There are some elements present which are their own inverses and the commutation property do not hold for every group. Such group for whom the commutation property exists are known as the Abelian groups.

1.3.1 Special Unitary SU(2) Group

Let us consider, we have two vectors x and y in 2-dimensional vector space which is defined over the complex numbers field [19]. When we apply the rotational

transformation on these vectors x and y their linear transformation equations can be written as

$$\begin{aligned} x' &= ax + by, & v' &= cx + dy; \\ \text{or} \\ [x', y'] &= [x, y] \begin{pmatrix} a & c \\ b & d \end{pmatrix}, \end{aligned} \quad (1.20)$$

where a, b, c, d are the transformation coefficients (complex numbers) and hence there are 8-parameters involved in the transformation matrix. For the case, where we only consider such rotations which leaves $xx^* + yy^* = |x|^2 + |y|^2$ invariant, we can see that the above matrix defined in Eq.(1.20) is a unitary matrix. Specifically, if we want that $|x'|^2 + |y'|^2 = |x|^2 + |y|^2$, we can get the conditions from Eq.(1.20)

$$a^*a + c^*c = 1, \quad b^*b + d^*d = 1, \quad b^*a + d^*c = 0. \quad (1.21)$$

As these scalars are complex and Eq.(1.21) is the sum of the two conditions. The condition defined in Eq.(1.21) reduces the 8 parameters defined in Eq.(1.20) to four parameters. Now by using these all conditions defined in Eq.(1.21) we can defined a unitary matrix (most general) containing these real four parameters of order-2 and such matrix can written as

$$\begin{pmatrix} \cos(\theta)e^{i\alpha} & \sin(\theta)e^{i\gamma} \\ -\sin(\theta)e^{i(\beta-\gamma)} & \cos(\theta)e^{i(\beta-\alpha)} \end{pmatrix}, \quad (1.22)$$

with $e^{i\beta}$ the determinant of this matrix. Here α, β, γ and θ be the 4-real parameters.

All those conditions or transformation equation defined in Eq.(1.21) are from a $U(2)$ group which is similar to the group which is made up of all second order unitary matrices. Precisely saying, this group is a compact, four-parameter, continuous, Lie group.

$U(2)$ group has a subgroup which contains all second order matrices with determinant 1, is the group in which physics and specifically our work is interested. A general element for this group is written in form given below:

$$\begin{pmatrix} s & -t^* \\ t & s^* \end{pmatrix} \quad \text{with} \quad ss^* + tt^* = 1. \quad (1.23)$$

This group which contains only the second order matrices is known as the unitary uni-modular group or known as special unitary group and is symbolized by $SU(2)$.

1.3.2 Generator of $U(n)$ and $SU(n)$

A group which contains all unitary matrices of order- n is known as the unitary group and is denoted by $U(n)$. On the other hand, such group which contains all unitary matrices with determinant 1 is known as the special unitary group and is denoted by $SU(n)$. One can clearly see that $SU(n)$ is a subgroup of $U(n)$ group. As there are n^2 elements in a unitary matrix of order n , so it is a n^2 parameters, connected, compact, continuous, Lie group. There is one additional property to satisfy for the special unitary group($SU(n)$), that is it has the unitary matrices whose determinants are 1, so special unitary group is a $(n^2 - 1)$ parameter, continuous, compact, connected, Lie group. The generators of the $U(n)$ are comparatively easy to obtain. The term e^{iH} represent a unitary matrix, when H is a hermitian matrix. We can also see this in another way, if U is a unitary matrix we can represent this in the form

$$U = e^{iH}, \quad (1.24)$$

where H is a hermitian matrix. Linear combination of any number of hermitian matrices which contain the real coefficients is also a hermitian matrix. The number of the hermitian matrices(independent) of order n can never exceed the number n^2 . Let us say we have H_1, H_2, \dots, H_N hermitian matrices of order n , where we are assuming $N \equiv n^2$ for our convenience. Let us say, we have $n^2 a_j (1 \leq j \leq N)$ real independent parameters. Now any unitary matrix of order n can be written as

$$U = e^{i \sum_{j=1}^N a_j H_j}, \quad (1.25)$$

or we can say now any element of the unitary group can be written by using the expression given in Eq.(1.25), just by putting the suitable values of the n real independent parameter a_j . So, we can say these n hermitian matrices are the generators of the $U(n)$ unitary group and obviously they are not unique because for any n , the generator of $U(n)$ unitary group can be the linear combination of these hermitian matrices.

Consider a square matrix B , we can written an expression for this matrix i.e.

$$\det(e^B) = e^{\text{trace}B}. \quad (1.26)$$

By using the Eq.(1.24) we can see that

$$\det(U) = \det(e^{iH}) = e^{i \text{trace}H}. \quad (1.27)$$

As we known all of the diagonal element of these hermitain matrices are real, so we can write that $\text{trace}H \equiv \beta$ which is a real number.

Turning our attention towards the $SU(n)$, we take into account the very fact that elements of the this group have their determinants equal to 1. Therefore, if

an element of $SU(n)$ is represented by $U_0 = e^{iH_0}$, then the condition $\det(U_0) = 1$ demands the trace of H_0 to be equal to 0. We have seen before that the maximum number of the independent trace-less hermitian matrices of order- n is $n^2 - 1$. Also a convenient choice of these matrices can be made to be the generators of $SU(n)$ having $n^2 - 1$ real independent parameters. It is easy to choose $n^2 - 1$ generators initially and add to this set of the unit matrices of order- n afterwards in order to get n^2 generators of $U(n)$.

As an example, we know that the three generators of $SU(2)$ serve to be the Pauli spin matrices,

$$\sigma_x = \begin{pmatrix} 0 & 1 \\ 1 & 0 \end{pmatrix}, \quad \sigma_y = \begin{pmatrix} 0 & -i \\ i & 0 \end{pmatrix} \quad \text{and} \quad \begin{pmatrix} 1 & 0 \\ 0 & -1 \end{pmatrix}. \quad (1.28)$$

Which make a set of three independent trace-less hermitian matrices of order-2. For the generators of $U(2)$ one can choose the set $(E, \sigma_x, \sigma_y, \sigma_z)$ where E is the unit matrix of order-2.

1.3.3 Special Unitary $SU(3)$ Group

It is clear from the name that $SU(3)$ is the group of all unitary matrices of the order-3 having determinant equal to 1. The $SU(3)$ group has $n^2 - 1 = 3^2 - 1 = 8$ generators. These 8 generators can be represented as $\lambda_1, \lambda_2, \lambda_3, \dots, \lambda_8$. Although there are many ways one can choose, the generators of $SU(3)$ group and the following trace-less matrices are used as the generators of $SU(3)$ conventionally,

$$\begin{aligned} \lambda_1 &= \begin{pmatrix} 0 & 1 & 0 \\ 1 & 0 & 0 \\ 0 & 0 & 0 \end{pmatrix}, & \lambda_2 &= \begin{pmatrix} 0 & -i & 0 \\ i & 0 & 0 \\ 0 & 0 & 0 \end{pmatrix}, & \lambda_3 &= \begin{pmatrix} 1 & 0 & 0 \\ 0 & -1 & 0 \\ 0 & 0 & 0 \end{pmatrix}, \\ \lambda_4 &= \begin{pmatrix} 0 & 0 & 1 \\ 0 & 0 & 0 \\ 1 & 0 & 0 \end{pmatrix}, & \lambda_5 &= \begin{pmatrix} 0 & 0 & -i \\ 0 & 0 & 0 \\ i & 0 & 0 \end{pmatrix}, & \lambda_6 &= \begin{pmatrix} 0 & 0 & 0 \\ 0 & 0 & 1 \\ 0 & 1 & 0 \end{pmatrix}, \\ \lambda_7 &= \begin{pmatrix} 0 & 0 & 0 \\ 0 & 0 & -i \\ 0 & i & 0 \end{pmatrix}, & \lambda_8 &= \frac{1}{\sqrt{3}} \begin{pmatrix} 1 & 0 & 0 \\ 0 & 1 & 0 \\ 0 & 0 & -2 \end{pmatrix}. \end{aligned} \quad (1.29)$$

The commutators of these generators can be found out to be,

$$[\lambda_j, \lambda_k] = 2i \sum_l f_{jkl} \lambda_l, \quad (1.30)$$

where the only non-vanishing components of the f_{jkl} are

$$\begin{aligned} f_{123} &= 1, \\ f_{147} &= f_{516} = f_{246} = f_{257} = f_{345} = f_{537} = \frac{1}{2}, \\ f_{458} &= f_{678} = \frac{\sqrt{3}}{2}, \end{aligned} \tag{1.31}$$

and all the permutations with proper signs. One must have the realization that these structures constants happen to be a characteristic property of the $SU(3)$ and they do not depend on the particular representation chosen in Eq.(1.29). It can be seen from Eq.(1.29) that λ_3 and λ_8 are diagonal matrices and hence they commute with each other. It can be verified that no other matrix commute with both λ_3 and λ_8 . Therefore the rank of the $SU(3)$ is 2. Therefore, the group $SU(3)$ has two Casimir operators. One is the quadratic combination of generators.

$$C_l = \sum_{i=1}^8 \lambda_i^2. \tag{1.32}$$

Without difficulty it can be shown that C_2 commutes with all other generators i.e. $[C_2, \lambda_i] = 0$. The other Casimir operators come out as a complex tri-linear combination of the generators.

One can use two running indices to label the eigen values of the two Casimir operators of $SU(3)$. The irreducible representations can than be denoted by (p, q) , where p and q can have all non-negative integral values. The dimensions of this irreducible representation come out to be,

$$d = (1 + p)(1 + q)(2 + p + q)/2. \tag{1.33}$$

As a convention, an irreducible representation can be denoted merely by its dimension. This means that instead of (p, q) , an irreducible representation can be denoted by d and d^* depending upon $p < q$ or $p > q$. when $p = q$, there exist only one irreducible representation of the corresponding dimension denoted by d . Therefore $p = q = 0$ or $(0, 0) \equiv 1$ corresponds to the lowest order irreducible representation. Some other irreducible representation are $(0, 1) \equiv 3$, $(1, 0) \equiv 3^*$, $(0, 2) \equiv 6$, $(2, 0) \equiv 6^*$, $(1, 1) \equiv 8$, $(0, 3) \equiv 10$, etc.

The direction product of these irreducible representation can be taken and it can also be reduced in terms of the irreducible representations. we provide a few specific cases of the decomposition without going into details,

$$\begin{aligned} 3 \otimes 3 &= 6 \oplus 3^*, \\ 3 \otimes 3^* &= 8 \oplus 1, \\ 3 \otimes 3 \otimes 3 &= 10 \oplus 8 \oplus 8 \oplus 1. \end{aligned} \tag{1.34}$$

and many other.

Group theoretical concepts are useful in understanding scattering operation of S_n matrix and the distribution of photons at the input and output ports under permutation group S_n .

1.4 Outline of thesis

Now in the coming sections, we have discussed the quantum interferometry using the above-mentioned formalism and have discussed different cases with different input patterns and then we have observed coincidence counts for each type of the input pattern.

In chapter 2, We have reviewed $SU(2)$ and $S(3)$ quantum interferometry. In Sec.2.1 we have discussed the $SU(2)$ quantum interferometry using a four-port quantum interferometer (two input ports and two output ports) by shining single photon input pulse on each of the two input port and then observed the coincidence for the single click on each of the output port. Then we have plotted the coincidence probability against the time delays introduced between the arrivals of the photons at input ports and observed how the coincidence probability varies with the length of the time delays.

In the Sec.2.2, we have discussed the $SU(3)$ quantum interferometry using six port quantum interferometer (three input ports and three output ports) by shining single photon input pulse on each of the input port and then observed the coincidence probability for a single click on each of the output port. Then plotted this coincidence probability against the time delays introduced between the arrival of the photons at input ports and observed the variation in the output coincidence probability with the change in the length of the time delays.

In chapter 3, we have discussed the $SU(3)$ quantum interferometry using six port quantum interferometer (three input ports and three output ports) by shining bi-photon input pulse on any two input ports and then observed the coincidence probability for all possible output coincidence patterns. For example, we have injected a bi-photon input pulse in the input port-1 and one in input port-2 and then observed coincidence probability for all possible output coincidence patterns. In the Sec.3.5, we have generated a special condition for the which we got the maximum probability for single type output pattern by adjusting the values of octuples $\Omega(\alpha_1, \alpha_2, \alpha_3, \beta_1, \beta_2, \beta_3, \gamma_1, \gamma_2)$ of the transformation matrix in Eq.(2.13). We have observed that by using the created condition we get the maximum probability of getting a tetra-photon click at one of the output port.

In the Sec.3.4, we have discussed the comparison between the same kind of output patterns and their plots of coincidence probabilities against the time delays introduced between the arrival of the photons at input ports for a different type of

input pulses. Also, we have observed the variation and the similarities between these plots to predict a pattern.

In the Sec.3.6, we have discussed the permanents of the scattering matrix and the formation of the scattering matrix [20]. Where the permanent is a special case of the square matrix which is similar to the determinant of a matrix, both these determinants and permanents are the polynomials of the entries of the square matrix, but in permanents all signs in between the terms are positive [21]. Permanent is discussed thoroughly in the Sec.3.6. It is observed that in the plots of the coincidence probabilities against the time delays introduced between the arrival of the photons at input ports that value of the coincidence probability we get, when there are no time delays between the arrival of the photons or when the photon enters simultaneously the input ports of the passive quantum optical interferometer is equal to the value permanent of the adjacent scattering matrix. The formation that that scattering matrix is also discussed thoroughly in the Sec.3.6.

In the last chapter 4, we have concluded our work.

2

Quantum Interferometry with Single-Photon Input Pulses

In this section we shall see the action of the four port beam splitter two input ports and two output ports on two monochromatic photons. We have shinned a single-photon on each input port and then counted the number of stricks on each output port. The single-photon state is written as $|1(\omega)\rangle = \hat{a}_i^\dagger(\omega) |0\rangle$, with i representing the input port number ($i=1,2$.) and the rounded bra-ket here represents the frequency-explicit states and $\hat{a}_i^\dagger(\omega)$ is the creation operator [4, 5].

$$[\hat{a}_i^\dagger(\omega_a), \hat{a}_j^\dagger(\omega_b)] = \delta_{ij}\delta(\omega_a - \omega_b)\mathbb{1}, \quad (2.1)$$

where i and j represent the input port numbers and vary from 1 to 3. The single-photon state can also be written as,

$$|1(\omega_a)\rangle = \int_{-\infty}^{\infty} \phi(\omega_a) \hat{a}^\dagger(\omega_a) |0\rangle d\omega_a, \quad (2.2)$$

with,

$$\int_{-\infty}^{\infty} |\phi(\omega_a)|^2 d\omega_a = 1, \quad (2.3)$$

For convenience, we have taken the normalized Gaussian distribution function,

$$\phi(\omega) = \frac{1}{[2\pi\sigma_0^2]^{\frac{1}{4}}} \exp \frac{-[\omega - \omega_0]^2}{4\sigma_0^2}. \quad (2.4)$$

where $\phi(\omega)$ is a probability density function (with ω_0 , σ_0 and σ_0^2 as the mean value, standard deviation and variance of the distribution function respectively.) of the Gaussian distribution which is also known as the normal distribution. Normal distribution is one of the very well known continuous distribution of random variables [5, 22].

2.1 SU(2) Quantum Interferometry with Single-Photon Input Pulses

In this case, we have taken the four port passive quantum optical interferometer (2-input ports and 2-output ports) and injected two single photons at two input ports of this passive quantum optical interferometer as shown in Fig.(2.1). For this case the transformation matrix of the beam-splitter action is defined as,

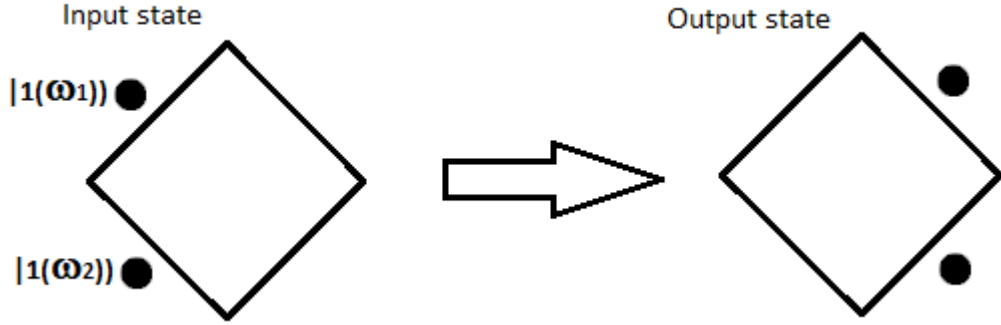


Figure 2.1: This diagram shows the simplest case where we have injected a single photon at each input port of the four passive quantum optical interferometer with two input ports and two output ports. Observed the coincidence probability of having single photon click at each of the output ports with time delay τ introduced between the arrival of these photons at input ports.

$$U = R(\Omega) \begin{pmatrix} e^{-\frac{i\phi}{2}} & 0 \\ 0 & e^{-\frac{i\phi}{2}} \end{pmatrix}, \quad (2.5)$$

To ensure the photon number conservation the transformation matrix of the beam-splitter is to be taken as the unitary matrix (such that $UU^\dagger = U^\dagger U = 1$). Here $R(\Omega)$ is the special unitary matrix with Ω contains α, β and γ . As $R(\Omega) \in SU(2)$ the reason behind, why we have used the group $SU(2)$ as the beam-splitter transformation matrix is because, we are using the loss-less passive quantum optical interferometer. The loss-less passive quantum optical interferometer conserves the total number of the photons that are entering the system through input ports and leaving the system through output ports [4]. The $R(\Omega)$ is define as,

$$R(\Omega) = \begin{pmatrix} e^{-i(\alpha+\gamma)/2} \cos(\beta/2) & -e^{-i(\alpha-\gamma)/2} \sin(\beta/2) \\ e^{i(\alpha-\gamma)/2} \sin(\beta/2) & e^{i(\alpha+\gamma)/2} \cos(\beta/2) \end{pmatrix}. \quad (2.6)$$

We have injected two photons with frequencies ω_a at time τ_1 and ω_b at time τ_2 in input port 1 and 2 of the 50/50 beam-splitter respectively and calculated the coincidence probability for the single click on each of the output ports. The coincidence probability is defined as,

$$P_{11,11} = \langle 11|^s U^\dagger \Pi_1 \otimes \Pi_2 U |11\rangle^s, \quad (2.7)$$

here $P_{11,11}$ shows we have injected single photon on each of the input port and the collected single photon at each output port [20]. Where Π_i are the single-photon output detection operators with,

$$\Pi_1 = \int_{-\infty}^{\infty} \hat{a}_1^\dagger(\omega_c) |0\rangle \langle 0| \hat{a}_1(\omega_c) d\omega_c \quad (2.8)$$

and

$$\Pi_2 = \int_{-\infty}^{\infty} \hat{a}_2^\dagger(\omega_d) |0\rangle \langle 0| \hat{a}_2(\omega_d) d\omega_d. \quad (2.9)$$

The action of the beam splitter is defined as,

$$U \hat{a}_{1in}^\dagger(\omega_a) \hat{a}_{2in}^\dagger(\omega_b) |00\rangle = A \hat{a}_{1out}^\dagger(\omega_a) \hat{a}_{2out}^\dagger(\omega_b) |00\rangle + B \hat{a}_{2out}^\dagger(\omega_a) \hat{a}_{1out}^\dagger(\omega_b) |00\rangle, \quad (2.10)$$

where A and B are the probability coefficients such that,

$$A = U_{11}U_{22}, \quad \text{and} \quad B = U_{21}U_{12}. \quad (2.11)$$

The coincidence probability for the dip where both of the output ports click is (for $\tau_1 = 0$, $\tau_2 = \tau$ and $\sigma_0 = 0.1$)

$$P_{11,11} = -2 \sin^2 \left(\frac{\beta}{2} \right) \cos^2 \left(\frac{\beta}{2} \right) e^{-\sigma^2 \tau^2} + \sin^4 \left(\frac{\beta}{2} \right) + \cos^4 \left(\frac{\beta}{2} \right). \quad (2.12)$$

As the coincidence is symmetric under the permutation of the frequencies, we can set $\beta = \pi/2$.

The coincidence probability plot for the case when both of the output ports click once

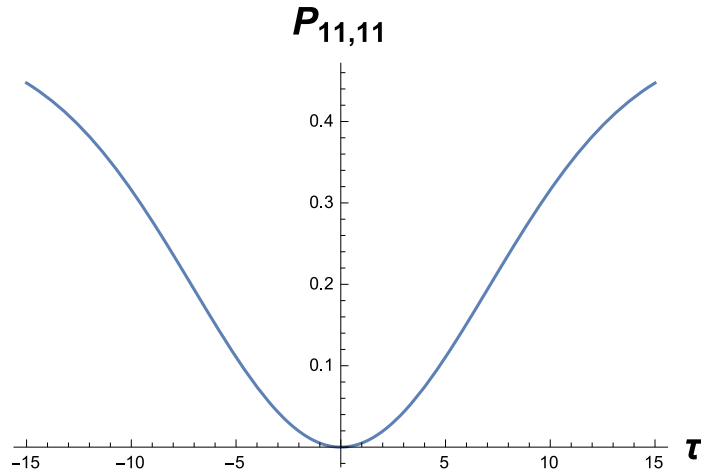


Figure 2.2: Coincidence probability plot against the time delay τ introduced between the arrival of the photons at input ports of the case where we have injected a single photon at each input port of the four passive quantum optical interferometer with two input ports and two output ports. Observed the coincidence probability of having single photon click at each of the output ports with time delay τ introduced between the arrival of these photons at input ports.

This plot in Fig.(2.2) shows, how the coincidence probability of having the single photon on each of the two output ports. As we can see the coincidence probability have the least value when there is no time delay between the arrival of the photons but it increases when we introduce the time interval between the arrival of the single photons. This means when there is no time delay between the arrival of the photon at input ports, the photons are identical in every manner. So, the probability that both photons will exit the different output port become zero, because they perfectly interfere destructively in time. Which means either both of the photons will exit one output port or the other and this effect is known as the Hong-Ou-mandel effect.

2.2 SU(3)Quantum Interferometry with Single-Photon Input Pulses

In this case, we have taken a six-port passive quantum optical interferometer (three-input ports and three-output ports) and injected three identical single-photons, one in each of the input ports with three different frequencies and separate them by introducing three time delays between the their arrival as shown in Fig.(2.3).

For this purpose the beam-splitter transformation matrix is

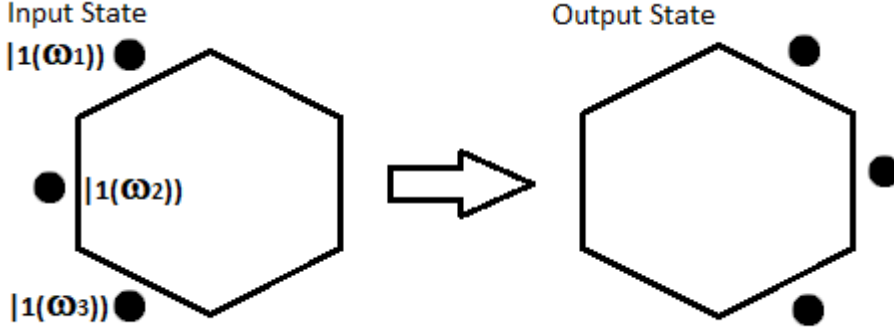


Figure 2.3: This diagram shows, we have injected three single photon one at each input port of the beam splitter and attached different frequency profile to each photon and then collected one photon at each output port with no specific frequency profile, which shows we are not interested in path of any photon.

$$U = R(\Omega) \begin{pmatrix} e^{-\frac{i\zeta}{3}} & 0 & 0 \\ 0 & e^{-\frac{i\zeta}{3}} & 0 \\ 0 & 0 & e^{-\frac{i\zeta}{3}} \end{pmatrix}, \quad (2.13)$$

to conserve the total number of photons, the U matrix is taken to the unitary matrix. Here $R(\Omega)$ is the special unitary matrix with Ω as the 8-tuple of angles [4]. The $R(\Omega)$ matrix is as a product

$$R(\Omega) = T_{23}(\alpha_1, \beta_1, -\alpha_1) T_{12}(\alpha_2, \beta_2, -\alpha_2) T_{23}(\alpha_3, \beta_3, -\alpha_3) \Phi(\gamma_1, \gamma_2), \quad (2.14)$$

with

$$\Omega := \Omega(\alpha_1, \alpha_2, \alpha_3, \beta_1, \beta_2, \beta_3, \gamma_1, \gamma_2). \quad (2.15)$$

The $T_{ij}(\alpha, \beta, \gamma)$ matrix can be written as,

$$T_{12}(\alpha, \beta, \gamma) = \begin{pmatrix} e^{-i(\alpha+\gamma)/2} \cos(\beta/2) & -e^{-i(\alpha-\gamma)/2} \sin(\beta/2) & 0 \\ e^{i(\alpha-\gamma)/2} \sin(\beta/2) & e^{i(\alpha+\gamma)/2} \cos(\beta/2) & 0 \\ 0 & 0 & 1 \end{pmatrix}, \quad (2.16)$$

which is the beam-splitter between the port-1 and port-2.

$$T_{23}(\alpha, \beta, \gamma) = \begin{pmatrix} 1 & 0 & 0 \\ 0 & e^{-i(\alpha+\gamma)/2} \cos(\beta/2) & -e^{-i(\alpha-\gamma)/2} \sin(\beta/2) \\ 0 & e^{i(\alpha-\gamma)/2} \sin(\beta/2) & e^{i(\alpha+\gamma)/2} \cos(\beta/2) \end{pmatrix} \quad (2.17)$$

which is the beam-splitter between the port-2 and port-3 and

$$\Phi(\gamma_1, \gamma_2) = \begin{pmatrix} e^{-2i\gamma_1} & 0 & 0 \\ 0 & e^{i(\gamma_1-\gamma_2/2)} & 0 \\ 0 & 0 & e^{i(\gamma_1+\gamma_2/2)} \end{pmatrix}. \quad (2.18)$$

is the phase shifter. Thus SU(3) operations are the phase shifter operations followed by the beam-splitters. The coincidence probability for case when each of the output detectors clicks once is,

$$P_{111,111} = \langle 111 |^s U^\dagger \Pi_1 \otimes \Pi_2 \otimes \Pi_3 U | 111 \rangle^s, \quad (2.19)$$

and represents that we have injected single photon at each input port and collected single photon at each output ports. Here Π_i are the single photon output detection operators and defined as,

$$\Pi_1 = \int_{-\infty}^{\infty} \hat{a}_1^\dagger(\omega_4) |0\rangle \langle 0| \hat{a}_1(\omega_4) d\omega_4, \quad (2.20)$$

$$\Pi_2 = \int_{-\infty}^{\infty} \hat{a}_2^\dagger(\omega_5) |0\rangle \langle 0| \hat{a}_2(\omega_5) d\omega_5 \quad (2.21)$$

and

$$\Pi_3 = \int_{-\infty}^{\infty} \hat{a}_3^\dagger(\omega_6) |0\rangle \langle 0| \hat{a}_3(\omega_6) d\omega_6. \quad (2.22)$$

The input state is

$$\begin{aligned} |111\rangle^s = \int_{-\infty}^{\infty} \phi(\omega_1) \phi(\omega_2) \phi(\omega_3) \exp(-i\omega_1\tau_1) \exp(-i\omega_2\tau_2) \exp(-i\omega_3\tau_3) \\ \hat{a}_1^\dagger(\omega_1) \hat{a}_2^\dagger(\omega_2) \hat{a}_3^\dagger(\omega_3) |000\rangle d\omega_1 d\omega_2 d\omega_3, \end{aligned} \quad (2.23)$$

so,

$$\begin{aligned} P_{111,111} = & X_1(X_2)^* e^{-\sigma^2\tau^2} + X_1(X_3)^* e^{-\sigma^2\tau^2} + X_1(X_4)^* e^{-3\sigma^2\tau^2} + X_1(X_5)^* e^{-3\sigma^2\tau^2} + \\ & X_1(X_6)^* e^{-4\sigma^2\tau^2} + X_2(X_1)^* e^{-\sigma^2\tau^2} + X_2(X_3)^* e^{-3\sigma^2\tau^2} + X_2(X_4)^* e^{-4\sigma^2\tau^2} + \\ & X_2(X_5)^* e^{-\sigma^2\tau^2} + X_2(X_6)^* e^{-3\sigma^2\tau^2} + X_3(X_1)^* e^{-\sigma^2\tau^2} + X_3(X_2)^* e^{-3\sigma^2\tau^2} + \\ & X_3(X_4)^* e^{-\sigma^2\tau^2} + X_3(X_5)^* e^{-4\sigma^2\tau^2} + X_3(X_6)^* e^{-3\sigma^2\tau^2} + X_4(X_1)^* e^{-3\sigma^2\tau^2} + \\ & X_4(X_2)^* e^{-4\sigma^2\tau^2} + X_4(X_3)^* e^{-\sigma^2\tau^2} + X_4(X_5)^* e^{-3\sigma^2\tau^2} + X_4(X_6)^* e^{-\sigma^2\tau^2} + \\ & X_5(X_1)^* e^{-3\sigma^2\tau^2} + X_5(X_2)^* e^{-\sigma^2\tau^2} + X_5(X_3)^* e^{-4\sigma^2\tau^2} + X_5(X_4)^* e^{-3\sigma^2\tau^2} + \\ & X_5(X_6)^* e^{-\sigma^2\tau^2} + X_6(X_1)^* e^{-4\sigma^2\tau^2} + X_6(X_2)^* e^{-3\sigma^2\tau^2} + X_6(X_3)^* e^{-3\sigma^2\tau^2} + \\ & X_6(X_4)^* e^{-\sigma^2\tau^2} + X_6(X_5)^* e^{-\sigma^2\tau^2} + X_1(X_1)^* + X_2(X_2)^* + X_3(X_3)^* + \\ & X_4(X_4)^* + X_5(X_5)^* + X_6(X_6)^* \end{aligned} \quad (2.24)$$

where X 's are the probability coefficients

$$\begin{aligned} X_1 &= U_{11}U_{22}U_{33}; & X_2 &= U_{11}U_{23}U_{32}; & X_3 &= U_{12}U_{21}U_{33}; \\ X_4 &= U_{12}U_{23}U_{31}; & X_5 &= U_{13}U_{21}U_{32}; & X_6 &= U_{13}U_{22}U_{31} \end{aligned} \quad (2.25)$$

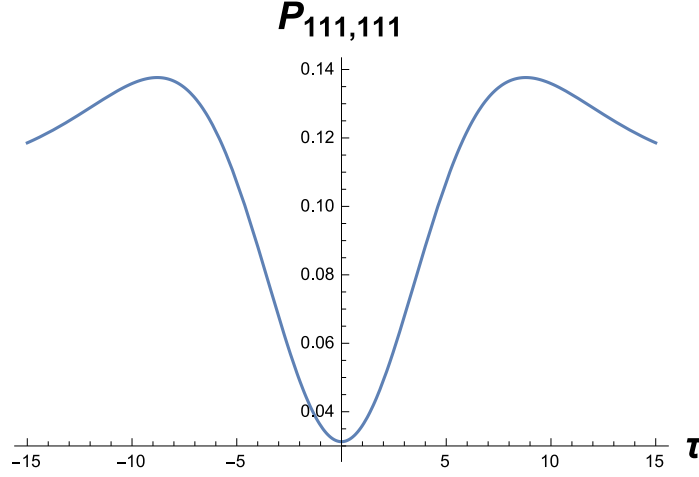


Figure 2.4: (with $\tau(\tau_1, \tau_2, \tau_3) = \tau(-\tau, 0, \tau)$, $\sigma_o = 0.1$ and $\Omega(\alpha_1, \alpha_2, \alpha_3, \beta_1, \beta_2, \beta_3, \gamma_1, \gamma_2) = \Omega(0, 0, 0, \pi/2, \pi/2, \pi/2, 0, 0)$)

The plot in Fig.(2.4) shows, how the coincidence probability of having the single photon on each of the three output ports varies with time-delay τ . Here each of the input pulse is delayed with respect to next one by time τ . As we can see the coincidence probability have the least value when there is no time delay between the arrival of the photons but it increases when we introduce the time interval between the arrival of the single photons and again decreases when the time delay exceeds a certain limit.

In this section, we have discussed the quantum interferometry for the case, where we injected single photon at each input port then calculated and plotted the coincidence probability rate against the time-delays introduced between the arrival of the photons at input ports. Now in the next chapter, we shall discuss the quantum interferometry with bi-photon input pulses at two of the three input ports of a six channel beam splitter with three input ports and three output ports and then discuss the coincidence probabilities for all possible output form one by one.

3

Quantum Interferometry with Bi-Photon Input Pulses

The calculation of the coincidence probability for the case, where single photon input pulses have injected at input ports of four-port passive quantum optical interferometer (with 2 input ports and 2 output ports) and six-port passive quantum optical interferometer (with 3 input ports and 3 output ports) and observing single photon clicks at output ports have already been done [4, 5]. The coincidence probability for the case where a combination of single photon input pulses and bi-photon pulses have injected at input ports of six port passive quantum optical interferometer (with 3 input ports and 3 output ports) and observed the output coincidence patterns in which we got bi-photon clicks at output ports have already been done [20].

We have regenerated the results for the single photon pulses at input ports of four port passive quantum optical interferometer and six port passive quantum optical interferometer. We have discussed the regenerated results in chapter 2.

We have calculated the coincidence probabilities for the cases where we have injected bi-photon input pulses at any two input ports of the six-port passive quantum optical interferometer and observed all possible output coincidence patterns. And then analyzed these coincidence probabilities against the time delays τ introduced between the arrival of the photons at input ports.

3.1 Bi-Photon Input pulses at Input-1 and Input-2

In this case, we have taken conventional 6-port beam splitter and injected four photons with different frequency profiles, two in each of the input-1 and input-2 (nothing at input-3) as shown in Fig.(3.1) and introduced a time delay τ between the arrival of each of the photon at the input ports. Here we shall discuss the coincidence probabilities for different possible outputs and see how these coincidences vary with the change in the length of the time-delays introduced between the arrival of the photons at input ports.

3.1.1 Bi-Photon Clicks on Output-1 and Output-2

In this section, we have injected four photons at input ports such that two at each of the input port-1 and input port-2. To create distinguishability, we have introduced a time-delay τ between the arrival of each of the photon at input ports and then calculated the coincidence probability for the output coincidence pattern where we have a bi-photon clicks at output port-1 and output port-2 as shown in Fig.(3.1). The coincidence probability for such problem can be written as,

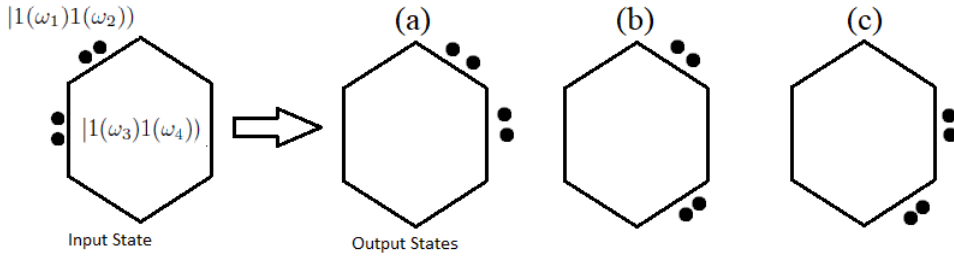


Figure 3.1: This diagram shows we have injected two bi-photon input pulses, one at input port-1 and one at input port-2 and then collected two bi-photon pulses at any of the two output ports as shown above.

$$P_{220,220} = \langle 1111 |^s U^\dagger \Pi_1 \otimes \Pi_2 U | 1111 \rangle^s, \quad (3.1)$$

the output operators for the cases where we get the bi-photon click on any of the two output ports are defined as

$$\Pi_1 = \int_{-\infty}^{\infty} \hat{a}_1^\dagger(\omega_5) \hat{a}_1^\dagger(\omega_8) |00\rangle \langle 00| \hat{a}_1(\omega_5) \hat{a}_1(\omega_8) d\omega_5 d\omega_8, \quad (3.2)$$

36 3. QUANTUM INTERFEROMETRY WITH BI-PHOTON INPUT PULSES

$$\Pi_2 = \int_{-\infty}^{\infty} \hat{a}_2^\dagger(\omega_6) \hat{a}_2^\dagger(\omega_9) |00\rangle \langle 00| \hat{a}_2(\omega_6) \hat{a}_2(\omega_9) d\omega_6 d\omega_9, \quad (3.3)$$

and

$$\Pi_3 = \int_{-\infty}^{\infty} \hat{a}_3^\dagger(\omega_7) \hat{a}_3^\dagger(\omega_{10}) |00\rangle \langle 00| \hat{a}_3(\omega_7) \hat{a}_3(\omega_{10}) d\omega_7 d\omega_{10}, \quad (3.4)$$

the output operators used for this specific case are defined in Eq.(3.2) and Eq.(3.3) and the input state is define as

$$|1111\rangle^s = \int_{-\infty}^{\infty} \phi(\omega_1) \phi(\omega_2) \phi(\omega_3) \phi(\omega_4) \exp(-i\omega_1\tau_1) \exp(-i\omega_2\tau_2) \exp(-i\omega_3\tau_3) \\ \exp(-i\omega_4\tau_4) \hat{a}_1^\dagger(\omega_1) \hat{a}_1^\dagger(\omega_2) \hat{a}_2^\dagger(\omega_3) \hat{a}_2^\dagger(\omega_4) |0000\rangle d\omega_1 d\omega_2 d\omega_3 d\omega_4, \quad (3.5)$$

so,

$$P_{220,220} = A_1 (A_2)^* e^{-\sigma^2\tau^2} + A_1 (A_3)^* e^{-3\sigma^2\tau^2} + A_1 (A_4)^* e^{-3\sigma^2\tau^2} + A_1 (A_5)^* e^{-5\sigma^2\tau^2} + \\ A_1 (A_6)^* e^{-8\sigma^2\tau^2} + A_2 (A_1)^* e^{-\sigma^2\tau^2} + A_2 (A_3)^* e^{-\sigma^2\tau^2} + A_2 (A_4)^* e^{-\sigma^2\tau^2} + \\ A_2 (A_5)^* e^{-2\sigma^2\tau^2} + A_2 (A_6)^* e^{-5\sigma^2\tau^2} + A_3 (A_1)^* e^{-3\sigma^2\tau^2} + A_3 (A_2)^* e^{-\sigma^2\tau^2} + \\ A_3 (A_4)^* e^{-2\sigma^2\tau^2} + A_3 (A_5)^* e^{-\sigma^2\tau^2} + A_3 (A_6)^* e^{-3\sigma^2\tau^2} + A_4 (A_1)^* e^{-3\sigma^2\tau^2} + \\ A_4 (A_2)^* e^{-\sigma^2\tau^2} + A_4 (A_3)^* e^{-2\sigma^2\tau^2} + A_4 (A_5)^* e^{-\sigma^2\tau^2} + A_4 (A_6)^* e^{-3\sigma^2\tau^2} + \\ A_5 (A_1)^* e^{-5\sigma^2\tau^2} + A_5 (A_2)^* e^{-2\sigma^2\tau^2} + A_5 (A_3)^* e^{-\sigma^2\tau^2} + A_5 (A_4)^* e^{-\sigma^2\tau^2} + \\ A_5 (A_6)^* e^{-\sigma^2\tau^2} + A_6 (A_1)^* e^{-8\sigma^2\tau^2} + A_6 (A_2)^* e^{-5\sigma^2\tau^2} + A_6 (A_3)^* e^{-3\sigma^2\tau^2} + \\ A_6 (A_4)^* e^{-3\sigma^2\tau^2} + A_6 (A_5)^* e^{-\sigma^2\tau^2} + A_1 (A_1)^* + A_2 (A_2)^* + A_3 (A_3)^* + \\ A_4 (A_4)^* + A_5 (A_5)^* + A_6 (A_6)^*. \quad (3.6)$$

Where the A's are the probability coefficients and are defined as

$$A_1 = U_{11}^2 U_{22}^2; \quad A_2 = U_{11} U_{21} U_{12} U_{22}; \quad A_3 = U_{11} U_{21} U_{22} U_{12}; \quad A_4 = U_{21} U_{11} U_{12} U_{22}; \\ A_5 = U_{21} U_{11} U_{22} U_{12}; \quad A_6 = U_{21}^2 U_{12}^2; \quad A_7 = U_{11}^2 U_{32}^2; \quad A_8 = U_{11} U_{31} U_{12} U_{22}; \\ A_9 = U_{11} U_{31} U_{32} U_{12}; \quad A_{10} = U_{31} U_{11} U_{12} U_{32}; \quad A_{11} = U_{31} U_{11} U_{32} U_{12}; \quad A_{12} = U_{31}^2 U_{12}^2; \\ A_{13} = U_{21}^2 U_{32}^2; \quad A_{14} = U_{21} U_{31} U_{22} U_{32}; \quad A_{15} = U_{21} U_{31} U_{32} U_{22}; \quad A_{16} = U_{31} U_{21} U_{22} U_{32}; \\ A_{17} = U_{31} U_{21} U_{32} U_{22}; \quad A_{18} = U_{31}^2 U_{22}^2; \quad (3.7)$$

The plot of the coincidence probability against the time delays introduced between the arrival of the photons at input ports is shown in the Fig.(3.2). This plot shows that we get the maximum probability of having the desired the output when there is no time-delays between the arrival of the photons at input ports and this value of the coincidence probability for this case with zero time delay is equal to the value of the permanent of the adjacent scattering matrix. The probability of having the

desired output starts decreasing as the length of time delays between the arrival of the photons at input ports start increasing as shown in Fig.(3.2). Rest of the cases as mentioned in Fig.(3.1) are discussed in Appendix(A.1,A.2.)

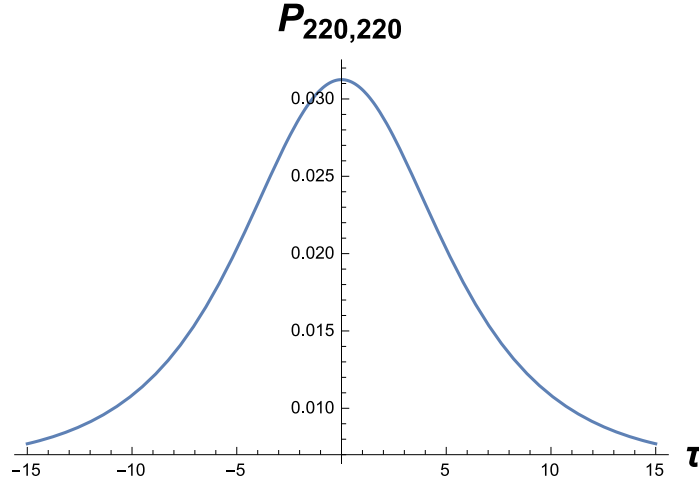


Figure 3.2: (with $T(\tau_1, \tau_2, \tau_3, \tau_4) = T(-\tau, 0, \tau, 2\tau)$, $\sigma_o = 0.1$ and $\Omega(\alpha_1, \alpha_2, \alpha_3, \beta_1, \beta_2, \beta_3, \gamma_1, \gamma_2) = \Omega(0, 0, 0, \pi/2, \pi/2, \pi/2, 0, 0)$)

3.1.2 Bi-Photon Click on Output-1 and Single-Photon Click on Output-2 and Output-3

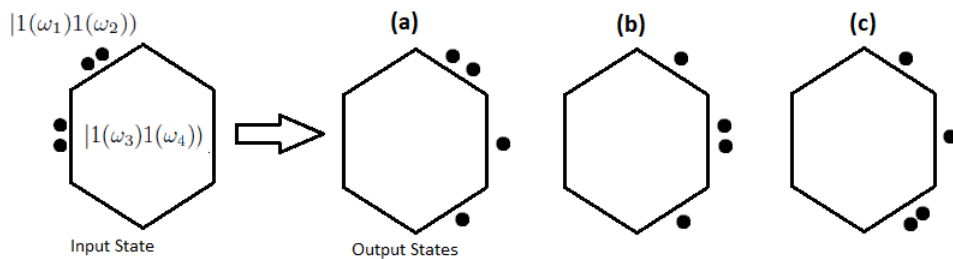


Figure 3.3: The input pattern is the same as before but in this case the output coincidence pattern is such that a bi-photon click on any of the one output ports and a single-photon click on each rest of the output ports.

38 3. QUANTUM INTERFEROMETRY WITH BI-PHOTON INPUT PULSES

In this case, we shall discuss the coincidence probability for a bi-photon click on the output port-1 and a single-photon click on output port-2 and output port-3 for the same input state, in which we inject bi-photon input pulse in input port-1 and input port-2 with time-delay between every arrival of the photons at input ports as shown in Fig.(3.3). The input state for this case is the same as defined before in the Eq.(3.5). The output operators for this case are defined as

$$\Pi_1 = \int_{-\infty}^{\infty} \hat{a}_1^\dagger(\omega_5) \hat{a}_1^\dagger(\omega_8) |00\rangle \langle 00| \hat{a}_1(\omega_5) \hat{a}_1(\omega_8) d\omega_5 d\omega_8, \quad (3.8)$$

$$\Pi_2 = \int_{-\infty}^{\infty} \hat{a}_2^\dagger(\omega_6) |0\rangle \langle 0| \hat{a}_2(\omega_6) d\omega_6, \quad (3.9)$$

and

$$\Pi_3 = \int_{-\infty}^{\infty} \hat{a}_3^\dagger(\omega_7) |0\rangle \langle 0| \hat{a}_3(\omega_7) d\omega_7, \quad (3.10)$$

the coincidence probability for this case is defined as

$$P_{220,211} = \langle 1111 |^s U^\dagger \Pi_1 \otimes \Pi_2 \otimes \Pi_3 U | 1111 \rangle^s, \quad (3.11)$$

The probability coefficients for this case are defined as,

$$\begin{aligned} L_1 &= U_{11}^2 U_{22} U_{32}; & L_2 &= U_{11}^2 U_{22} U_{32}; & L_3 &= U_{11} U_{12} U_{21} U_{32}; & L_4 &= U_{11} U_{12} U_{22} U_{31}; \\ L_5 &= U_{11} U_{12} U_{21} U_{32}; & L_6 &= U_{11} U_{12} U_{22} U_{31}; & L_7 &= U_{11} U_{12} U_{21} U_{32}; & L_8 &= U_{11} U_{12} U_{22} U_{31}; \\ L_9 &= U_{11} U_{12} U_{21} U_{32}; & L_{10} &= U_{11} U_{12} U_{22} U_{31}; & L_{11} &= U_{12}^2 U_{21} U_{31}; & L_{12} &= U_{12}^2 U_{21} U_{31}; \end{aligned} \quad (3.12)$$

so the coincidence probability for this case is,

$$\begin{aligned} P_{220,211} &= (L_1)^* L_1 + e^{-\sigma^2 \tau^2} (L_2)^* L_1 + e^{-\sigma^2 \tau^2} (L_3)^* L_1 + e^{-3\sigma^2 \tau^2} (L_4)^* L_1 + \\ &e^{-3\sigma^2 \tau^2} (L_5)^* L_1 + e^{-4\sigma^2 \tau^2} (L_6)^* L_1 + e^{-3\sigma^2 \tau^2} (L_7)^* L_1 + e^{-6\sigma^2 \tau^2} (L_8)^* L_1 + \\ &e^{-5\sigma^2 \tau^2} (L_9)^* L_1 + e^{-7\sigma^2 \tau^2} (L_{10})^* L_1 + e^{-8\sigma^2 \tau^2} (L_{11})^* L_1 + e^{-9\sigma^2 \tau^2} (L_{12})^* L_1 + \\ &e^{-\sigma^2 \tau^2} (L_1)^* L_2 + (L_2)^* L_2 + e^{-3\sigma^2 \tau^2} (L_3)^* L_2 + e^{-\sigma^2 \tau^2} (L_4)^* L_2 + \\ &e^{-4\sigma^2 \tau^2} (L_5)^* L_2 + e^{-3\sigma^2 \tau^2} (L_6)^* L_2 + e^{-6\sigma^2 \tau^2} (L_7)^* L_2 + e^{-3\sigma^2 \tau^2} (L_8)^* L_2 + \\ &e^{-7\sigma^2 \tau^2} (L_9)^* L_2 + e^{-5\sigma^2 \tau^2} (L_{10})^* L_2 + e^{-9\sigma^2 \tau^2} (L_{11})^* L_2 + e^{-8\sigma^2 \tau^2} (L_{12})^* L_2 + \\ &e^{-\sigma^2 \tau^2} (L_1)^* L_3 + e^{-3\sigma^2 \tau^2} (L_2)^* L_3 + (L_3)^* L_3 + e^{-4\sigma^2 \tau^2} (L_4)^* L_3 + \\ &e^{-\sigma^2 \tau^2} (L_5)^* L_3 + e^{-3\sigma^2 \tau^2} (L_6)^* L_3 + e^{-\sigma^2 \tau^2} (L_7)^* L_3 + e^{-7\sigma^2 \tau^2} (L_8)^* L_3 + \\ &e^{-2\sigma^2 \tau^2} (L_9)^* L_3 + e^{-6\sigma^2 \tau^2} (L_{10})^* L_3 + e^{-5\sigma^2 \tau^2} (L_{11})^* L_3 + e^{-7\sigma^2 \tau^2} (L_{12})^* L_3 + \\ &e^{-3\sigma^2 \tau^2} (L_1)^* L_4 + e^{-\sigma^2 \tau^2} (L_2)^* L_4 + e^{-4\sigma^2 \tau^2} (L_3)^* L_4 + (L_4)^* L_4 + \end{aligned}$$

$$\begin{aligned}
& e^{-3\sigma^2\tau^2} (L_5) * L_4 + e^{-\sigma^2\tau^2} (L_6) * L_4 + e^{-7\sigma^2\tau^2} (L_7) * L_4 + e^{-\sigma^2\tau^2} (L_8) * L_4 + \\
& e^{-6\sigma^2\tau^2} (L_9) * L_4 + e^{-2\sigma^2\tau^2} (L_{10}) * L_4 + e^{-7\sigma^2\tau^2} (L_{11}) * L_4 + e^{-5\sigma^2\tau^2} (L_{12}) * L_4 + \\
& e^{-3\sigma^2\tau^2} (L_1) * L_5 + e^{-4\sigma^2\tau^2} (L_2) * L_5 + e^{-\sigma^2\tau^2} (L_3) * L_5 + e^{-3\sigma^2\tau^2} (L_4) * L_5 + \\
& (L_5) * L_5 + e^{-\sigma^2\tau^2} (L_6) * L_5 + e^{-2\sigma^2\tau^2} (L_7) * L_5 + e^{-5\sigma^2\tau^2} (L_8) * L_5 + \\
& e^{-\sigma^2\tau^2} (L_9) * L_5 + e^{-3\sigma^2\tau^2} (L_{10}) * L_5 + e^{-3\sigma^2\tau^2} (L_{11}) * L_5 + e^{-4\sigma^2\tau^2} (L_{12}) * L_5 + \\
& e^{-4\sigma^2\tau^2} (L_1) * L_6 + e^{-3\sigma^2\tau^2} (L_2) * L_6 + e^{-3\sigma^2\tau^2} (L_3) * L_6 + e^{-\sigma^2\tau^2} (L_4) * L_6 + \\
& e^{-\sigma^2\tau^2} (L_5) * L_6 + (L_6) * L_6 + e^{-5\sigma^2\tau^2} (L_7) * L_6 + e^{-2\sigma^2\tau^2} (L_8) * L_6 + \\
& e^{-3\sigma^2\tau^2} (L_9) * L_6 + e^{-\sigma^2\tau^2} (L_{10}) * L_6 + e^{-4\sigma^2\tau^2} (L_{11}) * L_6 + e^{-3\sigma^2\tau^2} (L_{12}) * L_6 + \\
& e^{-3\sigma^2\tau^2} (L_1) * L_7 + e^{-6\sigma^2\tau^2} (L_2) * L_7 + e^{-\sigma^2\tau^2} (L_3) * L_7 + e^{-7\sigma^2\tau^2} (L_4) * L_7 + \\
& e^{-2\sigma^2\tau^2} (L_5) * L_7 + e^{-5\sigma^2\tau^2} (L_6) * L_7 + (L_7) * L_7 + e^{-9\sigma^2\tau^2} (L_8) * L_7 + \\
& e^{-\sigma^2\tau^2} (L_9) * L_7 + e^{-7\sigma^2\tau^2} (L_{10}) * L_7 + e^{-3\sigma^2\tau^2} (L_{11}) * L_7 + e^{-6\sigma^2\tau^2} (L_{12}) * L_7 + \\
& e^{-6\sigma^2\tau^2} (L_1) * L_8 + e^{-3\sigma^2\tau^2} (L_2) * L_8 + e^{-7\sigma^2\tau^2} (L_3) * L_8 + e^{-\sigma^2\tau^2} (L_4) * L_8 + \\
& e^{-5\sigma^2\tau^2} (L_5) * L_8 + e^{-2\sigma^2\tau^2} (L_6) * L_8 + e^{-9\sigma^2\tau^2} (L_7) * L_8 + (L_8) * L_8 + \\
& e^{-7\sigma^2\tau^2} (L_9) * L_8 + e^{-\sigma^2\tau^2} (L_{10}) * L_8 + e^{-6\sigma^2\tau^2} (L_{11}) * L_8 + e^{-3\sigma^2\tau^2} (L_{12}) * L_8 + \\
& e^{-5\sigma^2\tau^2} (L_1) * L_9 + e^{-7\sigma^2\tau^2} (L_2) * L_9 + e^{-2\sigma^2\tau^2} (L_3) * L_9 + e^{-6\sigma^2\tau^2} (L_4) * L_9 + \\
& e^{-\sigma^2\tau^2} (L_5) * L_9 + e^{-3\sigma^2\tau^2} (L_6) * L_9 + e^{-\sigma^2\tau^2} (L_7) * L_9 + e^{-7\sigma^2\tau^2} (L_8) * L_9 + \\
& (L_9) * L_9 + e^{-4\sigma^2\tau^2} (L_{10}) * L_9 + e^{-\sigma^2\tau^2} (L_{11}) * L_9 + e^{-3\sigma^2\tau^2} (L_{12}) * L_9 + \\
& e^{-7\sigma^2\tau^2} (L_1) * L_{10} + e^{-5\sigma^2\tau^2} (L_2) * L_{10} + e^{-6\sigma^2\tau^2} (L_3) * L_{10} + e^{-2\sigma^2\tau^2} (L_4) * L_{10} + \\
& e^{-3\sigma^2\tau^2} (L_5) * L_{10} + e^{-\sigma^2\tau^2} (L_6) * L_{10} + e^{-7\sigma^2\tau^2} (L_7) * L_{10} + e^{-\sigma^2\tau^2} (L_8) * L_{10} + \\
& e^{-4\sigma^2\tau^2} (L_9) * L_{10} + (L_{10}) * L_{10} + e^{-3\sigma^2\tau^2} (L_{11}) * L_{10} + \\
& e^{-\sigma^2\tau^2} (L_{12}) * L_{10} + e^{-8\sigma^2\tau^2} (L_1) * L_{11} + e^{-9\sigma^2\tau^2} (L_2) * L_{11} + e^{-5\sigma^2\tau^2} (L_3) * L_{11} + \\
& e^{-7\sigma^2\tau^2} (L_4) * L_{11} + e^{-3\sigma^2\tau^2} (L_5) * L_{11} + e^{-4\sigma^2\tau^2} (L_6) * L_{11} + e^{-3\sigma^2\tau^2} (L_7) * L_{11} + \\
& e^{-6\sigma^2\tau^2} (L_8) * L_{11} + e^{-\sigma^2\tau^2} (L_9) * L_{11} + e^{-3\sigma^2\tau^2} (L_{10}) * L_{11} + (L_{11}) * L_{11} + \\
& e^{-\sigma^2\tau^2} (L_{12}) * L_{11} + e^{-9\sigma^2\tau^2} (L_1) * L_{12} + e^{-8\sigma^2\tau^2} (L_2) * L_{12} + e^{-7\sigma^2\tau^2} (L_3) * L_{12} + \\
& e^{-5\sigma^2\tau^2} (L_4) * L_{12} + e^{-4\sigma^2\tau^2} (L_5) * L_{12} + e^{-3\sigma^2\tau^2} (L_6) * L_{12} + e^{-6\sigma^2\tau^2} (L_7) * L_{12} + \\
& e^{-3\sigma^2\tau^2} (L_8) * L_{12} + e^{-3\sigma^2\tau^2} (L_9) * L_{12} + e^{-\sigma^2\tau^2} (L_{10}) * L_{12} + e^{-\sigma^2\tau^2} (L_{11}) * L_{12} + \\
& (L_{12}) * L_{12}. \tag{3.13}
\end{aligned}$$

The plot of the coincidence probability against the time delays introduced between the arrival of the photons at input ports is shown in Fig.(3.4). This plot shows that the probability of having the desired output pattern is comparatively high, when

there is no time delays τ between the arrival of the photon at input ports and this value of the coincidence probability with zero time delay is equal to the value of the permanent of the adjacent scattering matrix for this specific case. Afterwards it slightly increases with increase in the length of the time delay τ and we two adjacent peaks and then we get a sharp drop with further increase in the length of the time delays. Rest of the cases as mentioned in Fig.(3.1) are discussed in Appendix(A.3,A.4).

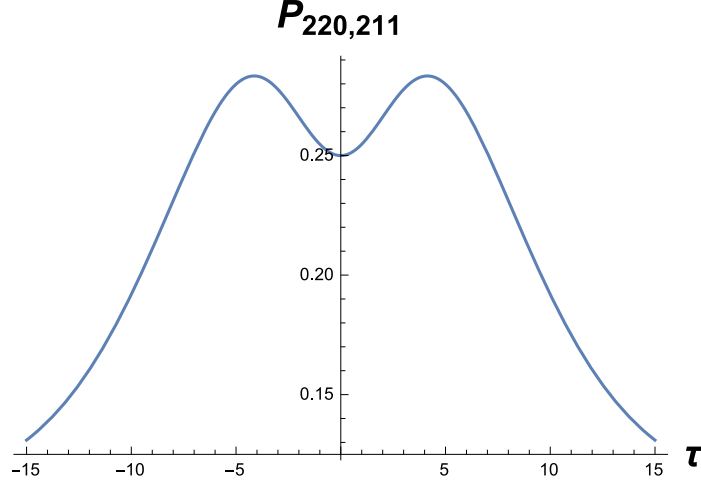


Figure 3.4: (with $T(\tau_1, \tau_2, \tau_3, \tau_4) = T(-\tau, 0, \tau, 2\tau)$, $\sigma_o = 0.1$ and $\Omega(\alpha_1, \alpha_2, \alpha_3, \beta_1, \beta_2, \beta_3, \gamma_1, \gamma_2) = \Omega(0, 0, 0, \pi/2, \pi/2, \pi/2, 0, 0)$)

3.1.3 Tri-Photon Click on Output-1, Single-Photon Click on Output-2 and no click on Output-3

In this section, we shall discuss the coincidence probability for the case when we get a tri-photon click and a single photon click simultaneously for the incidence of bi-photon clicks on input port-1 and input port-2 with time-delay τ is introduced between the arrival of photons at input ports. As we can see from the Fig.(3.5). For this specific case, we shall discuss first output in above Fig.(3.5). in which we get a tri-photon click at output port-1 and a single photon click at output port-2. The Input state will be same as we defined in Eq.(3.5) and the output operators for this case are defined as,

$$\Pi_1 = \int_{-\infty}^{\infty} \hat{a}_1^\dagger(\omega_5) \hat{a}_1^\dagger(\omega_8) \hat{a}_1^\dagger(\omega_{11}) |000\rangle \langle 000| \hat{a}_1(\omega_5) \hat{a}_1(\omega_8) \hat{a}_1(\omega_{11}) d\omega_5 d\omega_8 d\omega_{11}, \quad (3.14)$$

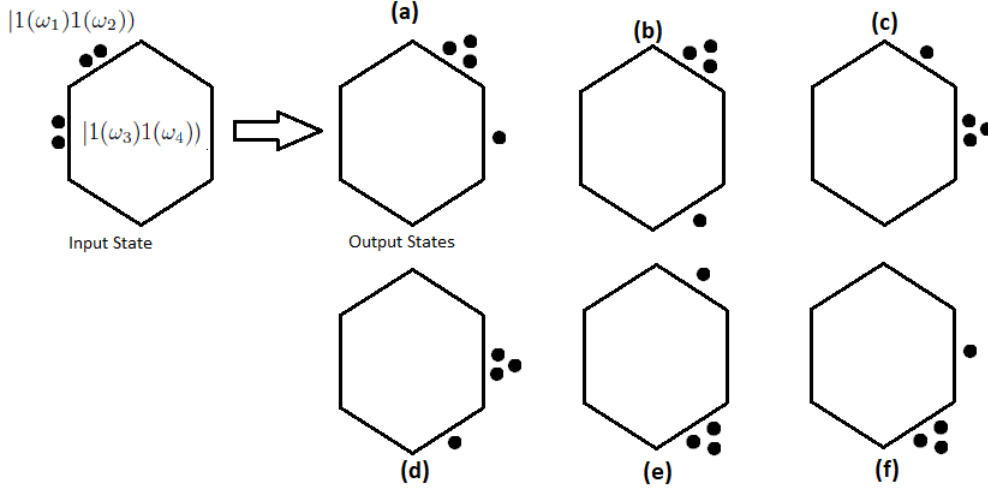


Figure 3.5: As we can see the input state is same but this time the output pattern is different in which we have observed the coincidence probabilities for the cases where we get a tri-photon click at one of the output ports, a single-photon click at another of output ports and one remains in click-less.

and

$$\Pi_2 = \int_{-\infty}^{\infty} \hat{a}_2^\dagger(\omega_6) |0\rangle \langle 0| \hat{a}_2^\dagger(\omega_6) d\omega_6, \quad (3.15)$$

the coincidence probability for this case can be written as

$$P_{220,310} = {}^s \langle 1111 | U^\dagger \Pi_1 \otimes \Pi_2 U | 1111 \rangle^s, \quad (3.16)$$

the probability coefficients for this case are defined as

$$\begin{aligned} D_1 &= U_{11}^2 U_{12} U_{22}; & D_2 &= U_{11}^2 U_{12} U_{22}; & D_3 &= U_{11} U_{12}^2 U_{21}; & D_4 &= U_{11} U_{12}^2 U_{21}; \\ D_5 &= U_{11} U_{21} U_{22}^2; & D_6 &= U_{11} U_{21} U_{22}^2; & D_7 &= U_{12} U_{21}^2 U_{22}; & D_8 &= U_{12} U_{21}^2 U_{22}; \\ D_9 &= U_{11}^2 U_{12} U_{32}; & D_{10} &= U_{11}^2 U_{12} U_{32}; & D_{11} &= U_{11} U_{12}^2 U_{31}; & D_{12} &= U_{11} U_{12}^2 U_{31}; \\ D_{13} &= U_{21}^2 U_{22} U_{32}; & D_{14} &= U_{21}^2 U_{22} U_{32}; & D_{15} &= U_{21} U_{22}^2 U_{31}; & D_{16} &= U_{21} U_{22}^2 U_{31}; \\ D_{17} &= U_{11} U_{31} U_{32}^2; & D_{18} &= U_{11} U_{31} U_{32}^2; & D_{19} &= U_{12} U_{31}^2 U_{32}; & D_{20} &= U_{12} U_{31}^2 U_{32}; \\ D_{21} &= U_{21} U_{31} U_{32}^2; & D_{22} &= U_{21} U_{31} U_{32}^2; & D_{23} &= U_{22} U_{31}^2 U_{32}; & D_{24} &= U_{22} U_{31}^2 U_{32}; \end{aligned} \quad (3.17)$$

so the Coincidence probability for this case is

$$P_{220,310} = D_1 (D_2)^* e^{-\sigma^2 \tau^2} + D_1 (D_3)^* e^{-3\sigma^2 \tau^2} + D_1 (D_4)^* e^{-6\sigma^2 \tau^2} + D_2 (D_1)^* e^{-\sigma^2 \tau^2} +$$

$$\begin{aligned}
& D_2(D_3)^* e^{-\sigma^2 \tau^2} + D_2(D_4)^* e^{-3\sigma^2 \tau^2} + D_3(D_1)^* e^{-3\sigma^2 \tau^2} + D_3(D_2)^* e^{-\sigma^2 \tau^2} + \\
& D_3(D_4)^* e^{-\sigma^2 \tau^2} + D_4(D_1)^* e^{-6\sigma^2 \tau^2} + D_4(D_2)^* e^{-3\sigma^2 \tau^2} + D_4(D_3)^* e^{-\sigma^2 \tau^2} + \\
& D_1(D_1)^* + D_2(D_2)^* + D_3(D_3)^* + D_4(D_4)^*.
\end{aligned} \tag{3.18}$$

The plot for the coincidence probability against the time-delay introduced between the arrival of the photons at input ports is shown in Fig.(3.6). This plot shows that the coincidence probability of having the a tri-photon click at output port-1 and a single-photon click at the output port-2 for the case when we inject a bi-photon pulse in the input port-1 and input port-2 of the balanced beam splitter such there is a time-delay τ between the arrival of the each photon is maximum, when there is no time delay τ introduced between the arrival of the input photons and is equal to the value of the permanent of the adjacent scattering matrix. the coincidence probability starts gradually decreasing as the length of the time delay τ increases. Rest of the cases as mentioned in Fig.(3.1) are discussed in Appendix(A.5,...,A.9).

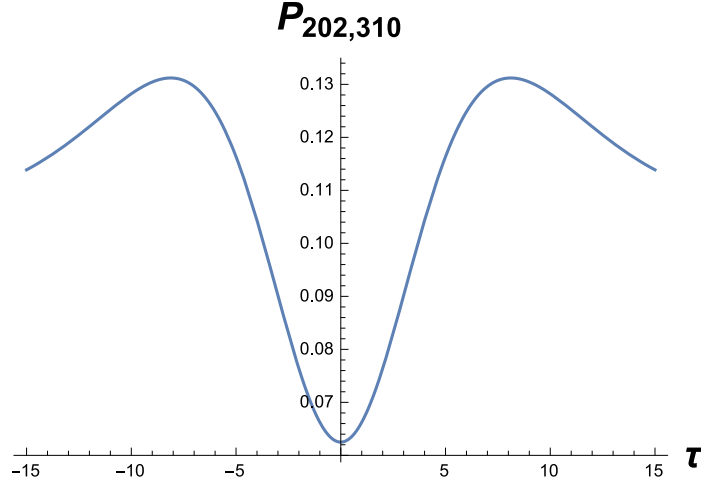


Figure 3.6: (with $T(\tau_1, \tau_2, \tau_3, \tau_4) = T(-\tau, 0, \tau, 2\tau)$, $\sigma_o = 0.1$ and $\Omega(\alpha_1, \alpha_2, \alpha_3, \beta_1, \beta_2, \beta_3, \gamma_1, \gamma_2) = \Omega(0, 0, 0, \pi/2, \pi/2, \pi/2, 0, 0)$)

3.1.4 Tetra-Photon Click on Output-1 and no Click on Output-2 and Output-3

In this section, we shall discuss the coincidence probability of having a tetra-photon click on any of the three output ports, when we inject bi-photon pulses at input port-1 and input port-2 of a balanced beam-splitter. Which can be visualized from Fig.(3.7) First of all, we shall discuss the coincidence probability for the first output

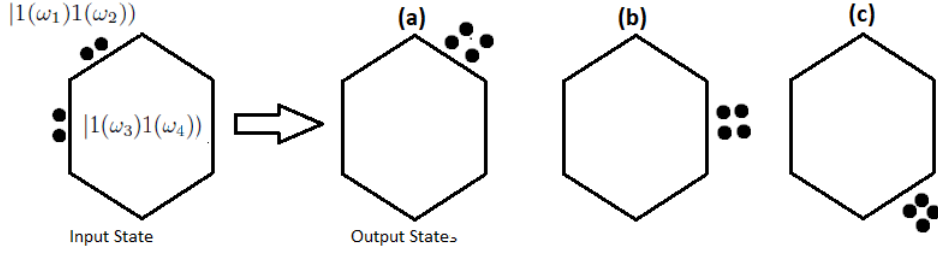


Figure 3.7

in Fig.(3.7), which shows that we get a tetra-photon pulse at output port-1 and no clicks on output port-2 and output port-3. The input state for this case is same as defined in Eq.(3.5) and the output operator for this specific case is define as,

$$\Pi_1 = \int_{-\infty}^{\infty} \hat{a}_1^\dagger(\omega_5) \hat{a}_1^\dagger(\omega_8) \hat{a}_1^\dagger(\omega_{11}) \hat{a}_1^\dagger(\omega_{14}) |0000\rangle \langle 0000| \hat{a}_1(\omega_5) \hat{a}_1(\omega_8) \hat{a}_1(\omega_{11}) \hat{a}_1(\omega_{14}) d\omega_5 d\omega_8 d\omega_{11} d\omega_{14}, \quad (3.19)$$

the coincidence probability for this case can be written as,

$$P_{220,400} = {}^s \langle 1111 | U^\dagger \Pi_1 U | 1111 \rangle^s, \quad (3.20)$$

and the probability coefficient for this case are defined as,

$$V_1 = U_{11}^2 U_{12}^2; , \quad (3.21)$$

so, coincidence probability for this case is

$$P_{220,400} = V_1 (V_1)^*. \quad (3.22)$$

We can clearly see. the coincidence probability for this specific case does not depend on the time delay introduced between the arrival of the photons at input ports of a balanced beam splitter. Rest of the cases as mentioned in Fig.(3.1) are discussed in Appendix(A.10,A.11).

3.2 Bi-Photon Input pulses at Input-1 and Input-3

In this section, we shall discuss the coincidence probabilities for all possible output coincidence patterns for the case, where we have injected a bi-photon pulses in input port-1 and in input port-3 but the input port-2 remains in dark. After

calculating these coincidence probabilities, we shall plot them against the time-delays introduced between the arrivals of these input photons at input ports and shall see how these coincidence probabilities varies with the increase and decrease in lengths of the time-delays " τ " introduced between the arrival of the photons at input ports.

3.2.1 Bi-Photon Click on Output-1 and Output-2 and no Click on Output-3

In this case, we shall discuss the coincidence probability for one of the possible output coincidence pattern such that we have a bi-photon click at output port-1 and at output port-2. For this kind of the output we have taken the same input pattern in which, we have injected a bi-photon pulse in input port-1 and in input port-3 as shown in Fig.(3.8). The output operators for this specific case are the same as defined in Eq.(3.2) and Eq.(3.3) and the input state is defined as

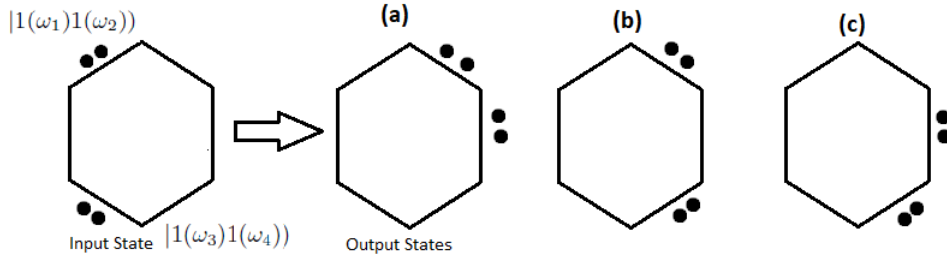


Figure 3.8

$$\begin{aligned}
 |1111\rangle^s = & \int_{-\infty}^{\infty} \phi(\omega_1)\phi(\omega_2)\phi(\omega_3)\phi(\omega_4) \exp(-i\omega_1\tau_1) \exp(-i\omega_2\tau_2) \exp(-i\omega_3\tau_3) \\
 & \exp(-i\omega_4\tau_4) \hat{a}_1^\dagger(\omega_1)\hat{a}_1^\dagger(\omega_2)\hat{a}_3^\dagger(\omega_3)\hat{a}_3^\dagger(\omega_4) |0000\rangle d\omega_1 d\omega_2 d\omega_3 d\omega_4,
 \end{aligned} \tag{3.23}$$

the coincidence probability for this case is defined as

$$P_{202,220} = {}^s \langle 1111 | U^\dagger \Pi_1 \otimes \Pi_2 U | 1111 \rangle^s, \tag{3.24}$$

the probability coefficients defined for the cases where we get bi-photon pulses at output ports are defined as

$$\begin{aligned}
 B_1 = U_{11}^2 U_{23}^2; \quad B_2 = U_{11} U_{21} U_{13} U_{23}; \quad B_3 = U_{11} U_{21} U_{23} U_{13}; \quad B_4 = U_{21} U_{11} U_{13} U_{23}; \\
 B_5 = U_{21} U_{11} U_{23} U_{13}; \quad B_6 = U_{21}^2 U_{13}^2; \quad B_7 = U_{11}^2 U_{33}^2; \quad B_8 = U_{11} U_{31} U_{13} U_{33};
 \end{aligned}$$

$$\begin{aligned}
B_9 &= U_{11}U_{31}U_{33}U_{13}; & B_{10} &= U_{31}U_{11}U_{13}U_{33}; & B_{11} &= U_{31}U_{11}U_{33}U_{13}; & B_{12} &= U_{31}^2U_{13}^2; \\
B_{13} &= U_{21}^2U_{33}^2; & B_{14} &= U_{21}U_{31}U_{23}U_{33}; & B_{15} &= U_{21}U_{31}U_{33}U_{23}; & B_{16} &= U_{31}U_{21}U_{23}U_{33}; \\
B_{17} &= U_{31}U_{21}U_{33}U_{23}; & B_{18} &= U_{31}^2U_{23}^2;
\end{aligned} \tag{3.25}$$

so,

$$\begin{aligned}
P_{202,220} &= B_1(B_2)^*e^{-\sigma^2\tau^2} + B_1(B_3)^*e^{-3\sigma^2\tau^2} + B_1(B_4)^*e^{-3\sigma^2\tau^2} + B_1(B_5)^*e^{-5\sigma^2\tau^2} + \\
& B_1(B_6)^*e^{-8\sigma^2\tau^2} + B_2(B_1)^*e^{-\sigma^2\tau^2} + B_2(B_3)^*e^{-\sigma^2\tau^2} + B_2(B_4)^*e^{-\sigma^2\tau^2} + \\
& B_2(B_5)^*e^{-2\sigma^2\tau^2} + B_2(B_6)^*e^{-5\sigma^2\tau^2} + B_3(B_1)^*e^{-3\sigma^2\tau^2} + B_3(B_2)^*e^{-\sigma^2\tau^2} + \\
& B_3(B_4)^*e^{-2\sigma^2\tau^2} + B_3(B_5)^*e^{-\sigma^2\tau^2} + B_3(B_6)^*e^{-3\sigma^2\tau^2} + B_4(B_1)^*e^{-3\sigma^2\tau^2} + \\
& B_4(B_2)^*e^{-\sigma^2\tau^2} + B_4(B_3)^*e^{-2\sigma^2\tau^2} + B_4(B_5)^*e^{-\sigma^2\tau^2} + B_4(B_6)^*e^{-3\sigma^2\tau^2} + \\
& B_5(B_1)^*e^{-5\sigma^2\tau^2} + B_5(B_2)^*e^{-2\sigma^2\tau^2} + B_5(B_3)^*e^{-\sigma^2\tau^2} + B_5(B_4)^*e^{-\sigma^2\tau^2} + \\
& B_5(B_6)^*e^{-\sigma^2\tau^2} + B_6(B_1)^*e^{-8\sigma^2\tau^2} + B_6(B_2)^*e^{-5\sigma^2\tau^2} + B_6(B_3)^*e^{-3\sigma^2\tau^2} + \\
& B_6(B_4)^*e^{-3\sigma^2\tau^2} + B_6(B_5)^*e^{-\sigma^2\tau^2} + B_1(B_1)^* + B_2(B_2)^* + B_3(B_3)^* + \\
& B_4(B_4)^* + B_5(B_5)^* + B_6(B_6)^*.
\end{aligned} \tag{3.26}$$

The plot of the coincidence probability against the time-delays introduced between the arrivals of the photons at input ports of a balanced beam-splitter is shown in Fig.(3.9). This plot shows that the coincidence probability of getting a bi-photon click at output port-1 and output port-2 is minimum but not zero when there is no time-delay introduced between the arrival of the photons at input ports and is equal to the value of the permanent of the adjacent scattering matrix. The coincidence probability of having this output increases with the increase in length of the time-delay τ between the arrival of the photons at input ports but at specific point it again starts decreasing. Rest of the cases as mentioned in Fig.(3.1) are discussed in Appendix(B.1,B.2).

3.2.2 Bi-Photon Click on Output-1 and Single-Photon Click on Output-2 and Output-3

In this section, we shall discuss one of the possible output coincidence pattern such that each of the output detectors clicks. As we have four incident photons these four photons are distributed over the output ports in such way that one of the output port clicks twice and rest of the two output port click once. Such output can be observed in three different ways which can be visualized from Fig.(3.10). First of all, we discuss the first output state from the left, which shows the output port-1 clicks twice but output port-2 and output port-3 click once. The input state for this case has already been defined in Eq.(3.23) and the output operators are defined as

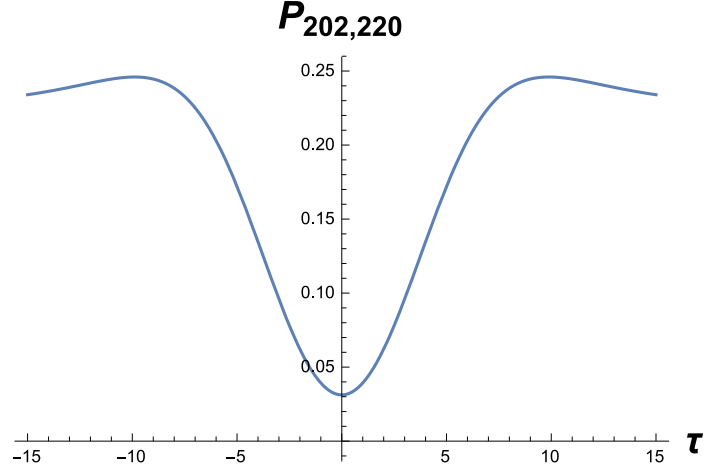


Figure 3.9: (with $T(\tau_1, \tau_2, \tau_3, \tau_4) = T(-\tau, 0, \tau, 2\tau)$, $\sigma_o = 0.1$ and $\Omega(\alpha_1, \alpha_2, \alpha_3, \beta_1, \beta_2, \beta_3, \gamma_1, \gamma_2) = \Omega(0, 0, 0, \pi/2, \pi/2, \pi/2, 0, 0)$)

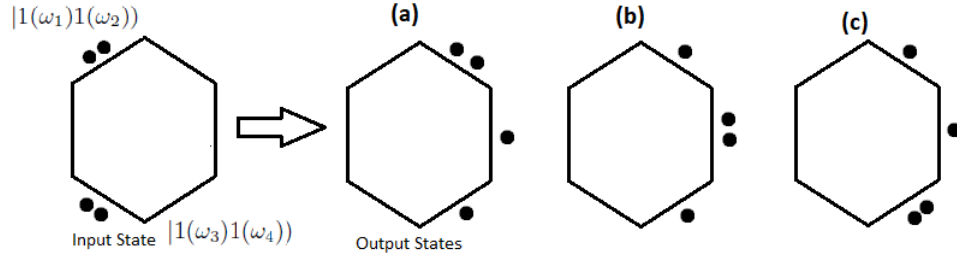


Figure 3.10

$$\Pi_1 = \int_{-\infty}^{\infty} \hat{a}_1^\dagger(\omega_5) \hat{a}_1^\dagger(\omega_8) |00\rangle \langle 00| \hat{a}_1(\omega_5) \hat{a}_1(\omega_8) d\omega_5 d\omega_8, \quad (3.27)$$

$$\Pi_2 = \int_{-\infty}^{\infty} \hat{a}_2^\dagger(\omega_6) |0\rangle \langle 0| \hat{a}_2(\omega_6) d\omega_6, \quad (3.28)$$

and

$$\Pi_3 = \int_{-\infty}^{\infty} \hat{a}_3^\dagger(\omega_7) |0\rangle \langle 0| \hat{a}_3(\omega_7) d\omega_7, \quad (3.29)$$

the coincidence probability for this case is defined as

$$P_{202,211} = \langle 1111 |^s U^\dagger \Pi_1 \otimes \Pi_2 \otimes \Pi_3 U |1111\rangle^s, \quad (3.30)$$

so the coincidence probability for this case is,

$$\begin{aligned}
P_{202,211} = & (O_1) * O_1 + e^{-\sigma^2 \tau^2} (O_2) * O_1 + e^{-\sigma^2 \tau^2} (O_3) * O_1 + e^{-3\sigma^2 \tau^2} (O_4) * O_1 + \\
& e^{-3\sigma^2 \tau^2} (O_5) * O_1 + e^{-4\sigma^2 \tau^2} (O_6) * O_1 + e^{-3\sigma^2 \tau^2} (O_7) * O_1 + e^{-6\sigma^2 \tau^2} (O_8) * O_1 + \\
& e^{-5\sigma^2 \tau^2} (O_9) * O_1 + e^{-7\sigma^2 \tau^2} (O_{10}) * O_1 + e^{-8\sigma^2 \tau^2} (O_{11}) * O_1 + e^{-9\sigma^2 \tau^2} (O_{12}) * O_1 + \\
& e^{-\sigma^2 \tau^2} (O_1) * O_2 + (O_2) * O_2 + e^{-3\sigma^2 \tau^2} (O_3) * O_2 + e^{-\sigma^2 \tau^2} (O_4) * O_2 + \\
& e^{-4\sigma^2 \tau^2} (O_5) * O_2 + e^{-3\sigma^2 \tau^2} (O_6) * O_2 + e^{-6\sigma^2 \tau^2} (O_7) * O_2 + e^{-3\sigma^2 \tau^2} (O_8) * O_2 + \\
& e^{-7\sigma^2 \tau^2} (O_9) * O_2 + e^{-5\sigma^2 \tau^2} (O_{10}) * O_2 + e^{-9\sigma^2 \tau^2} (O_{11}) * O_2 + e^{-8\sigma^2 \tau^2} (O_{12}) * O_2 + \\
& e^{-\sigma^2 \tau^2} (O_1) * O_3 + e^{-3\sigma^2 \tau^2} (O_2) * O_3 + (O_3) * O_3 + e^{-4\sigma^2 \tau^2} (O_4) * O_3 + \\
& e^{-\sigma^2 \tau^2} (O_5) * O_3 + e^{-3\sigma^2 \tau^2} (O_6) * O_3 + e^{-\sigma^2 \tau^2} (O_7) * O_3 + e^{-7\sigma^2 \tau^2} (O_8) * O_3 + \\
& e^{-2\sigma^2 \tau^2} (O_9) * O_3 + e^{-6\sigma^2 \tau^2} (O_{10}) * O_3 + e^{-5\sigma^2 \tau^2} (O_{11}) * O_3 + e^{-7\sigma^2 \tau^2} (O_{12}) * O_3 + \\
& e^{-3\sigma^2 \tau^2} (O_1) * O_4 + e^{-\sigma^2 \tau^2} (O_2) * O_4 + e^{-4\sigma^2 \tau^2} (O_3) * O_4 + (O_4) * O_4 + \\
& e^{-3\sigma^2 \tau^2} (O_5) * O_4 + e^{-\sigma^2 \tau^2} (O_6) * O_4 + e^{-7\sigma^2 \tau^2} (O_7) * O_4 + e^{-\sigma^2 \tau^2} (O_8) * O_4 + \\
& e^{-6\sigma^2 \tau^2} (O_9) * O_4 + e^{-2\sigma^2 \tau^2} (O_{10}) * O_4 + e^{-7\sigma^2 \tau^2} (O_{11}) * O_4 + e^{-5\sigma^2 \tau^2} (O_{12}) * O_4 + \\
& e^{-3\sigma^2 \tau^2} (O_1) * O_5 + e^{-4\sigma^2 \tau^2} (O_2) * O_5 + e^{-\sigma^2 \tau^2} (O_3) * O_5 + e^{-3\sigma^2 \tau^2} (O_4) * O_5 + \\
& (O_5) * O_5 + e^{-\sigma^2 \tau^2} (O_6) * O_5 + e^{-2\sigma^2 \tau^2} (O_7) * O_5 + e^{-5\sigma^2 \tau^2} (O_8) * O_5 + \\
& e^{-\sigma^2 \tau^2} (O_9) * O_5 + e^{-3\sigma^2 \tau^2} (O_{10}) * O_5 + e^{-3\sigma^2 \tau^2} (O_{11}) * O_5 + e^{-4\sigma^2 \tau^2} (O_{12}) * O_5 + \\
& e^{-4\sigma^2 \tau^2} (O_1) * O_6 + e^{-3\sigma^2 \tau^2} (O_2) * O_6 + e^{-3\sigma^2 \tau^2} (O_3) * O_6 + e^{-\sigma^2 \tau^2} (O_4) * O_6 + \\
& e^{-\sigma^2 \tau^2} (O_5) * O_6 + (O_6) * O_6 + e^{-5\sigma^2 \tau^2} (O_7) * O_6 + e^{-2\sigma^2 \tau^2} (O_8) * O_6 + \\
& e^{-3\sigma^2 \tau^2} (O_9) * O_6 + e^{-\sigma^2 \tau^2} (O_{10}) * O_6 + e^{-4\sigma^2 \tau^2} (O_{11}) * O_6 + e^{-3\sigma^2 \tau^2} (O_{12}) * O_6 + \\
& e^{-3\sigma^2 \tau^2} (O_1) * O_7 + e^{-6\sigma^2 \tau^2} (O_2) * O_7 + e^{-\sigma^2 \tau^2} (O_3) * O_7 + e^{-7\sigma^2 \tau^2} (O_4) * O_7 + \\
& e^{-2\sigma^2 \tau^2} (O_5) * O_7 + e^{-5\sigma^2 \tau^2} (O_6) * O_7 + (O_7) * O_7 + e^{-9\sigma^2 \tau^2} (O_8) * O_7 + \\
& e^{-\sigma^2 \tau^2} (O_9) * O_7 + e^{-7\sigma^2 \tau^2} (O_{10}) * O_7 + e^{-3\sigma^2 \tau^2} (O_{11}) * O_7 + e^{-6\sigma^2 \tau^2} (O_{12}) * O_7 + \\
& e^{-6\sigma^2 \tau^2} (O_1) * O_8 + e^{-3\sigma^2 \tau^2} (O_2) * O_8 + e^{-7\sigma^2 \tau^2} (O_3) * O_8 + e^{-\sigma^2 \tau^2} (O_4) * O_8 + \\
& e^{-5\sigma^2 \tau^2} (O_5) * O_8 + e^{-2\sigma^2 \tau^2} (O_6) * O_8 + e^{-9\sigma^2 \tau^2} (O_7) * O_8 + (O_8) * O_8 + \\
& e^{-7\sigma^2 \tau^2} (O_9) * O_8 + e^{-\sigma^2 \tau^2} (O_{10}) * O_8 + e^{-6\sigma^2 \tau^2} (O_{11}) * O_8 + e^{-3\sigma^2 \tau^2} (O_{12}) * O_8 + \\
& e^{-5\sigma^2 \tau^2} (O_1) * O_9 + e^{-7\sigma^2 \tau^2} (O_2) * O_9 + e^{-2\sigma^2 \tau^2} (O_3) * O_9 + e^{-6\sigma^2 \tau^2} (O_4) * O_9 + \\
& e^{-\sigma^2 \tau^2} (O_5) * O_9 + e^{-3\sigma^2 \tau^2} (O_6) * O_9 + e^{-\sigma^2 \tau^2} (O_7) * O_9 + e^{-7\sigma^2 \tau^2} (O_8) * O_9 + \\
& (O_9) * O_9 + e^{-4\sigma^2 \tau^2} (O_{10}) * O_9 + e^{-\sigma^2 \tau^2} (O_{11}) * O_9 + e^{-3\sigma^2 \tau^2} (O_{12}) * O_9 + \\
& e^{-7\sigma^2 \tau^2} (O_1) * O_{10} + e^{-5\sigma^2 \tau^2} (O_2) * O_{10} + e^{-6\sigma^2 \tau^2} (O_3) * O_{10} + e^{-2\sigma^2 \tau^2} (O_4) * O_{10} + \\
& e^{-3\sigma^2 \tau^2} (O_5) * O_{10} + e^{-\sigma^2 \tau^2} (O_6) * O_{10} + e^{-7\sigma^2 \tau^2} (O_7) * O_{10} + e^{-\sigma^2 \tau^2} (O_8) * O_{10} +
\end{aligned}$$

$$\begin{aligned}
 & e^{-4\sigma^2\tau^2} (O_9) * O_{10} + (O_{10}) * O_{10} + e^{-3\sigma^2\tau^2} (O_{11}) * O_{10} + e^{-\sigma^2\tau^2} (O_{12}) * O_{10} + \\
 & e^{-8\sigma^2\tau^2} (O_1) * O_{11} + e^{-9\sigma^2\tau^2} (O_2) * O_{11} + e^{-5\sigma^2\tau^2} (O_3) * O_{11} + e^{-7\sigma^2\tau^2} (O_4) * O_{11} + \\
 & e^{-3\sigma^2\tau^2} (O_5) * O_{11} + e^{-4\sigma^2\tau^2} (O_6) * O_{11} + e^{-3\sigma^2\tau^2} (O_7) * O_{11} + e^{-6\sigma^2\tau^2} (O_8) * O_{11} + \\
 & e^{-\sigma^2\tau^2} (O_9) * O_{11} + e^{-3\sigma^2\tau^2} (O_{10}) * O_{11} + (O_{11}) * O_{11} + e^{-\sigma^2\tau^2} (O_{12}) * O_{11} + \\
 & e^{-9\sigma^2\tau^2} (O_1) * O_{12} + e^{-8\sigma^2\tau^2} (O_2) * O_{12} + e^{-7\sigma^2\tau^2} (O_3) * O_{12} + e^{-5\sigma^2\tau^2} (O_4) * O_{12} + \\
 & e^{-4\sigma^2\tau^2} (O_5) * O_{12} + e^{-3\sigma^2\tau^2} (O_6) * O_{12} + e^{-6\sigma^2\tau^2} (O_7) * O_{12} + e^{-3\sigma^2\tau^2} (O_8) * O_{12} + \\
 & e^{-3\sigma^2\tau^2} (O_9) * O_{12} + e^{-\sigma^2\tau^2} (O_{10}) * O_{12} + e^{-\sigma^2\tau^2} (O_{11}) * O_{12} + (O_{12}) * O_{12}.
 \end{aligned} \tag{3.31}$$

Where O 's are the probability coefficients and are given as

$$\begin{aligned}
 O_1 &= U_{11}^2 U_{23} U_{33}; & O_2 &= U_{11}^2 U_{23} U_{33}; & O_3 &= U_{11} U_{13} U_{21} U_{33}; & O_4 &= U_{11} U_{13} U_{23} U_{31}; \\
 O_5 &= U_{11} U_{13} U_{21} U_{33}; & O_6 &= U_{11} U_{13} U_{23} U_{31}; & O_7 &= U_{11} U_{13} U_{21} U_{33}; & O_8 &= U_{11} U_{13} U_{23} U_{31}; \\
 O_9 &= U_{11} U_{13} U_{21} U_{33}; & O_{10} &= U_{11} U_{13} U_{23} U_{31}; & O_{11} &= U_{13}^2 U_{21} U_{31}; & O_{12} &= U_{13}^2 U_{21} U_{31}; .
 \end{aligned} \tag{3.32}$$

The coincidence probability plot for the case when we have above defined output coincidence pattern against time-delays τ introduced between the arrival photons at input ports is shown in Fig.(3.11). The plot shows that the coincidence probability of having the above defined output coincidence pattern is relatively high and equal to the value of the permanent of the adjacent scattering matrix, when time-delays τ introduced between the arrival of the incident photons is zero. As the length of the time-delays τ introduced between the arrival of the photon at input ports increases we get a slightly increase in the value of the coincidence probability and we get two relative maximas. With further increase in the length of the time-delays we get a sharp decrease in the value of the coincidence probability. Rest of the cases as mentioned in Fig.(3.1) are discussed in Appendix(B.3,B.4).

3.2.3 Tri-Photon Click on Output-1, Single-Photon Click on Output-2 and no click on Output-3

In this section, we shall discuss the coincidence probability for the case when we get a tri-photon click at one output port and a single photon click one the other output port simultaneously for the incidence of bi-photon pulse at input port-1 and input port-3 with time-delay τ introduced between arrival of the photons at input ports. The input state has already been defined in Eq.(3.23). This kind of input and output pattern can be visualized from Fig.(3.12). For this specific case, we shall discuss the coincidence probability of first output coincidence pattern as shown in Fig.(3.12), in which we have a tri-photon click at output port-1 and a

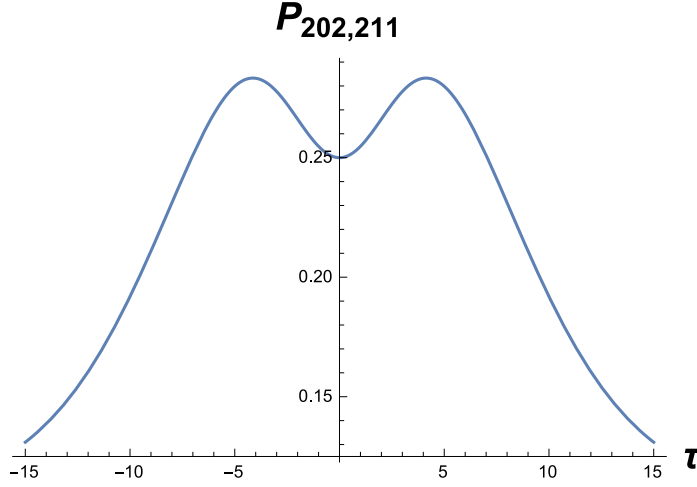


Figure 3.11: (with $T(\tau_1, \tau_2, \tau_3, \tau_4) = T(-\tau, 0, \tau, 2\tau)$, $\sigma_o = 0.1$ and $\Omega(\alpha_1, \alpha_2, \alpha_3, \beta_1, \beta_2, \beta_3, \gamma_1, \gamma_2) = \Omega(0, 0, 0, \pi/2, \pi/2, \pi/2, 0, 0)$)

single-photon click at output port-2. The output operators for this case are defined as

$$\Pi_1 = \int_{-\infty}^{\infty} \hat{a}_1^\dagger(\omega_5) \hat{a}_1^\dagger(\omega_8) \hat{a}_1^\dagger(\omega_{11}) |000\rangle \langle 000| \hat{a}_1(\omega_5) \hat{a}_1(\omega_8) \hat{a}_1(\omega_{11}) d\omega_5 d\omega_8 d\omega_{11}, \quad (3.33)$$

and

$$\Pi_2 = \int_{-\infty}^{\infty} \hat{a}_2^\dagger(\omega_6) |0\rangle \langle 0| \hat{a}_2^\dagger(\omega_6) d\omega_6, \quad (3.34)$$

the coincidence probability for this case can be written as

$$P_{202,310} = {}^s \langle 1111 | U^\dagger \Pi_1 \otimes \Pi_2 U | 1111 \rangle^s, \quad (3.35)$$

so the coincidence probability is

$$\begin{aligned} P_{202,310} = & F_9 (F_{10})^* e^{-\sigma^2 \tau^2} + F_9 (F_{11})^* e^{-3\sigma^2 \tau^2} + F_9 (F_{12})^* e^{-6\sigma^2 \tau^2} + \\ & F_{10} (F_9)^* e^{-\sigma^2 \tau^2} + F_{10} (F_{11})^* e^{-\sigma^2 \tau^2} + F_{10} (F_{12})^* e^{-3\sigma^2 \tau^2} + \\ & F_{11} (F_9)^* e^{-3\sigma^2 \tau^2} + F_{11} (F_{10})^* e^{-\sigma^2 \tau^2} + F_{11} (F_{12})^* e^{-\sigma^2 \tau^2} + \\ & F_{12} (F_9)^* e^{-6\sigma^2 \tau^2} + F_{12} (F_{10})^* e^{-3\sigma^2 \tau^2} + F_{12} (F_{11})^* e^{-\sigma^2 \tau^2} + \\ & F_9 (F_9)^* + F_{10} (F_{10})^* + F_{11} (F_{11})^* + F_{12} (F_{12})^* \end{aligned} \quad (3.36)$$

Where F's are the probability coefficients and are given as

$$F_1 = U_{11}^2 U_{13} U_{33}; \quad F_2 = U_{11}^2 U_{13} U_{33}; \quad F_3 = U_{11} U_{13}^2 U_{31}; \quad F_4 = U_{11} U_{13}^2 U_{31};$$

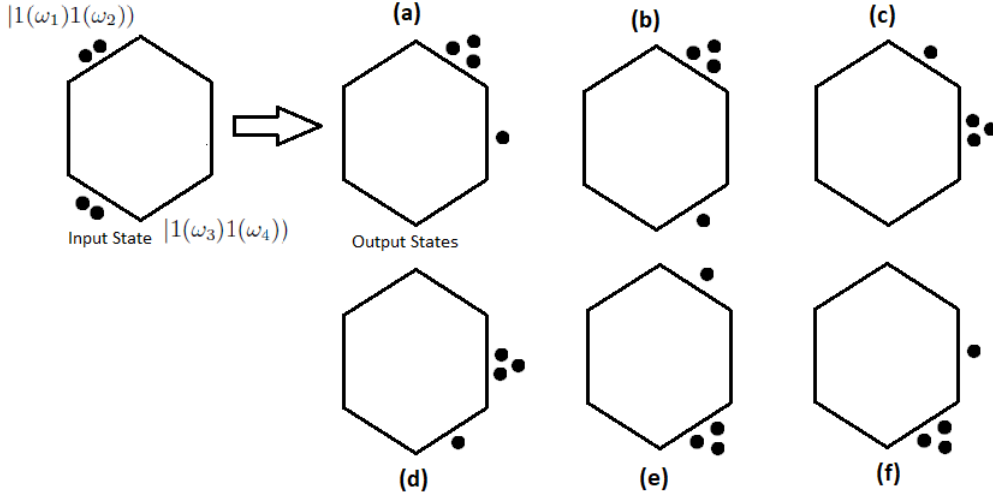


Figure 3.12

$$\begin{aligned}
 F_5 &= U_{11}U_{31}U_{33}^2; & F_6 &= U_{11}U_{31}U_{33}^2; & F_7 &= U_{13}U_{31}^2U_{33}; & F_8 &= U_{13}U_{31}^2U_{33}; \\
 F_9 &= U_{11}^2U_{13}U_{23}; & F_{10} &= U_{11}^2U_{13}U_{23}; & F_{11} &= U_{11}U_{13}^2U_{21}; & F_{12} &= U_{11}U_{13}^2U_{21}; \\
 F_{13} &= U_{11}U_{21}U_{23}^2; & F_{14} &= U_{11}U_{21}U_{23}^2; & F_{15} &= U_{13}U_{21}^2U_{23}; & F_{16} &= U_{13}U_{21}^2U_{23}; \\
 F_{17} &= U_{21}^2U_{23}U_{33}; & F_{18} &= U_{21}^2U_{23}U_{33}; & F_{19} &= U_{21}U_{23}^2U_{31}; & F_{20} &= U_{21}U_{23}^2U_{31}; \\
 F_{21} &= U_{21}U_{31}U_{33}^2; & F_{22} &= U_{21}U_{31}U_{33}^2; & F_{23} &= U_{23}U_{31}^2U_{33}; & F_{24} &= U_{23}U_{31}^2U_{33};
 \end{aligned}
 \tag{3.37}$$

The coincidence probability plot against the time-delays introduced between the arrival of the photons at input ports of the balanced beam-splitter is shown in Fig.(3.13). This Coincidence probability plot shows that the probability of having the above defined output coincidence pattern is minimum and is equal to the value of the permanent of the adjacent scattering matrix, when there is no time-delays introduced between the arrival of the photon at the input ports. This Coincidence probability increases with the increase in the length of the time-delays introduced between the arrival of the photons till specific point and then again starts decreasing. Rest of the cases as mentioned in Fig.(3.1) are discussed in Appendix(B.5,...,B.9).

3.2.4 Tetra-Photon Click on Output-1 and no Click on Output-2 and Output-3

In this section, we shall discuss the coincidence probability of having a tetra-photon click on any of the three output ports when we inject bi-photon pulses at input port-1 and at input port-3 of a balanced beam-splitter. Which can be visualized

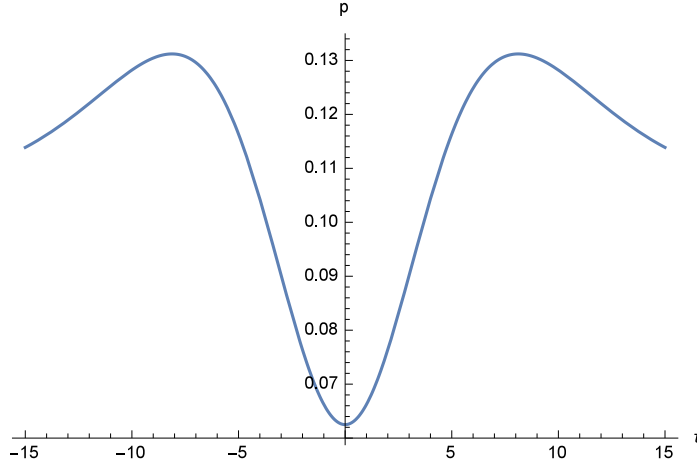


Figure 3.13: (with $T(\tau_1, \tau_2, \tau_3, \tau_4) = T(-\tau, 0, \tau, 2\tau)$, $\sigma_o = 0.1$ and $\Omega(\alpha_1, \alpha_2, \alpha_3, \beta_1, \beta_2, \beta_3, \gamma_1, \gamma_2) = \Omega(0, 0, 0, \pi/2, \pi/2, \pi/2, 0, 0)$)

from Fig.(3.14) First of all, we shall discuss the coincidence probability for the first

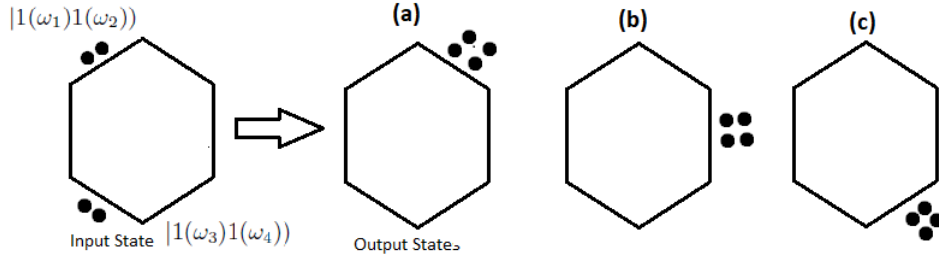


Figure 3.14

output coincidence pattern in Fig.(3.14) which shows that we get a tetra-photon click at output port-1 and no clicks on output port-2 and output port-3. The input state for this case is same as defined in Eq.(3.23) and the output operator is define as,

$$\Pi_1 = \int_{-\infty}^{\infty} \hat{a}_1^\dagger(\omega_5) \hat{a}_1^\dagger(\omega_8) \hat{a}_1^\dagger(\omega_{11}) \hat{a}_1^\dagger(\omega_{14}) |0000\rangle \langle 0000| \hat{a}_1(\omega_5) \hat{a}_1(\omega_8) \hat{a}_1(\omega_{11}) \hat{a}_1(\omega_{14}) d\omega_5 d\omega_8 d\omega_{11} d\omega_{14}, \quad (3.38)$$

the coincidence probability for this case can be written as,

$$P_{202,400} = {}^s \langle 1111 | U^\dagger \Pi_1 U | 1111 \rangle^s, \quad (3.39)$$

the probability coefficient for this case are defined as,

$$V_4 = U_{11}^2 U_{13}^2 \quad (3.40)$$

so,

$$P_{202,400} = V_4 (V_4)^*. \quad (3.41)$$

One can clearly see from this relation, the coincidence probability for this case does not depend of the time-delays τ introduced between the arrival of the photons at input ports of the balanced beam-splitter. Rest of the cases as mentioned in Fig.(3.1) are discussed in Appendix(B.10,B.11).

3.3 Bi-Photon Input pulses at Input-2 and Input-3

In this section, we shall discuss the possible output coincidence patterns for the case, where we inject a bi-photon pulses in input port-2 and input port-3 but the input port-1 remains in dark and shall calculate the coincidence probabilities for these possible output coincidence patterns. After calculating these coincidence probabilities, we shall plot them against the time-delays τ introduced between the arrivals of these input photons at input ports and shall see how these coincidence probabilities varies with the increase and decrease in the length of the time-delays " τ " introduced between the arrival of the photons at input ports.

3.3.0.1 Bi-Photon Click on Output-1 and Output-2 and no Click on Output-3

In this case, we shall discuss one of the possible output coincidence pattern, in which we get a bi-photon click at output port-1 and output port-2 for the case where we have injected a bi-photon pulse in input port-2 and port-3 as shown in Fig.(3.15). The output operators for this specific case are the same as defined in Eq.(3.2) and Eq.(3.3) and the input state is defined as

$$\begin{aligned} |1111\rangle^s = & \int_{-\infty}^{\infty} \phi(\omega_1)\phi(\omega_2)\phi(\omega_3)\phi(\omega_4) \exp(-i\omega_1\tau_1) \exp(-i\omega_2\tau_2) \exp(-i\omega_3\tau_3) \\ & \exp(-i\omega_4\tau_4) \hat{a}_2^\dagger(\omega_1) \hat{a}_2^\dagger(\omega_2) \hat{a}_3^\dagger(\omega_3) \hat{a}_3^\dagger(\omega_4) |0000\rangle d\omega_1 d\omega_2 d\omega_3 d\omega_4, \end{aligned} \quad (3.42)$$

the coincidence probability for this case is defined as

$$P_{022,220} = {}^s \langle 1111 | U^\dagger \Pi_1 \otimes \Pi_2 U | 1111 \rangle^s, \quad (3.43)$$

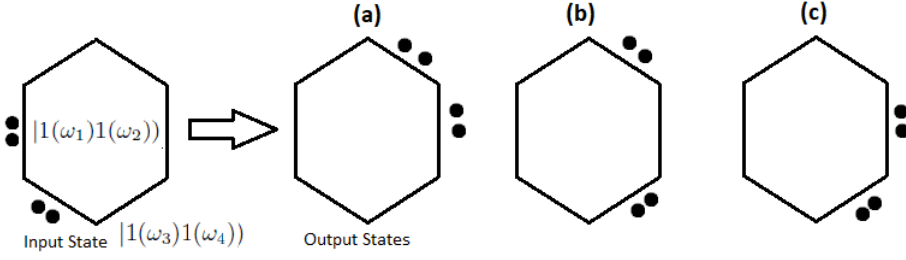


Figure 3.15

the probability coefficients defined for the cases where we get bi-photon pulses at output ports are defined as

$$\begin{aligned}
C_1 &= U_{12}^2 U_{23}^2; & C_2 &= U_{12} U_{22} U_{13} U_{23}; & C_3 &= U_{12} U_{22} U_{23} U_{13}; & C_4 &= U_{22} U_{12} U_{13} U_{23}; \\
C_5 &= U_{22} U_{12} U_{23} U_{13}; & C_6 &= U_{22}^2 U_{13}^2; & C_7 &= U_{12}^2 U_{33}^2; & C_8 &= U_{12} U_{32} U_{13} U_{33}; \\
C_9 &= U_{12} U_{32} U_{33} U_{13}; & C_{10} &= U_{32} U_{12} U_{13} U_{33}; & C_{11} &= U_{32} U_{12} U_{33} U_{13}; & C_{12} &= U_{32}^2 U_{13}^2; \\
C_{13} &= U_{22}^2 U_{33}^2; & C_{14} &= U_{22} U_{32} U_{23} U_{33}; & C_{15} &= U_{22} U_{32} U_{33} U_{23}; & C_{16} &= U_{32} U_{22} U_{23} U_{33}; \\
C_{17} &= U_{32} U_{22} U_{33} U_{23}; & C_{18} &= U_{32}^2 U_{23}^2;
\end{aligned} \tag{3.44}$$

so the coincidence probability is

$$\begin{aligned}
P_{022,220} &= C_1 (C_2)^* e^{-\sigma^2 \tau^2} + C_1 (C_3)^* e^{-3\sigma^2 \tau^2} + C_1 (C_4)^* e^{-3\sigma^2 \tau^2} + C_1 (C_5)^* e^{-5\sigma^2 \tau^2} + \\
& C_1 (C_6)^* e^{-8\sigma^2 \tau^2} + C_2 (C_1)^* e^{-\sigma^2 \tau^2} + C_2 (C_3)^* e^{-\sigma^2 \tau^2} + C_2 (C_4)^* e^{-\sigma^2 \tau^2} + \\
& C_2 (C_5)^* e^{-2\sigma^2 \tau^2} + C_2 (C_6)^* e^{-5\sigma^2 \tau^2} + C_3 (C_1)^* e^{-3\sigma^2 \tau^2} + C_3 (C_2)^* e^{-\sigma^2 \tau^2} + \\
& C_3 (C_4)^* e^{-2\sigma^2 \tau^2} + C_3 (C_5)^* e^{-\sigma^2 \tau^2} + C_3 (C_6)^* e^{-3\sigma^2 \tau^2} + C_4 (C_1)^* e^{-3\sigma^2 \tau^2} + \\
& C_4 (C_2)^* e^{-\sigma^2 \tau^2} + C_4 (C_3)^* e^{-2\sigma^2 \tau^2} + C_4 (C_5)^* e^{-\sigma^2 \tau^2} + C_4 (C_6)^* e^{-3\sigma^2 \tau^2} + \\
& C_5 (C_1)^* e^{-5\sigma^2 \tau^2} + C_5 (C_2)^* e^{-2\sigma^2 \tau^2} + C_5 (C_3)^* e^{-\sigma^2 \tau^2} + C_5 (C_4)^* e^{-\sigma^2 \tau^2} + \\
& C_5 (C_6)^* e^{-\sigma^2 \tau^2} + C_6 (C_1)^* e^{-8\sigma^2 \tau^2} + C_6 (C_2)^* e^{-5\sigma^2 \tau^2} + C_6 (C_3)^* e^{-3\sigma^2 \tau^2} + \\
& C_6 (C_4)^* e^{-3\sigma^2 \tau^2} + C_6 (C_5)^* e^{-\sigma^2 \tau^2} + C_1 (C_1)^* + C_2 (C_2)^* + C_3 (C_3)^* + \\
& C_4 (C_4)^* + C_5 (C_5)^* + C_6 (C_6)^*.
\end{aligned} \tag{3.45}$$

The plot of the coincidence probability against the time-delays τ introduced between the arrivals of the photons at input ports of a balanced beam-splitter is shown in Fig.(3.16). This plot shows that the coincidence probability of getting a bi-photon click at output port-1 and output port-2 is minimum and is equal to the value of the permanent of the adjacent scattering matrix but not zero when there is no time-delay introduced between the arrival of the photons at input ports. The

coincidence probability of having this desired output increases with the increase in length of the time-delay τ but at specific point it gradually becomes constant. Rest of the cases as mentioned in Fig.(3.1) are discussed in Appendix(C.1,C.2).

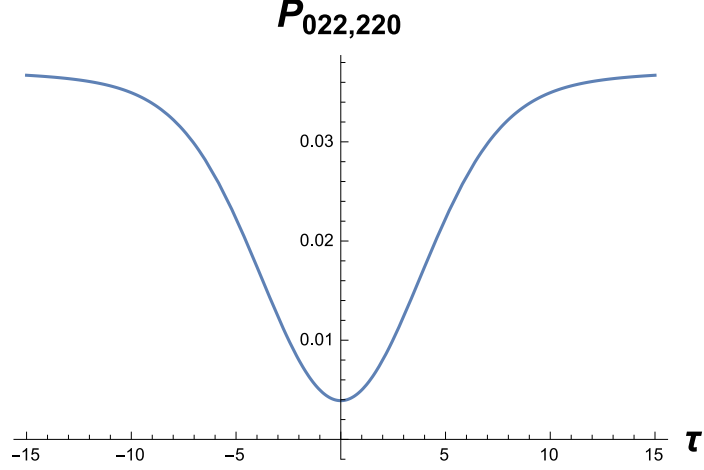


Figure 3.16: (with $T(\tau_1, \tau_2, \tau_3, \tau_4) = T(-\tau, 0, \tau, 2\tau)$, $\sigma_o = 0.1$ and $\Omega(\alpha_1, \alpha_2, \alpha_3, \beta_1, \beta_2, \beta_3, \gamma_1, \gamma_2) = \Omega(0, 0, 0, \pi/2, \pi/2, \pi/2, 0, 0)$)

3.3.1 Bi-Photon Click on Output-1 and Single-Photon Click on Output-2 and Output-3

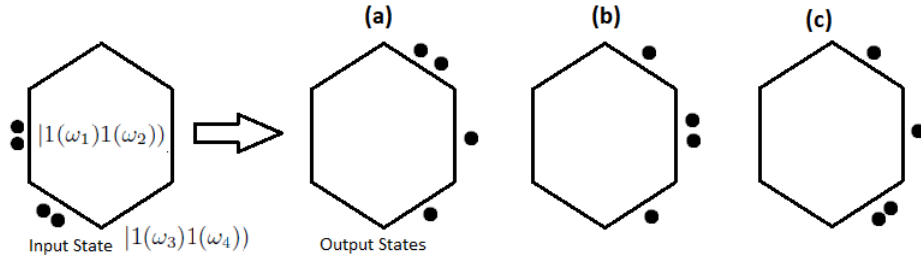


Figure 3.17

In this section, we shall discuss the case where we get a bi-photon click at one output port and single-photon clicks at other output ports. Four photons can be distributed in this pattern in three ways which can be visualized from Fig.(3.17). First of all, we shall discuss the first output coincidence pattern from the left in

Fig.(??), which shows the output port-1 clicks twice and port-2 and port-3 click once. The input state for this case is already been defined in Eq.(3.42) and the output operators are defined as

$$\Pi_1 = \int_{-\infty}^{\infty} \hat{a}_1^\dagger(\omega_5) \hat{a}_1^\dagger(\omega_8) |00\rangle \langle 00| \hat{a}_1(\omega_5) \hat{a}_1(\omega_8) d\omega_5 d\omega_8, \quad (3.46)$$

$$\Pi_2 = \int_{-\infty}^{\infty} \hat{a}_2^\dagger(\omega_6) |0\rangle \langle 0| \hat{a}_2(\omega_6) d\omega_6, \quad (3.47)$$

and

$$\Pi_3 = \int_{-\infty}^{\infty} \hat{a}_3^\dagger(\omega_7) |0\rangle \langle 0| \hat{a}_3(\omega_7) d\omega_7, \quad (3.48)$$

the coincidence probability for this case is defined as

$$P_{022,211} = \langle 1111|^s U^\dagger \Pi_1 \otimes \Pi_2 \otimes \Pi_3 U |1111\rangle^s, \quad (3.49)$$

so the coincidence probability for this case is,

$$\begin{aligned} P_{022,211} = & (R_1)^* R_1 + e^{-\sigma^2 \tau^2} (R_2)^* R_1 + e^{-\sigma^2 \tau^2} (R_3)^* R_1 + e^{-3\sigma^2 \tau^2} (R_4)^* R_1 + \\ & e^{-3\sigma^2 \tau^2} (R_5)^* R_1 + e^{-4\sigma^2 \tau^2} (R_6)^* R_1 + e^{-3\sigma^2 \tau^2} (R_7)^* R_1 + e^{-6\sigma^2 \tau^2} (R_8)^* R_1 + \\ & e^{-5\sigma^2 \tau^2} (R_9)^* R_1 + e^{-7\sigma^2 \tau^2} (R_{10})^* R_1 + e^{-8\sigma^2 \tau^2} (R_{11})^* R_1 + e^{-9\sigma^2 \tau^2} (R_{12})^* R_1 + \\ & e^{-\sigma^2 \tau^2} (R_1)^* R_2 + (R_2)^* R_2 + e^{-3\sigma^2 \tau^2} (R_3)^* R_2 + e^{-\sigma^2 \tau^2} (R_4)^* R_2 + \\ & e^{-4\sigma^2 \tau^2} (R_5)^* R_2 + e^{-3\sigma^2 \tau^2} (R_6)^* R_2 + e^{-6\sigma^2 \tau^2} (R_7)^* R_2 + e^{-3\sigma^2 \tau^2} (R_8)^* R_2 + \\ & e^{-7\sigma^2 \tau^2} (R_9)^* R_2 + e^{-5\sigma^2 \tau^2} (R_{10})^* R_2 + e^{-9\sigma^2 \tau^2} (R_{11})^* R_2 + e^{-8\sigma^2 \tau^2} (R_{12})^* R_2 + \\ & e^{-\sigma^2 \tau^2} (R_1)^* R_3 + e^{-3\sigma^2 \tau^2} (R_2)^* R_3 + (R_3)^* R_3 + e^{-4\sigma^2 \tau^2} (R_4)^* R_3 + \\ & e^{-\sigma^2 \tau^2} (R_5)^* R_3 + e^{-3\sigma^2 \tau^2} (R_6)^* R_3 + e^{-\sigma^2 \tau^2} (R_7)^* R_3 + e^{-7\sigma^2 \tau^2} (R_8)^* R_3 + \\ & e^{-2\sigma^2 \tau^2} (R_9)^* R_3 + e^{-6\sigma^2 \tau^2} (R_{10})^* R_3 + e^{-5\sigma^2 \tau^2} (R_{11})^* R_3 + e^{-7\sigma^2 \tau^2} (R_{12})^* R_3 + \\ & e^{-3\sigma^2 \tau^2} (R_1)^* R_4 + e^{-\sigma^2 \tau^2} (R_2)^* R_4 + e^{-4\sigma^2 \tau^2} (R_3)^* R_4 + (R_4)^* R_4 + \\ & e^{-3\sigma^2 \tau^2} (R_5)^* R_4 + e^{-\sigma^2 \tau^2} (R_6)^* R_4 + e^{-7\sigma^2 \tau^2} (R_7)^* R_4 + e^{-\sigma^2 \tau^2} (R_8)^* R_4 + \\ & e^{-6\sigma^2 \tau^2} (R_9)^* R_4 + e^{-2\sigma^2 \tau^2} (R_{10})^* R_4 + e^{-7\sigma^2 \tau^2} (R_{11})^* R_4 + e^{-5\sigma^2 \tau^2} (R_{12})^* R_4 + \\ & e^{-3\sigma^2 \tau^2} (R_1)^* R_5 + e^{-4\sigma^2 \tau^2} (R_2)^* R_5 + e^{-\sigma^2 \tau^2} (R_3)^* R_5 + e^{-3\sigma^2 \tau^2} (R_4)^* R_5 + \\ & (R_5)^* R_5 + e^{-\sigma^2 \tau^2} (R_6)^* R_5 + e^{-2\sigma^2 \tau^2} (R_7)^* R_5 + e^{-5\sigma^2 \tau^2} (R_8)^* R_5 + \\ & e^{-\sigma^2 \tau^2} (R_9)^* R_5 + e^{-3\sigma^2 \tau^2} (R_{10})^* R_5 + e^{-3\sigma^2 \tau^2} (R_{11})^* R_5 + e^{-4\sigma^2 \tau^2} (R_{12})^* R_5 + \\ & e^{-4\sigma^2 \tau^2} (R_1)^* R_6 + e^{-3\sigma^2 \tau^2} (R_2)^* R_6 + e^{-3\sigma^2 \tau^2} (R_3)^* R_6 + e^{-\sigma^2 \tau^2} (R_4)^* R_6 + \\ & e^{-\sigma^2 \tau^2} (R_5)^* R_6 + (R_6)^* R_6 + e^{-5\sigma^2 \tau^2} (R_7)^* R_6 + e^{-2\sigma^2 \tau^2} (R_8)^* R_6 + \end{aligned}$$

56 3. QUANTUM INTERFEROMETRY WITH BI-PHOTON INPUT PULSES

$$\begin{aligned}
 & e^{-3\sigma^2\tau^2} (R_9) * R_6 + e^{-\sigma^2\tau^2} (R_{10}) * R_6 + e^{-4\sigma^2\tau^2} (R_{11}) * R_6 + e^{-3\sigma^2\tau^2} (R_{12}) * R_6 + \\
 & e^{-3\sigma^2\tau^2} (R_1) * R_7 + e^{-6\sigma^2\tau^2} (R_2) * R_7 + e^{-\sigma^2\tau^2} (R_3) * R_7 + e^{-7\sigma^2\tau^2} (R_4) * R_7 + \\
 & e^{-2\sigma^2\tau^2} (R_5) * R_7 + e^{-5\sigma^2\tau^2} (R_6) * R_7 + (R_7) * R_7 + e^{-9\sigma^2\tau^2} (R_8) * R_7 + \\
 & e^{-\sigma^2\tau^2} (R_9) * R_7 + e^{-7\sigma^2\tau^2} (R_{10}) * R_7 + e^{-3\sigma^2\tau^2} (R_{11}) * R_7 + e^{-6\sigma^2\tau^2} (R_{12}) * R_7 + \\
 & e^{-6\sigma^2\tau^2} (R_1) * R_8 + e^{-3\sigma^2\tau^2} (R_2) * R_8 + e^{-7\sigma^2\tau^2} (R_3) * R_8 + e^{-\sigma^2\tau^2} (R_4) * R_8 + \\
 & e^{-5\sigma^2\tau^2} (R_5) * R_8 + e^{-2\sigma^2\tau^2} (R_6) * R_8 + e^{-9\sigma^2\tau^2} (R_7) * R_8 + (R_8) * R_8 + \\
 & e^{-7\sigma^2\tau^2} (R_9) * R_8 + e^{-\sigma^2\tau^2} (R_{10}) * R_8 + e^{-6\sigma^2\tau^2} (R_{11}) * R_8 + e^{-3\sigma^2\tau^2} (R_{12}) * R_8 + \\
 & e^{-5\sigma^2\tau^2} (R_1) * R_9 + e^{-7\sigma^2\tau^2} (R_2) * R_9 + e^{-2\sigma^2\tau^2} (R_3) * R_9 + e^{-6\sigma^2\tau^2} (R_4) * R_9 + \\
 & e^{-\sigma^2\tau^2} (R_5) * R_9 + e^{-3\sigma^2\tau^2} (R_6) * R_9 + e^{-\sigma^2\tau^2} (R_7) * R_9 + e^{-7\sigma^2\tau^2} (R_8) * R_9 + \\
 & (R_9) * R_9 + e^{-4\sigma^2\tau^2} (R_{10}) * R_9 + e^{-\sigma^2\tau^2} (R_{11}) * R_9 + e^{-3\sigma^2\tau^2} (R_{12}) * R_9 + \\
 & e^{-7\sigma^2\tau^2} (R_1) * R_{10} + e^{-5\sigma^2\tau^2} (R_2) * R_{10} + e^{-6\sigma^2\tau^2} (R_3) * R_{10} + e^{-2\sigma^2\tau^2} (R_4) * R_{10} + \\
 & e^{-3\sigma^2\tau^2} (R_5) * R_{10} + e^{-\sigma^2\tau^2} (R_6) * R_{10} + e^{-7\sigma^2\tau^2} (R_7) * R_{10} + e^{-\sigma^2\tau^2} (R_8) * R_{10} + \\
 & e^{-4\sigma^2\tau^2} (R_9) * R_{10} + (R_{10}) * R_{10} + e^{-3\sigma^2\tau^2} (R_{11}) * R_{10} + e^{-\sigma^2\tau^2} (R_{12}) * R_{10} + \\
 & e^{-8\sigma^2\tau^2} (R_1) * R_{11} + e^{-9\sigma^2\tau^2} (R_2) * R_{11} + e^{-5\sigma^2\tau^2} (R_3) * R_{11} + e^{-7\sigma^2\tau^2} (R_4) * R_{11} + \\
 & e^{-3\sigma^2\tau^2} (R_5) * R_{11} + e^{-4\sigma^2\tau^2} (R_6) * R_{11} + e^{-3\sigma^2\tau^2} (R_7) * R_{11} + e^{-6\sigma^2\tau^2} (R_8) * R_{11} + \\
 & e^{-\sigma^2\tau^2} (R_9) * R_{11} + e^{-3\sigma^2\tau^2} (R_{10}) * R_{11} + (R_{11}) * R_{11} + e^{-\sigma^2\tau^2} (R_{12}) * R_{11} + \\
 & e^{-9\sigma^2\tau^2} (R_1) * R_{12} + e^{-8\sigma^2\tau^2} (R_2) * R_{12} + e^{-7\sigma^2\tau^2} (R_3) * R_{12} + e^{-5\sigma^2\tau^2} (R_4) * R_{12} + \\
 & e^{-4\sigma^2\tau^2} (R_5) * R_{12} + e^{-3\sigma^2\tau^2} (R_6) * R_{12} + e^{-6\sigma^2\tau^2} (R_7) * R_{12} + e^{-3\sigma^2\tau^2} (R_8) * R_{12} + \\
 & e^{-3\sigma^2\tau^2} (R_9) * R_{12} + e^{-\sigma^2\tau^2} (R_{10}) * R_{12} + e^{-\sigma^2\tau^2} (R_{11}) * R_{12} + (R_{12}) * R_{12}.
 \end{aligned} \tag{3.50}$$

Where R's are the probability coefficients and are defined as

$$\begin{aligned}
 R_1 &= U_{12}^2 U_{23} U_{33}; & R_2 &= U_{12}^2 U_{23} U_{33}; & R_3 &= U_{12} U_{13} U_{22} U_{33}; & R_4 &= U_{12} U_{13} U_{23} U_{32}; \\
 R_5 &= U_{12} U_{13} U_{22} U_{33}; & R_6 &= U_{12} U_{13} U_{23} U_{32}; & R_7 &= U_{12} U_{13} U_{22} U_{33}; & R_8 &= U_{12} U_{13} U_{23} U_{32}; \\
 R_9 &= U_{12} U_{13} U_{22} U_{33}; & R_{10} &= U_{12} U_{13} U_{23} U_{32}; & R_{11} &= U_{13}^2 U_{22} U_{32}; & R_{12} &= U_{13}^2 U_{22} U_{32};
 \end{aligned} \tag{3.51}$$

The plot of coincidence probability against time-delays τ introduced between the incident photons at input ports of a balanced beam-splitter is shown in Fig.(3.18). The plot shows the coincidence probability of having the above-mentioned output coincidence pattern is maximum and is equal to the value of the permanent of the adjacent scattering matrix when time-delays τ introduced between the arrival of the incident photons is zero. The coincidence probability decreases with the increase in the length of the time-delays introduced between the arrival of the

photons at input ports of the balanced beam-splitter and eventually becomes zero at a specific value of the time-delay. Rest of the cases as mentioned in Fig.(3.1) are discussed in Appendix(C.3,C.4).

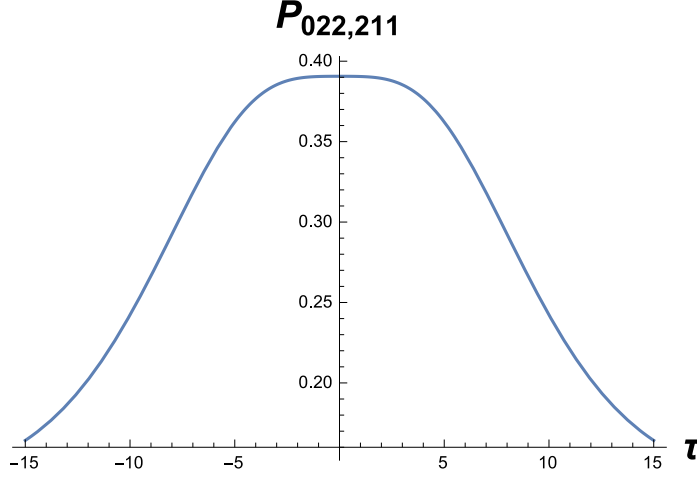


Figure 3.18: (with $T(\tau_1, \tau_2, \tau_3, \tau_4) = T(-\tau, 0, \tau, 2\tau)$, $\sigma_o = 0.1$ and $\Omega(\alpha_1, \alpha_2, \alpha_3, \beta_1, \beta_2, \beta_3, \gamma_1, \gamma_2) = \Omega(0, 0, 0, \pi/2, \pi/2, \pi/2, 0, 0)$)

3.3.2 Tri-Photon Click on Output-1, Single-Photon Click on Output-2 and no click on Output-3

In this section, we shall discuss the coincidence probability for the case when we get a tri-photon click at one output port, a single photon click at other output port and one output port remains click-less as show in Fig.(3.19) for the incidence of bi-photon clicks on input port-2 and input port-3 with time-delay τ is introduced between their arrival at input ports. The input state has already been defined in Eq.(3.42). The probability coefficients for this kind of output coincidence pattern are defined as,

$$\begin{aligned}
G_1 &= U_{22}^2 U_{23} U_{33}; & G_2 &= U_{22}^2 U_{23} U_{33}; & G_3 &= U_{22} U_{23}^2 U_{32}; & G_4 &= U_{22} U_{23}^2 U_{32} \\
G_5 &= U_{22} U_{32} U_{33}^2; & G_6 &= U_{22} U_{32} U_{33}^2; & G_7 &= U_{23} U_{32}^2 U_{33}; & G_8 &= U_{23} U_{32}^2 U_{33}; \\
G_9 &= U_{12}^2 U_{13} U_{23}; & G_{10} &= U_{12}^2 U_{13} U_{23}; & G_{11} &= U_{12} U_{13}^2 U_{22}; & G_{12} &= U_{12} U_{13}^2 U_{22}; \\
G_{13} &= U_{12}^2 U_{13} U_{33}; & G_{14} &= U_{12}^2 U_{13} U_{33}; & G_{15} &= U_{12} U_{13}^2 U_{32}; & G_{16} &= U_{12} U_{13}^2 U_{32}; \\
G_{17} &= U_{12} U_{22} U_{23}^2; & G_{18} &= U_{12} U_{22} U_{23}^2; & G_{19} &= U_{13} U_{22}^2 U_{23}; & G_{20} &= U_{13} U_{22}^2 U_{23}; \\
G_{21} &= U_{12} U_{32} U_{33}^2; & G_{22} &= U_{12} U_{32} U_{33}^2; & G_{23} &= U_{13} U_{32}^2 U_{33}; & G_{24} &= U_{13} U_{32}^2 U_{33};
\end{aligned} \tag{3.52}$$

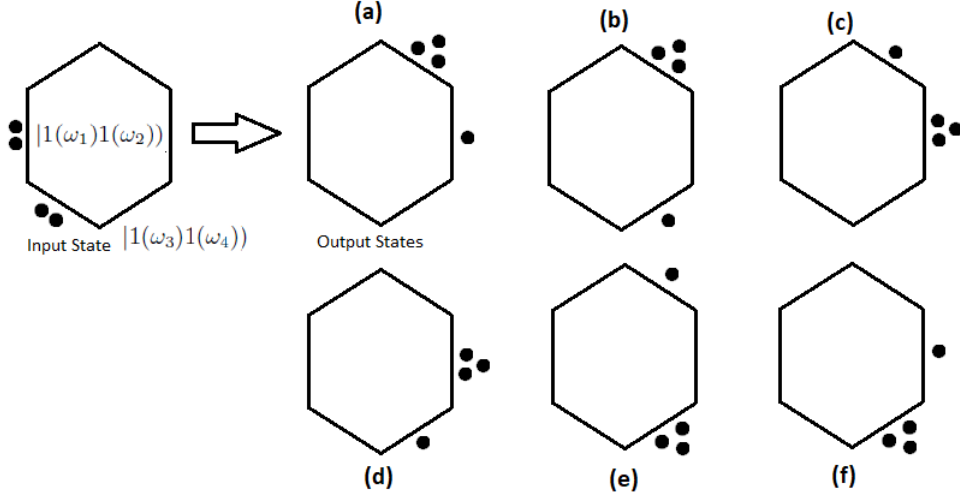


Figure 3.19

For this specific case, we shall discuss coincidence probability of the first output coincidence pattern as shown in Fig.(3.19, in which we get a tri-photon click at output port-1, a single-photon click at output port-2 and no click at output port-3. The Input state will be the same as we defined in Eq.(3.42) and the output operators for this case are defined as,

$$\Pi_1 = \int_{-\infty}^{\infty} \hat{a}_1^\dagger(\omega_5) \hat{a}_1^\dagger(\omega_8) \hat{a}_1^\dagger(\omega_{11}) |000\rangle \langle 000| \hat{a}_1(\omega_5) \hat{a}_1(\omega_8) \hat{a}_1(\omega_{11}) d\omega_5 d\omega_8 d\omega_{11}, \quad (3.53)$$

and

$$\Pi_2 = \int_{-\infty}^{\infty} \hat{a}_2^\dagger(\omega_6) |0\rangle \langle 0| \hat{a}_2^\dagger(\omega_6) d\omega_6, \quad (3.54)$$

the coincidence probability for this case can be written as

$$P_{202,310} = {}^s \langle 1111 | U^\dagger \Pi_1 \otimes \Pi_2 U | 1111 \rangle^s, \quad (3.55)$$

so the coincidence probability is

$$\begin{aligned} P_{202,310} = & G_9 (G_{10})^* e^{-\sigma^2 \tau^2} + G_9 (G_{11})^* e^{-3\sigma^2 \tau^2} + G_9 (G_{12})^* e^{-6\sigma^2 \tau^2} + \\ & G_{10} (G_9)^* e^{-\sigma^2 \tau^2} + G_{10} (G_{11})^* e^{-\sigma^2 \tau^2} + G_{10} (G_{12})^* e^{-3\sigma^2 \tau^2} + \\ & G_{11} (G_9)^* e^{-3\sigma^2 \tau^2} + G_{11} (G_{10})^* e^{-\sigma^2 \tau^2} + G_{11} (G_{12})^* e^{-\sigma^2 \tau^2} + \\ & G_{12} (G_9)^* e^{-6\sigma^2 \tau^2} + G_{12} (G_{10})^* e^{-3\sigma^2 \tau^2} + G_{12} (G_{11})^* e^{-\sigma^2 \tau^2} + \\ & G_9 (G_9)^* + G_{10} (G_{10})^* + G_{11} (G_{11})^* + G_{12} (G_{12})^*. \end{aligned} \quad (3.56)$$

The plot of coincidence probability against the time-delays introduced between the arrival of the photons at input ports of the balanced beam-splitter is shown in Fig.(3.20). This plot shows that the probability of having the desired output is relatively high and is equal to the value of the permanent of the adjacent scattering matrix when the time-delays τ introduced between the arrival of the photon at inputs of the beam-splitter is zero. The coincidence probability slightly increases with the increase in the length of the time-delays τ and then gradually decreases to zero with further increase in the length of the time-delays τ . Rest of the cases as mentioned in Fig.(3.1) are discussed in Appendix(C.5,....,C.9).

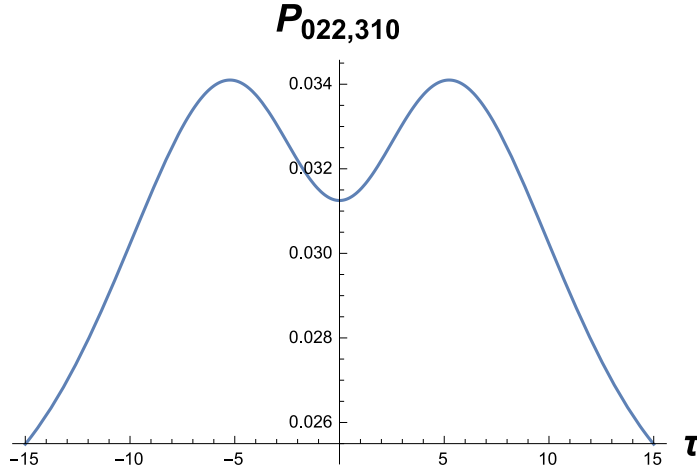


Figure 3.20: (with $T(\tau_1, \tau_2, \tau_3, \tau_4) = T(-\tau, 0, \tau, 2\tau)$, $\sigma_o = 0.1$ and $\Omega(\alpha_1, \alpha_2, \alpha_3, \beta_1, \beta_2, \beta_3, \gamma_1, \gamma_2) = \Omega(0, 0, 0, \pi/2, \pi/2, \pi/2, 0, 0)$)

3.3.3 Tetra-Photon Click on Output-1 and no Click on Output-2 and Output-3

In this section, we shall discuss the coincidence probability of having a tetra-photon click on any of the three output ports when we inject bi-photon pulses at input port-2 and at input port-3 of a balanced beam-splitter. Which can be visualized from Fig.(3.21)

First of all, we shall discuss the coincidence probability of the first output coincidence pattern as shown Fig.(3.21) which shows that we get a tetra-photon pulse at output port-1 and no clicks at output-2 and at output-3. The input state

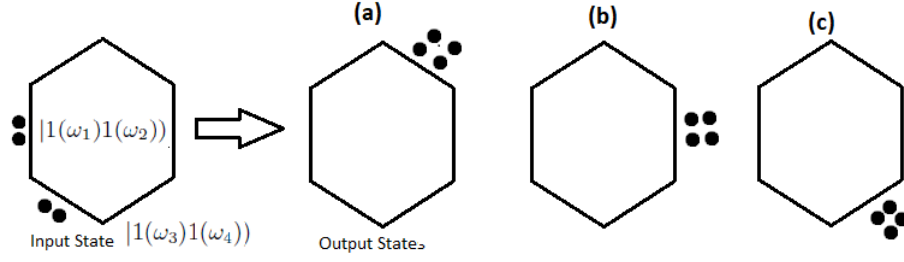


Figure 3.21

for this case is same as defined in Eq.(3.42) and the output operator is define as,

$$\Pi_1 = \int_{-\infty}^{\infty} \hat{a}_1^\dagger(\omega_5) \hat{a}_1^\dagger(\omega_8) \hat{a}_1^\dagger(\omega_{11}) \hat{a}_1^\dagger(\omega_{14}) |0000\rangle \langle 0000| \hat{a}_1(\omega_5) \hat{a}_1(\omega_8) \hat{a}_1(\omega_{11}) \hat{a}_1(\omega_{14}) d\omega_5 d\omega_8 d\omega_{11} d\omega_{14}, \quad (3.57)$$

the coincidence probability for this case can be written as,

$$P_{022,400} = {}^s \langle 1111 | U^\dagger \Pi_1 U | 1111 \rangle^s, \quad (3.58)$$

the probability coefficient for this case are defined as,

$$V_7 = U_{12}^2 U_{13}^2; \quad (3.59)$$

so the coincidence probability is

$$P_{202,400} = V_7 (V_7)^*. \quad (3.60)$$

One can clearly see from this relation, the coincidence probability for this case does not depend on the time-delays introduced between the arrival of the photons at input ports of the balanced beam-splitter. Rest of the cases as mentioned in Fig.(3.1) are discussed in Appendix(C.10,C.11).

3.4 Comparison between the Coincidence Probability Plots

Here in the section we have compiled the coincidence probability plots to conclude our work. We have compared the plots for the three type of input modes, we discussed in earlier sections and divided them in three different types based on the output modes. First mode in which two bi-photon clicks at any two output ports(one on each) are observed, the second output mode is in which a bi-photon click at one output port and two single-photon clicks at other two output port are observed and the third output mode is in which a tri-photon click at one output port, single-photon click at other output port and one output port remains click-less are observed as shown in Fig.(3.1), Fig.(3.3) and Fig.(3.5) respectively and there coincidence plot comparisons are shown in Fig.(3.22), Fig.(3.23) and Fig.(3.24) respectively.

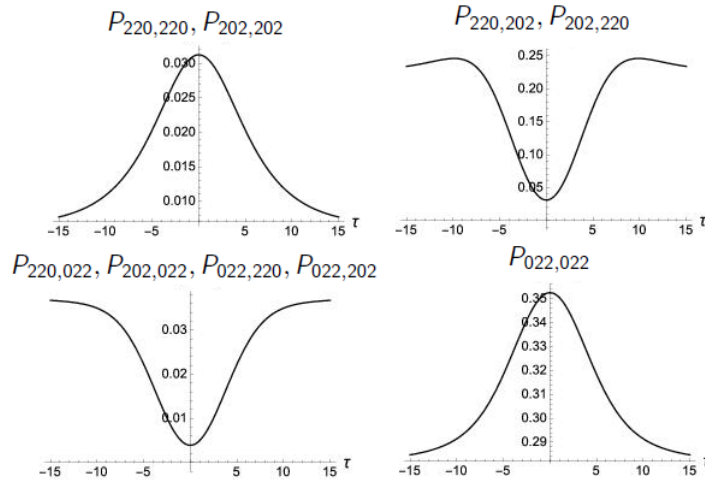


Figure 3.22: Comparison of the coincidence plots for the output mode when two bi-photon clicks are observed at the output ports.

62 3. QUANTUM INTERFEROMETRY WITH BI-PHOTON INPUT PULSES

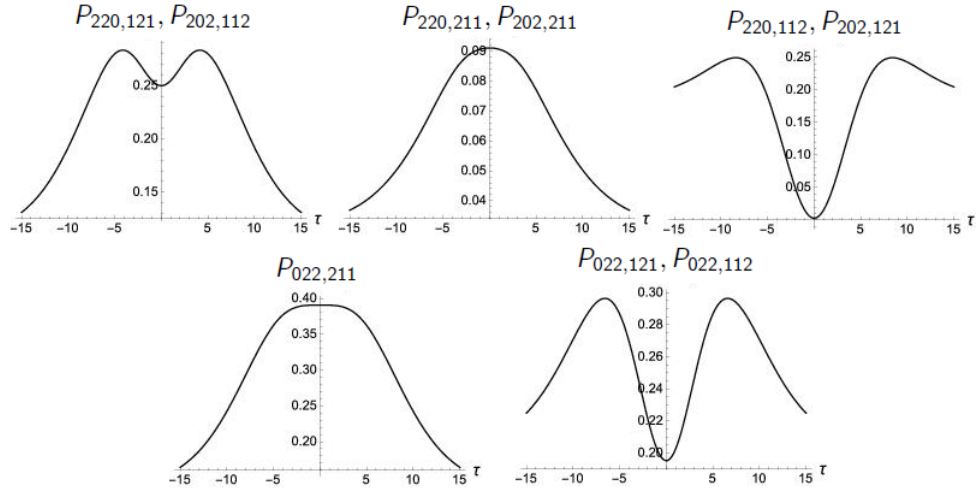


Figure 3.23: Comparison of the coincidence plots for the output mode when a bi-photon click and two single-photon clicks at output ports are observed.

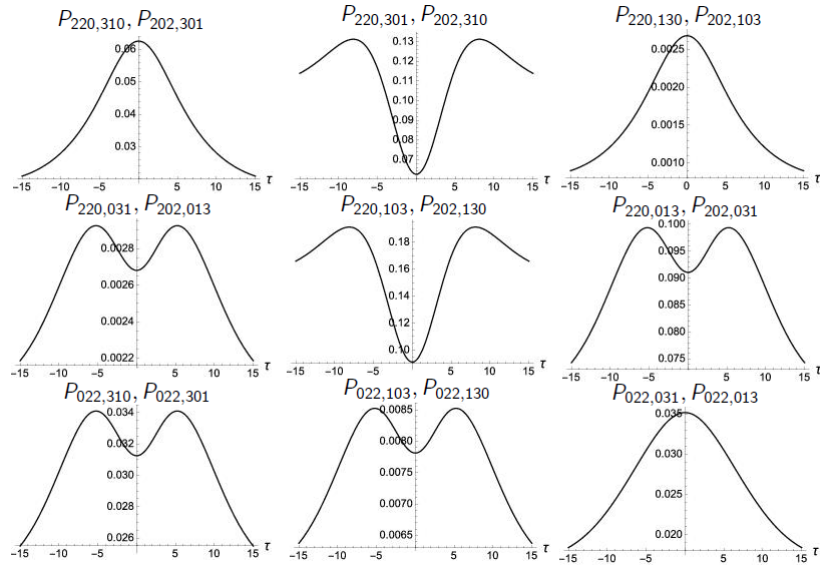


Figure 3.24: Comparison of the coincidence plots for the output mode when a tri-photon click and a single-photon click at any of the three output ports are observed.

3.5 Maximizing the Probabilities of the Outputs

We have generated a condition by varying the value of octuples $\Omega(\alpha_1, \alpha_2, \alpha_3, \beta_1, \beta_2, \beta_3, \gamma_1, \gamma_2)$ to reach a point where the distribution of the photon entering from input ports at output port of a balanced beam-splitter breaks and we get the maximum probability for one type of the output coincidence pattern and minimum for the other type of output coincidence patterns. The condition is defined as,

$$\Omega(\alpha_1, \alpha_2, \alpha_3, \beta_1, \beta_2, \beta_3, \gamma_1, \gamma_2) = \Omega(0, 0, 0, \pi, \pi, \pi, 0, 0), \quad (3.61)$$

for this condition, we get the matrix form such as

$$R(\Omega) = \begin{pmatrix} 0 & 0 & 1 \\ 0 & -1 & 0 \\ 1 & 0 & 0 \end{pmatrix}. \quad (3.62)$$

By using this condition for first kind of the input state in which we have injected a bi-photon pulse at input port-1 and port-2, we get maximum probability of having a bi-photon click at output port-2 and port-3 and minimum for all rest of the output coincidence patterns,

$$\begin{aligned} P_{220,022} &= 1, \\ P_{220,220} &= P_{220,202} = P_{220,211} = P_{220,121} = P_{220,112} = P_{220,310} = P_{220,301} = \\ P_{220,130} &= P_{220,031} = P_{220,103} = P_{220,013} = P_{220,400} = P_{220,040} = P_{220,004} = 0. \end{aligned} \quad (3.63)$$

For second kind of the input state in which we have injected a bi-photon pulse at input port-1 and port-3, we get maximum probability of having a bi-photon click at output port-1 and port-3 and minimum for all rest of the output coincidence patterns,

$$\begin{aligned} P_{202,202} &= 1, \\ P_{202,220} &= P_{202,022} = P_{202,211} = P_{202,121} = P_{202,112} = P_{202,310} = P_{202,301} = \\ P_{202,130} &= P_{202,031} = P_{202,103} = P_{202,013} = P_{202,400} = P_{202,040} = P_{202,004} = 0. \end{aligned} \quad (3.64)$$

For third kind of the input state in which we have injected a bi-photon pulse at input port-2 and port-3, we get maximum probability of having a bi-photon click at output port-1 and port-2 and minimum for all rest of the output coincidence patterns,

$$\begin{aligned} P_{022,220} &= 1, \\ P_{022,202} &= P_{022,022} = P_{022,211} = P_{022,121} = P_{022,112} = P_{022,310} = P_{022,301} = \\ P_{022,130} &= P_{022,031} = P_{022,103} = P_{022,013} = P_{022,400} = P_{022,040} = P_{022,004} = 0. \end{aligned} \quad (3.65)$$

We can maximize the probability of having any other kind of the output coincidence by just adjusting the values of the octuples.

3.6 Permanents and the Scattering Matrices

In this section we shall discuss, the permanents of matrices, the scattering matrices and their formation.

3.6.1 Permanents

For a square matrix of any order, the permanents are similar kind of the function to the determinants of the matrices. Both determinants and the permanents are polynomials of the elements of the matrices. There is one function which more general than the determinant and the permanent of a matrix is known as the immanent of a matrix [21]. For a $n \times n$ matrix $T = (t_{ij})$ the permanent can be written as

$$\text{Perm}(T) = \sum_{\sigma \in S_n} \prod_{i=1}^n t_{i,\sigma(i)}. \quad (3.66)$$

Where we can see that summation in above equation is over all elements σ of the S_n symmetric group. Which covers all the numbers 1,2,3.....n and their permutations. So the permanent of a 2×2 matrix can written as,

$$\text{Perm} \begin{pmatrix} t_{11} & t_{12} \\ t_{21} & t_{22} \end{pmatrix} = t_{11}t_{22} + t_{12}t_{21}, \quad (3.67)$$

now the permanent of a 3×3 matrix,

$$\begin{aligned} \text{Perm} \begin{pmatrix} t_{11} & t_{12} & t_{13} \\ t_{21} & t_{22} & t_{23} \\ t_{31} & t_{32} & t_{33} \end{pmatrix} &= t_{11}t_{22}t_{33} + t_{11}t_{23}t_{32} + t_{12}t_{21}t_{33} + t_{12}t_{23}t_{311} \\ &+ t_{13}t_{21}t_{32} + t_{13}t_{22}t_{31}. \end{aligned} \quad (3.68)$$

We can see the permanents are similar to the determinant, the only difference is that in a permanent all signs between term are positive. That means all sign that comes with permutations of the elements of the matrix T are ignored.

3.6.2 Scattering Matrices

The scattering matrix in reference to the combination of single photon pulses and bi-photon pulses has been studied for the case where a bi-photon pulse and two single photon pulses have injected at three input ports of a six port passive quantum optical interferometer (with three input ports and three output ports) and observed two bi-photon click at output ports [20]. We are using the same

concept to calculate the scattering matrix for our work. The scattering matrix is defined as

$$T_{ij} := U_{a_i, b_j}. \quad (3.69)$$

Where a_i and b_j show the number of clicks at input ports and at output ports respectively. For example, for a case where we have injected a bi-photon pulse at input port-1 and at input port-2 which can be written as a(220). Then observed a bi-photon click at output port-1 and at output port-2 which can be written as b(220). The scattering matrix for this case can be written as,

$$T_{220,220} = \begin{pmatrix} U_{11} & U_{11} & U_{12} & U_{12} \\ U_{11} & U_{11} & U_{12} & U_{12} \\ U_{21} & U_{21} & U_{22} & U_{22} \\ U_{21} & U_{21} & U_{22} & U_{22} \end{pmatrix}, \quad (3.70)$$

permanent of this matrix is

$$T_{220,220} = 4U_{12}^2 U_{21}^2 + 16U_{11} U_{12} U_{22} U_{21} + 4U_{11}^2 U_{22}^2. \quad (3.71)$$

Now for the case where we have the same input pattern but observed a bi-photon click at output port-1 and single-photon click at output port-2 and at output port-3. The scattering matrix for this case can be written as,

$$T_{220,211} = \begin{pmatrix} U_{11} & U_{11} & U_{12} & U_{13} \\ U_{11} & U_{11} & U_{12} & U_{13} \\ U_{21} & U_{21} & U_{22} & U_{23} \\ U_{21} & U_{21} & U_{22} & U_{23} \end{pmatrix}, \quad (3.72)$$

permanent of this matrix is

$$T_{220,211} = 4U_{22} U_{23} U_{11}^2 + 8U_{13} U_{21} U_{22} U_{11} + 8U_{12} U_{21} U_{23} U_{11} + 4U_{12} U_{13} U_{21}^2. \quad (3.73)$$

Now for the case where we have the same input pattern but observed a tri-photon click at output port-1, single-photon click at output port-2 and output port-3 remains click-less. The scattering matrix for this case can be written as,

$$T_{220,310} = \begin{pmatrix} U_{11} & U_{11} & U_{11} & U_{12} \\ U_{11} & U_{11} & U_{11} & U_{12} \\ U_{21} & U_{21} & U_{21} & U_{22} \\ U_{21} & U_{21} & U_{21} & U_{22} \end{pmatrix}, \quad (3.74)$$

permanent of this matrix is

$$T_{220,310} = 12U_{21} U_{22} U_{11}^2 + 12U_{12} U_{21}^2 U_{11}. \quad (3.75)$$

Similarly, we can form the scattering matrices for all rest of the cases and can also calculate the permanent of those matrices.

4

Conclusion

We have studied $SU(3)$ quantum photon interferometry using four photons with bi-photon input pulses at each input port (at any two of three input ports) of the 6-channel passive optical quantum interferometer (three input and three output channels).

We have observed all possible output coincidence patterns at output ports, calculated their coincidence probabilities and plotted them against the time-delay τ introduced between the arrival of the photons at input ports of the passive optical quantum interferometer. For the ground knowledge of the quantum interferometry and for the related knowledge of our problem, we have reviewed three research papers. We have reviewed single-photon quantum interferometry by using the $SU(3)$ group theoretical approach and their coincidence landscape [4, 5] and the quantum interferometry with multiple channel quantum interferometer and multiple photons observing the permutational symmetries present in them [20].

We have then extensively studied various patterns in $SU(3)$ quantum interferometry with bi-photon injections, with time-delay τ between the arrival of the photons at input ports. We have observed the peaks and dips for different coincidence for different occurrences of the output photons at output ports of a six-channel passive quantum optical interferometer with same input states. These dips and the peaks are occurring due to the different combinations of the transmissions and reflections of the input photons at interferometer. These dips and the peaks of the coincidence plots are equal to the value of the permanents of the adjacent scattering matrices related to the different output coincidence patterns.

We got three different kind of the plots, dips, peaks and bi-model distributions. According to Hong-Ou-Mandel effect when the photons reach the output ports after combination of reflections and transmissions, they form a specific output coincidence pattern. We get a dip in output coincidence probability plot when the photons reaches the output ports after specific combination of reflections and transmissions with zero time delay τ between the arrival of the photons at input

ports, destructively interfere at output ports to form a dip in coincidence pattern. Similarly, we get a peak in output coincidence probability plot when the photons reaches the output ports after specific combination of reflections and transmissions with zero time delay τ between the arrival of the photons at input ports, constructively interfere at output ports to form a specific output coincidence pattern. We get a bi-model distribution in coincidence probability plot when the photons reach the output ports after specific combination of the transmissions and reflection to form a specific output coincidence pattern, interfere constructively and equal interfere destructively at output ports. We have also observed a pattern in the occurrences of the dips and the peaks. According to that pattern, we get a peak when the photons leave the output ports in the way that they entered the input ports. Which mean we get a peak when the photons enter the input port-1 and input port-2 and leave the output port-1 and output port-2 irrespective of the arrangements of the clicks. In some cases we get a divergence from the pattern.

We have observed that by just adjusting the value of the octuples $\Omega(\alpha_1, \alpha_2, \alpha_3, \beta_1, \beta_2, \beta_3, \gamma_1, \gamma_2)$, we can break the superposition between different output coincidence patterns and can create condition to get maximum probability of having the desired output coincidence pattern which can be helpful in many problems. By using this theory developed in our analysis, we can study the properties of the $SU(3)$ transition matrix.

Appendix A

Appendix

A Rest of the Cases of Section 3.1

In this case, we have injected a bi-photon input pulse at input port 1, input port 2 and nothing input port 3 of a six port passive quantum optical interferometer and then calculate and plotted the coincidence probabilities of all output coincidence patterns as shown in Fig.3.1, Fig.3.3, Fig.3.5 and Fig.3.7.

A.1 Bi-Photon Clicks on Output-1 and Output-3

In this section, we shall discuss the coincidence probability for the case, where we get a bi-photon clicks on the output port-1 and output port-3 and shall see how the coincidence probability varies with the change in length of time-delays τ between the arrival of the photons at input ports as shown in Fig.(3.1). The coincidence probability for this case is define as,

$$P_{220,202} = \langle 1111 |^s U^\dagger \Pi_1 \otimes \Pi_3 U | 1111 \rangle^s, \quad (\text{A.1})$$

the output operators used for this specific case are already been defined in Eq.(3.2) and Eq.(3.4) and the input state will be the same as before in Eq.(3.5). We are discussing the different output for the same input state. The Coincidence probability is defined as,

$$\begin{aligned} P_{220,202} = & A_7 (A_8) * e^{-\sigma^2 \tau^2} + A_7 (A_9) * e^{-3\sigma^2 \tau^2} + A_7 (A_{10}) * e^{-3\sigma^2 \tau^2} + A_7 (A_{11}) * e^{-5\sigma^2 \tau^2} \\ & + A_7 (A_{12}) * e^{-8\sigma^2 \tau^2} + A_8 (A_7) * e^{-\sigma^2 \tau^2} + A_8 (A_9) * e^{-\sigma^2 \tau^2} + A_8 (A_{10}) * e^{-\sigma^2 \tau^2} + \\ & A_8 (A_{11}) * e^{-2\sigma^2 \tau^2} + A_8 (A_{12}) * e^{-5\sigma^2 \tau^2} + A_9 (A_7) * e^{-3\sigma^2 \tau^2} + A_9 (A_8) * e^{-\sigma^2 \tau^2} + \\ & A_9 (A_{10}) * e^{-2\sigma^2 \tau^2} + A_9 (A_{11}) * e^{-\sigma^2 \tau^2} + A_9 (A_{12}) * e^{-3\sigma^2 \tau^2} + A_{10} (A_7) * e^{-3\sigma^2 \tau^2} + \\ & A_{10} (A_8) * e^{-\sigma^2 \tau^2} + A_{10} (A_9) * e^{-2\sigma^2 \tau^2} + A_{10} (A_{11}) * e^{-\sigma^2 \tau^2} + A_{10} (A_{12}) * e^{-3\sigma^2 \tau^2} + \end{aligned}$$

$$\begin{aligned}
& A_{11} (A_7)^* e^{-5\sigma^2\tau^2} + A_{11} (A_8)^* e^{-2\sigma^2\tau^2} + A_{11} (A_9)^* e^{-\sigma^2\tau^2} + A_{11} (A_{10})^* e^{-\sigma^2\tau^2} + \\
& A_{11} (A_{12})^* e^{-\sigma^2\tau^2} + A_{12} (A_7)^* e^{-8\sigma^2\tau^2} + A_{12} (A_8)^* e^{-5\sigma^2\tau^2} + A_{12} (A_9)^* e^{-3\sigma^2\tau^2} + \\
& A_{12} (A_{10})^* e^{-3\sigma^2\tau^2} + A_{12} (A_{11})^* e^{-\sigma^2\tau^2} + A_7 (A_7)^* + A_8 (A_8)^* + A_9 (A_9)^* + \\
& A_{10} (A_{10})^* + A_{11} (A_{11})^* + A_{12} (A_{12})^*. \tag{A.2}
\end{aligned}$$

The probability coefficients are defined in Eq.(3.7) and the plot of the coincidence probability against the time delay τ introduced between the arrival of the photons at input ports is shown in Fig.(A.1). This plot shows that the probability of having the desired output is least when there is no time delay τ introduced between the arrival of the photons and this value of the coincidence probability with zero time delay is equal to the permanent of adjacent scattering matrix and it starts increasing as the length of the time-delay increases and at specific limit it again starts decreasing as shown in Fig.(A.1).

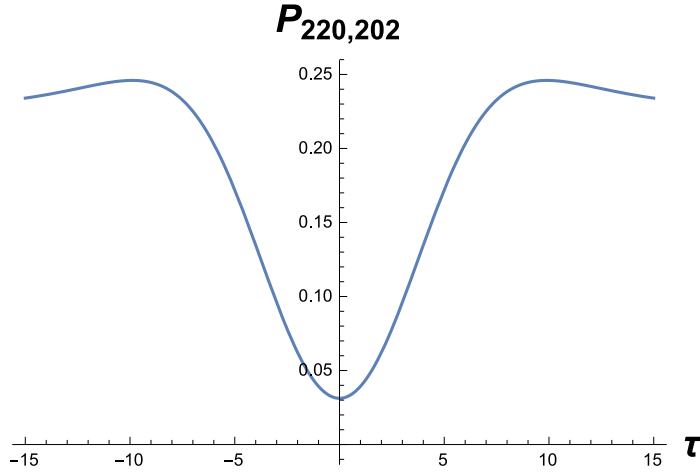


Figure A.1: (with $T(\tau_1, \tau_2, \tau_3, \tau_4) = T(-\tau, 0, \tau, 2\tau)$, $\sigma_o = 0.1$ and $\Omega(\alpha_1, \alpha_2, \alpha_3, \beta_1, \beta_2, \beta_3, \gamma_1, \gamma_2) = \Omega(0, 0, 0, \pi/2, \pi/2, \pi/2, 0, 0)$)

A.2 Bi-Photon Clicks on Output-2 and Output-3

In this section, we shall discuss the coincidence probability for the case, where we get a bi-photon clicks on the output port-2 and output port-3 and shall see how the coincidence probability changes with change in the length of the time-delays τ between the arrival of the photons at input ports as shown in Fig.(3.1). The coincidence probability for this case is defined as,

$$P_{220,022} = \langle 1111 |^s U^\dagger \Pi_2 \otimes \Pi_3 U | 1111 \rangle^s, \tag{A.3}$$

the output operators used for this specific case are already defined in Eq.(3.3) and Eq.(3.4) but the input state will remain the same as defined before in Eq.(3.5). We are discussing the different output pattern for the same input state. The coincidence probability is,

$$\begin{aligned}
P_{220,022} = & A_{13} (A_{14})^* e^{-\sigma^2 \tau^2} + A_{13} (A_{15})^* e^{-3\sigma^2 \tau^2} + A_{13} (A_{16})^* e^{-3\sigma^2 \tau^2} + \\
& A_{13} (A_{17})^* e^{-5\sigma^2 \tau^2} + A_{13} (A_{18})^* e^{-8\sigma^2 \tau^2} + A_{14} (A_{13})^* e^{-\sigma^2 \tau^2} + \\
& A_{14} (A_{15})^* e^{-\sigma^2 \tau^2} + A_{14} (A_{16})^* e^{-\sigma^2 \tau^2} + A_{14} (A_{17})^* e^{-2\sigma^2 \tau^2} + \\
& A_{14} (A_{18})^* e^{-5\sigma^2 \tau^2} + A_{15} (A_{13})^* e^{-3\sigma^2 \tau^2} + A_{15} (A_{14})^* e^{-\sigma^2 \tau^2} + \\
& A_{15} (A_{16})^* e^{-2\sigma^2 \tau^2} + A_{15} (A_{17})^* e^{-\sigma^2 \tau^2} + A_{15} (A_{18})^* e^{-3\sigma^2 \tau^2} + \\
& A_{16} (A_{13})^* e^{-3\sigma^2 \tau^2} + A_{16} (A_{14})^* e^{-\sigma^2 \tau^2} + A_{16} (A_{15})^* e^{-2\sigma^2 \tau^2} + \\
& A_{16} (A_{17})^* e^{-\sigma^2 \tau^2} + A_{16} (A_{18})^* e^{-3\sigma^2 \tau^2} + A_{17} (A_{13})^* e^{-5\sigma^2 \tau^2} + \\
& A_{17} (A_{14})^* e^{-2\sigma^2 \tau^2} + A_{17} (A_{15})^* e^{-\sigma^2 \tau^2} + A_{17} (A_{16})^* e^{-\sigma^2 \tau^2} + \\
& A_{17} (A_{18})^* e^{-\sigma^2 \tau^2} + A_{18} (A_{13})^* e^{-8\sigma^2 \tau^2} + A_{18} (A_{14})^* e^{-5\sigma^2 \tau^2} + \\
& A_{18} (A_{15})^* e^{-3\sigma^2 \tau^2} + A_{18} (A_{16})^* e^{-3\sigma^2 \tau^2} + A_{18} (A_{17})^* e^{-\sigma^2 \tau^2} + \\
& A_{13} (A_{13})^* + A_{14} (A_{14})^* + A_{15} (A_{15})^* + A_{16} (A_{16})^* + \\
& A_{17} (A_{17})^* + A_{18} (A_{18})^*
\end{aligned} \tag{A.4}$$

where the probability coefficients are defined in Eq.(3.7) and the coincidence plot against the time-delay τ between the arrival of the photons at the input ports of beam-splitter is shown in Fig.(A.2). This plot shows that the probability of having the desired output is least when there is no time-delays between the arrival of the photons at input ports and this value of the coincidence probability with no time delay between the arrival of the photons at input ports is equal to the value of the permanent of the adjacent scattering matrix. It starts increasing as the length of the time-delay introduced between the arrival of the photons at input ports increases as shown in Fig.(A.2).

A.3 Bi-Photon Click on Output-2 and Single-Photon Click on Output-1 and Output-3

In this case, we shall discuss the coincidence probability for the bi-photon click on the output port-2 and a single-photon click on output port-1 and output port-3 for the same input state in which we inject bi-photon pulse in input port-1 and input port-2 with time-delay τ between every arrival of the photon at input ports as shown in Fig.(3.3). The input state for this case is the same as defined before in

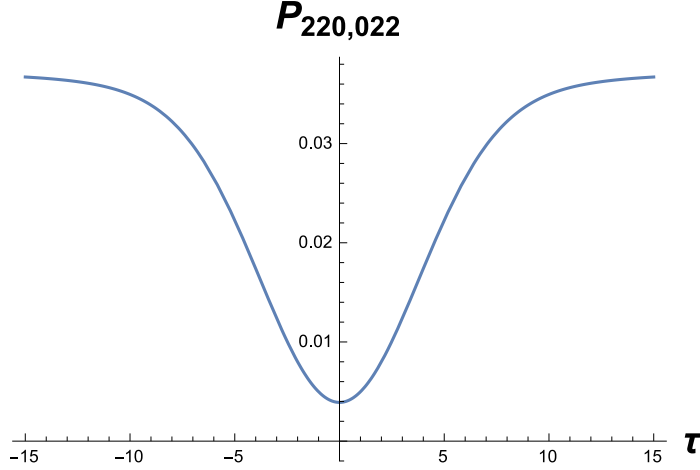


Figure A.2: (with $T(\tau_1, \tau_2, \tau_3, \tau_4) = T(-\tau, 0, \tau, 2\tau)$, $\sigma_o = 0.1$ and $\Omega(\alpha_1, \alpha_2, \alpha_3, \beta_1, \beta_2, \beta_3, \gamma_1, \gamma_2) = \Omega(0, 0, 0, \pi/2, \pi/2, \pi/2, 0, 0)$)

the Eq.(3.5). The output operators for this case are defined as,

$$\Pi_1 = \int_{-\infty}^{\infty} \hat{a}_1^\dagger(\omega_5) |0\rangle \langle 0| \hat{a}_1(\omega_5) d\omega_5, \quad (\text{A.5})$$

$$\Pi_2 = \int_{-\infty}^{\infty} \hat{a}_2^\dagger(\omega_6) \hat{a}_2^\dagger(\omega_9) |00\rangle \langle 00| \hat{a}_2(\omega_6) \hat{a}_2(\omega_9) d\omega_6 d\omega_9, \quad (\text{A.6})$$

and

$$\Pi_3 = \int_{-\infty}^{\infty} \hat{a}_3^\dagger(\omega_7) |0\rangle \langle 0| \hat{a}_3(\omega_7) d\omega_7, \quad (\text{A.7})$$

the coincidence probability for this case is defined as

$$P_{220,121} = \langle 1111 |^s U^\dagger \Pi_1 \otimes \Pi_2 \otimes \Pi_3 U |1111\rangle^s, \quad (\text{A.8})$$

The probability coefficients for this case are defined as,

$$\begin{aligned} M_1 &= U_{12} U_{21}^2 U_{32}; & M_2 &= U_{12} U_{21}^2 U_{32}; & M_3 &= U_{11} U_{21} U_{22} U_{32}; & M_4 &= U_{12} U_{21} U_{22} U_{31}; \\ M_5 &= U_{11} U_{21} U_{22} U_{32}; & M_6 &= U_{12} U_{21} U_{22} U_{31}; & M_7 &= U_{11} U_{21} U_{22} U_{32}; & M_8 &= U_{12} U_{21} U_{22} U_{31}; \\ M_9 &= U_{11} U_{21} U_{22} U_{32}; & M_{10} &= U_{12} U_{21} U_{22} U_{31}; & M_{11} &= U_{11} U_{22}^2 U_{31}; & M_{12} &= U_{11} U_{22}^2 U_{31}; \end{aligned} \quad (\text{A.9})$$

so the coincidence probability for this case is

$$P_{220,121} = (M_1)^* M_1 + e^{-\sigma^2 \tau^2} (M_2)^* M_1 + e^{-\sigma^2 \tau^2} (M_3)^* M_1 + e^{-3\sigma^2 \tau^2} (M_4)^* M_1 +$$

$$\begin{aligned}
& e^{-3\sigma^2\tau^2} (M_5) * M_1 + e^{-4\sigma^2\tau^2} (M_6) * M_1 + e^{-3\sigma^2\tau^2} (M_7) * M_1 + e^{-6\sigma^2\tau^2} (M_8) * M_1 + \\
& e^{-5\sigma^2\tau^2} (M_9) * M_1 + e^{-7\sigma^2\tau^2} (M_{10}) * M_1 + e^{-8\sigma^2\tau^2} (M_{11}) * M_1 + e^{-9\sigma^2\tau^2} (M_{12}) * M_1 + \\
& e^{-\sigma^2\tau^2} (M_1) * M_2 + (M_2) * M_2 + e^{-3\sigma^2\tau^2} (M_3) * M_2 + e^{-\sigma^2\tau^2} (M_4) * M_2 + \\
& e^{-4\sigma^2\tau^2} (M_5) * M_2 + e^{-3\sigma^2\tau^2} (M_6) * M_2 + e^{-6\sigma^2\tau^2} (M_7) * M_2 + e^{-3\sigma^2\tau^2} (M_8) * M_2 + \\
& e^{-7\sigma^2\tau^2} (M_9) * M_2 + e^{-5\sigma^2\tau^2} (M_{10}) * M_2 + e^{-9\sigma^2\tau^2} (M_{11}) * M_2 + e^{-8\sigma^2\tau^2} (M_{12}) * M_2 + \\
& e^{-\sigma^2\tau^2} (M_1) * M_3 + e^{-3\sigma^2\tau^2} (M_2) * M_3 + (M_3) * M_3 + e^{-4\sigma^2\tau^2} (M_4) * M_3 + \\
& e^{-\sigma^2\tau^2} (M_5) * M_3 + e^{-3\sigma^2\tau^2} (M_6) * M_3 + e^{-\sigma^2\tau^2} (M_7) * M_3 + e^{-7\sigma^2\tau^2} (M_8) * M_3 + \\
& e^{-2\sigma^2\tau^2} (M_9) * M_3 + e^{-6\sigma^2\tau^2} (M_{10}) * M_3 + e^{-5\sigma^2\tau^2} (M_{11}) * M_3 + e^{-7\sigma^2\tau^2} (M_{12}) * M_3 + \\
& e^{-3\sigma^2\tau^2} (M_1) * M_4 + e^{-\sigma^2\tau^2} (M_2) * M_4 + e^{-4\sigma^2\tau^2} (M_3) * M_4 + (M_4) * M_4 + \\
& e^{-3\sigma^2\tau^2} (M_5) * M_4 + e^{-\sigma^2\tau^2} (M_6) * M_4 + e^{-7\sigma^2\tau^2} (M_7) * M_4 + e^{-\sigma^2\tau^2} (M_8) * M_4 + \\
& e^{-6\sigma^2\tau^2} (M_9) * M_4 + e^{-2\sigma^2\tau^2} (M_{10}) * M_4 + e^{-7\sigma^2\tau^2} (M_{11}) * M_4 + e^{-5\sigma^2\tau^2} (M_{12}) * M_4 + \\
& e^{-3\sigma^2\tau^2} (M_1) * M_5 + e^{-4\sigma^2\tau^2} (M_2) * M_5 + e^{-\sigma^2\tau^2} (M_3) * M_5 + e^{-3\sigma^2\tau^2} (M_4) * M_5 + \\
& (M_5) * M_5 + e^{-\sigma^2\tau^2} (M_6) * M_5 + e^{-2\sigma^2\tau^2} (M_7) * M_5 + e^{-5\sigma^2\tau^2} (M_8) * M_5 + \\
& e^{-\sigma^2\tau^2} (M_9) * M_5 + e^{-3\sigma^2\tau^2} (M_{10}) * M_5 + e^{-3\sigma^2\tau^2} (M_{11}) * M_5 + e^{-4\sigma^2\tau^2} (M_{12}) * M_5 + \\
& e^{-4\sigma^2\tau^2} (M_1) * M_6 + e^{-3\sigma^2\tau^2} (M_2) * M_6 + e^{-3\sigma^2\tau^2} (M_3) * M_6 + e^{-\sigma^2\tau^2} (M_4) * M_6 + \\
& e^{-\sigma^2\tau^2} (M_5) * M_6 + (M_6) * M_6 + e^{-5\sigma^2\tau^2} (M_7) * M_6 + e^{-2\sigma^2\tau^2} (M_8) * M_6 + \\
& e^{-3\sigma^2\tau^2} (M_9) * M_6 + e^{-\sigma^2\tau^2} (M_{10}) * M_6 + e^{-4\sigma^2\tau^2} (M_{11}) * M_6 + e^{-3\sigma^2\tau^2} (M_{12}) * M_6 + \\
& e^{-3\sigma^2\tau^2} (M_1) * M_7 + e^{-6\sigma^2\tau^2} (M_2) * M_7 + e^{-\sigma^2\tau^2} (M_3) * M_7 + e^{-7\sigma^2\tau^2} (M_4) * M_7 + \\
& e^{-2\sigma^2\tau^2} (M_5) * M_7 + e^{-5\sigma^2\tau^2} (M_6) * M_7 + (M_7) * M_7 + e^{-9\sigma^2\tau^2} (M_8) * M_7 + \\
& e^{-\sigma^2\tau^2} (M_9) * M_7 + e^{-7\sigma^2\tau^2} (M_{10}) * M_7 + e^{-3\sigma^2\tau^2} (M_{11}) * M_7 + e^{-6\sigma^2\tau^2} (M_{12}) * M_7 + \\
& e^{-6\sigma^2\tau^2} (M_1) * M_8 + e^{-3\sigma^2\tau^2} (M_2) * M_8 + e^{-7\sigma^2\tau^2} (M_3) * M_8 + e^{-\sigma^2\tau^2} (M_4) * M_8 + \\
& e^{-5\sigma^2\tau^2} (M_5) * M_8 + e^{-2\sigma^2\tau^2} (M_6) * M_8 + e^{-9\sigma^2\tau^2} (M_7) * M_8 + (M_8) * M_8 + \\
& e^{-7\sigma^2\tau^2} (M_9) * M_8 + e^{-\sigma^2\tau^2} (M_{10}) * M_8 + e^{-6\sigma^2\tau^2} (M_{11}) * M_8 + e^{-3\sigma^2\tau^2} (M_{12}) * M_8 + \\
& e^{-5\sigma^2\tau^2} (M_1) * M_9 + e^{-7\sigma^2\tau^2} (M_2) * M_9 + e^{-2\sigma^2\tau^2} (M_3) * M_9 + e^{-6\sigma^2\tau^2} (M_4) * M_9 + \\
& e^{-\sigma^2\tau^2} (M_5) * M_9 + e^{-3\sigma^2\tau^2} (M_6) * M_9 + e^{-\sigma^2\tau^2} (M_7) * M_9 + e^{-7\sigma^2\tau^2} (M_8) * M_9 + \\
& (M_9) * M_9 + e^{-4\sigma^2\tau^2} (M_{10}) * M_9 + e^{-\sigma^2\tau^2} (M_{11}) * M_9 + e^{-3\sigma^2\tau^2} (M_{12}) * M_9 + \\
& e^{-7\sigma^2\tau^2} (M_1) * M_{10} + e^{-5\sigma^2\tau^2} (M_2) * M_{10} + e^{-6\sigma^2\tau^2} (M_3) * M_{10} + e^{-2\sigma^2\tau^2} (M_4) * M_{10} + \\
& e^{-3\sigma^2\tau^2} (M_5) * M_{10} + e^{-\sigma^2\tau^2} (M_6) * M_{10} + e^{-7\sigma^2\tau^2} (M_7) * M_{10} + e^{-\sigma^2\tau^2} (M_8) * M_{10} + \\
& e^{-4\sigma^2\tau^2} (M_9) * M_{10} + (M_{10}) * M_{10} + e^{-3\sigma^2\tau^2} (M_{11}) * M_{10} + e^{-\sigma^2\tau^2} (M_{12}) * M_{10} +
\end{aligned}$$

$$\begin{aligned}
& e^{-8\sigma^2\tau^2} (M_1) * M_{11} + e^{-9\sigma^2\tau^2} (M_2) * M_{11} + e^{-5\sigma^2\tau^2} (M_3) * M_{11} + e^{-7\sigma^2\tau^2} (M_4) * M_{11} + \\
& e^{-3\sigma^2\tau^2} (M_5) * M_{11} + e^{-4\sigma^2\tau^2} (M_6) * M_{11} + e^{-3\sigma^2\tau^2} (M_7) * M_{11} + e^{-6\sigma^2\tau^2} (M_8) * M_{11} + \\
& e^{-\sigma^2\tau^2} (M_9) * M_{11} + e^{-3\sigma^2\tau^2} (M_{10}) * M_{11} + (M_{11}) * M_{11} + e^{-\sigma^2\tau^2} (M_{12}) * M_{11} + \\
& e^{-9\sigma^2\tau^2} (M_1) * M_{12} + e^{-8\sigma^2\tau^2} (M_2) * M_{12} + e^{-7\sigma^2\tau^2} (M_3) * M_{12} + e^{-5\sigma^2\tau^2} (M_4) * M_{12} + \\
& e^{-4\sigma^2\tau^2} (M_5) * M_{12} + e^{-3\sigma^2\tau^2} (M_6) * M_{12} + e^{-6\sigma^2\tau^2} (M_7) * M_{12} + e^{-3\sigma^2\tau^2} (M_8) * M_{12} + \\
& e^{-3\sigma^2\tau^2} (M_9) * M_{12} + e^{-\sigma^2\tau^2} (M_{10}) * M_{12} + e^{-\sigma^2\tau^2} (M_{11}) * M_{12} + (M_{12}) * M_{12}.
\end{aligned} \tag{A.10}$$

The plot of coincidence probability against the time-delays between the arrival of the photons at input ports is shown Fig.(A.3). This plot shows, the coincidence probability of having desired output pattern is maximum when the time-delays between the arrival of the photons at input ports is zero and this value of the coincidence probability with no time delay is equal to the value of the permanent of the adjacent scattering matrix. Then coincidence probability gradually starts decreasing as the length of the time-delays increases between the arrival of the photons at the input ports, which can be visualized from Fig.(A.3)

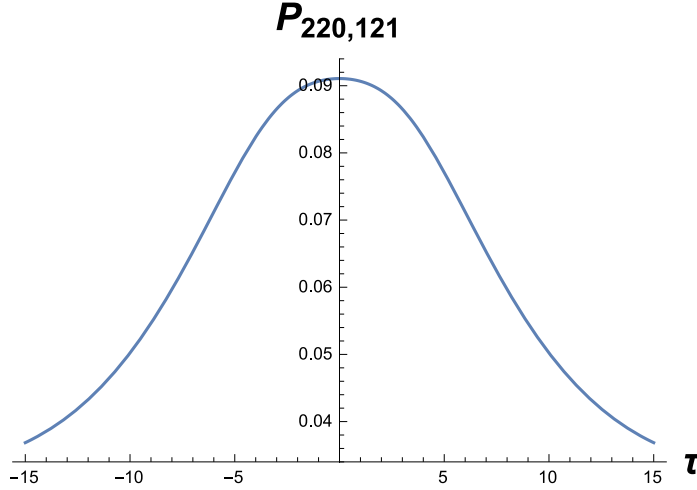


Figure A.3: (with $T(\tau_1, \tau_2, \tau_3, \tau_4) = T(-\tau, 0, \tau, 2\tau)$, $\sigma_o = 0.1$ and $\Omega(\alpha_1, \alpha_2, \alpha_3, \beta_1, \beta_2, \beta_3, \gamma_1, \gamma_2) = \Omega(0, 0, 0, \pi/2, \pi/2, \pi/2, 0, 0)$)

A.4 Bi-Photon Click on Output-3 and Single-Photon Click on Output-1 and Output-2

In this case, we shall discuss the coincidence probability of a bi-photon click on the output port-3 and a single-photon click on output port-1 and output port-2, for the same input state with a bi-photon click on input port-1 and input port-2 with time-delay between arrival of every the photon as shown in Fig.(3.3). The input state for this case is the same as defined before in the Eq.(3.5). The output operators for this case are defined as,

$$\Pi_1 = \int_{-\infty}^{\infty} \hat{a}_1^\dagger(\omega_5) |0\rangle \langle 0| \hat{a}_1(\omega_5) d\omega_5, \quad (\text{A.11})$$

$$\Pi_2 = \int_{-\infty}^{\infty} \hat{a}_2^\dagger(\omega_6) |0\rangle \langle 0| \hat{a}_2(\omega_6) d\omega_6, \quad (\text{A.12})$$

and

$$\Pi_3 = \int_{-\infty}^{\infty} \hat{a}_3^\dagger(\omega_7) \hat{a}_3^\dagger(\omega_{10}) |00\rangle \langle 00| \hat{a}_3(\omega_7) \hat{a}_3(\omega_{10}) d\omega_7 d\omega_{10}, \quad (\text{A.13})$$

the coincidence probability for this case is defined as,

$$P_{220,112} = \langle 1111 |^s U^\dagger \Pi_1 \otimes \Pi_2 \otimes \Pi_3 U |1111\rangle^s, \quad (\text{A.14})$$

and the probability coefficients for this case are,

$$\begin{aligned} N_1 &= U_{12}U_{22}U_{31}^2; & N_2 &= U_{12}U_{22}U_{31}^2; & N_3 &= U_{11}U_{22}U_{31}U_{32}; & N_4 &= U_{12}U_{21}U_{31}U_{32}; \\ N_5 &= U_{11}U_{22}U_{31}U_{32}; & N_6 &= U_{12}U_{21}U_{31}U_{32}; & N_7 &= U_{11}U_{22}U_{31}U_{32}; & N_8 &= U_{12}U_{21}U_{31}U_{32}; \\ N_9 &= U_{11}U_{22}U_{31}U_{32}; & N_{10} &= U_{12}U_{21}U_{31}U_{32}; & N_{11} &= U_{11}U_{21}U_{32}^2; & N_{12} &= U_{11}U_{21}U_{32}^2; \end{aligned} \quad (\text{A.15})$$

so the coincidence probability is

$$\begin{aligned} P_{220,112} &= (N_1)^* N_1 + e^{-\sigma^2 \tau^2} (N_2)^* N_1 + e^{-\sigma^2 \tau^2} (N_3)^* N_1 + e^{-3\sigma^2 \tau^2} (N_4)^* N_1 + \\ &e^{-3\sigma^2 \tau^2} (N_5)^* N_1 + e^{-4\sigma^2 \tau^2} (N_6)^* N_1 + e^{-3\sigma^2 \tau^2} (N_7)^* N_1 + e^{-6\sigma^2 \tau^2} (N_8)^* N_1 + \\ &e^{-5\sigma^2 \tau^2} (N_9)^* N_1 + e^{-7\sigma^2 \tau^2} (N_{10})^* N_1 + e^{-8\sigma^2 \tau^2} (N_{11})^* N_1 + e^{-9\sigma^2 \tau^2} (N_{12})^* N_1 + \\ &e^{-\sigma^2 \tau^2} (N_1)^* N_2 + (N_2)^* N_2 + e^{-3\sigma^2 \tau^2} (N_3)^* N_2 + e^{-\sigma^2 \tau^2} (N_4)^* N_2 + \\ &e^{-4\sigma^2 \tau^2} (N_5)^* N_2 + e^{-3\sigma^2 \tau^2} (N_6)^* N_2 + e^{-6\sigma^2 \tau^2} (N_7)^* N_2 + e^{-3\sigma^2 \tau^2} (N_8)^* N_2 + \\ &e^{-7\sigma^2 \tau^2} (N_9)^* N_2 + e^{-5\sigma^2 \tau^2} (N_{10})^* N_2 + e^{-9\sigma^2 \tau^2} (N_{11})^* N_2 + e^{-8\sigma^2 \tau^2} (N_{12})^* N_2 + \\ &e^{-\sigma^2 \tau^2} (N_1)^* N_3 + e^{-3\sigma^2 \tau^2} (N_2)^* N_3 + (N_3)^* N_3 + e^{-4\sigma^2 \tau^2} (N_4)^* N_3 + \\ &e^{-\sigma^2 \tau^2} (N_5)^* N_3 + e^{-3\sigma^2 \tau^2} (N_6)^* N_3 + e^{-\sigma^2 \tau^2} (N_7)^* N_3 + e^{-7\sigma^2 \tau^2} (N_8)^* N_3 + \end{aligned}$$

$$\begin{aligned}
& e^{-2\sigma^2\tau^2} (N_9) * N_3 + e^{-6\sigma^2\tau^2} (N_{10}) * N_3 + e^{-5\sigma^2\tau^2} (N_{11}) * N_3 + e^{-7\sigma^2\tau^2} (N_{12}) * N_3 + \\
& e^{-3\sigma^2\tau^2} (N_1) * N_4 + e^{-\sigma^2\tau^2} (N_2) * N_4 + e^{-4\sigma^2\tau^2} (N_3) * N_4 + (N_4) * N_4 + \\
& e^{-3\sigma^2\tau^2} (N_5) * N_4 + e^{-\sigma^2\tau^2} (N_6) * N_4 + e^{-7\sigma^2\tau^2} (N_7) * N_4 + e^{-\sigma^2\tau^2} (N_8) * N_4 + \\
& e^{-6\sigma^2\tau^2} (N_9) * N_4 + e^{-2\sigma^2\tau^2} (N_{10}) * N_4 + e^{-7\sigma^2\tau^2} (N_{11}) * N_4 + e^{-5\sigma^2\tau^2} (N_{12}) * N_4 + \\
& e^{-3\sigma^2\tau^2} (N_1) * N_5 + e^{-4\sigma^2\tau^2} (N_2) * N_5 + e^{-\sigma^2\tau^2} (N_3) * N_5 + e^{-3\sigma^2\tau^2} (N_4) * N_5 + \\
& (N_5) * N_5 + e^{-\sigma^2\tau^2} (N_6) * N_5 + e^{-2\sigma^2\tau^2} (N_7) * N_5 + e^{-5\sigma^2\tau^2} (N_8) * N_5 + \\
& e^{-\sigma^2\tau^2} (N_9) * N_5 + e^{-3\sigma^2\tau^2} (N_{10}) * N_5 + e^{-3\sigma^2\tau^2} (N_{11}) * N_5 + e^{-4\sigma^2\tau^2} (N_{12}) * N_5 + \\
& e^{-4\sigma^2\tau^2} (N_1) * N_6 + e^{-3\sigma^2\tau^2} (N_2) * N_6 + e^{-3\sigma^2\tau^2} (N_3) * N_6 + e^{-\sigma^2\tau^2} (N_4) * N_6 + \\
& e^{-\sigma^2\tau^2} (N_5) * N_6 + (N_6) * N_6 + e^{-5\sigma^2\tau^2} (N_7) * N_6 + e^{-2\sigma^2\tau^2} (N_8) * N_6 + \\
& e^{-3\sigma^2\tau^2} (N_9) * N_6 + e^{-\sigma^2\tau^2} (N_{10}) * N_6 + e^{-4\sigma^2\tau^2} (N_{11}) * N_6 + e^{-3\sigma^2\tau^2} (N_{12}) * N_6 + \\
& e^{-3\sigma^2\tau^2} (N_1) * N_7 + e^{-6\sigma^2\tau^2} (N_2) * N_7 + e^{-\sigma^2\tau^2} (N_3) * N_7 + e^{-7\sigma^2\tau^2} (N_4) * N_7 + \\
& e^{-2\sigma^2\tau^2} (N_5) * N_7 + e^{-5\sigma^2\tau^2} (N_6) * N_7 + (N_7) * N_7 + e^{-9\sigma^2\tau^2} (N_8) * N_7 + \\
& e^{-\sigma^2\tau^2} (N_9) * N_7 + e^{-7\sigma^2\tau^2} (N_{10}) * N_7 + e^{-3\sigma^2\tau^2} (N_{11}) * N_7 + e^{-6\sigma^2\tau^2} (N_{12}) * N_7 + \\
& e^{-6\sigma^2\tau^2} (N_1) * N_8 + e^{-3\sigma^2\tau^2} (N_2) * N_8 + e^{-7\sigma^2\tau^2} (N_3) * N_8 + e^{-\sigma^2\tau^2} (N_4) * N_8 + \\
& e^{-5\sigma^2\tau^2} (N_5) * N_8 + e^{-2\sigma^2\tau^2} (N_6) * N_8 + e^{-9\sigma^2\tau^2} (N_7) * N_8 + (N_8) * N_8 + \\
& e^{-7\sigma^2\tau^2} (N_9) * N_8 + e^{-\sigma^2\tau^2} (N_{10}) * N_8 + e^{-6\sigma^2\tau^2} (N_{11}) * N_8 + e^{-3\sigma^2\tau^2} (N_{12}) * N_8 + \\
& e^{-5\sigma^2\tau^2} (N_1) * N_9 + e^{-7\sigma^2\tau^2} (N_2) * N_9 + e^{-2\sigma^2\tau^2} (N_3) * N_9 + e^{-6\sigma^2\tau^2} (N_4) * N_9 + \\
& e^{-\sigma^2\tau^2} (N_5) * N_9 + e^{-3\sigma^2\tau^2} (N_6) * N_9 + e^{-\sigma^2\tau^2} (N_7) * N_9 + e^{-7\sigma^2\tau^2} (N_8) * N_9 + \\
& (N_9) * N_9 + e^{-4\sigma^2\tau^2} (N_{10}) * N_9 + e^{-\sigma^2\tau^2} (N_{11}) * N_9 + e^{-3\sigma^2\tau^2} (N_{12}) * N_9 + \\
& e^{-7\sigma^2\tau^2} (N_1) * N_{10} + e^{-5\sigma^2\tau^2} (N_2) * N_{10} + e^{-6\sigma^2\tau^2} (N_3) * N_{10} + e^{-2\sigma^2\tau^2} (N_4) * N_{10} + \\
& e^{-3\sigma^2\tau^2} (N_5) * N_{10} + e^{-\sigma^2\tau^2} (N_6) * N_{10} + e^{-7\sigma^2\tau^2} (N_7) * N_{10} + e^{-\sigma^2\tau^2} (N_8) * N_{10} + \\
& e^{-4\sigma^2\tau^2} (N_9) * N_{10} + (N_{10}) * N_{10} + e^{-3\sigma^2\tau^2} (N_{11}) * N_{10} + e^{-\sigma^2\tau^2} (N_{12}) * N_{10} + \\
& e^{-8\sigma^2\tau^2} (N_1) * N_{11} + e^{-9\sigma^2\tau^2} (N_2) * N_{11} + e^{-5\sigma^2\tau^2} (N_3) * N_{11} + e^{-7\sigma^2\tau^2} (N_4) * N_{11} + \\
& e^{-3\sigma^2\tau^2} (N_5) * N_{11} + e^{-4\sigma^2\tau^2} (N_6) * N_{11} + e^{-3\sigma^2\tau^2} (N_7) * N_{11} + e^{-6\sigma^2\tau^2} (N_8) * N_{11} + \\
& e^{-\sigma^2\tau^2} (N_9) * N_{11} + e^{-3\sigma^2\tau^2} (N_{10}) * N_{11} + (N_{11}) * N_{11} + e^{-\sigma^2\tau^2} (N_{12}) * N_{11} + \\
& e^{-9\sigma^2\tau^2} (N_1) * N_{12} + e^{-8\sigma^2\tau^2} (N_2) * N_{12} + e^{-7\sigma^2\tau^2} (N_3) * N_{12} + e^{-5\sigma^2\tau^2} (N_4) * N_{12} + \\
& e^{-4\sigma^2\tau^2} (N_5) * N_{12} + e^{-3\sigma^2\tau^2} (N_6) * N_{12} + e^{-6\sigma^2\tau^2} (N_7) * N_{12} + e^{-3\sigma^2\tau^2} (N_8) * N_{12} + \\
& e^{-3\sigma^2\tau^2} (N_9) * N_{12} + e^{-\sigma^2\tau^2} (N_{10}) * N_{12} + e^{-\sigma^2\tau^2} (N_{11}) * N_{12} + (N_{12}) * N_{12}.
\end{aligned}
\tag{A.16}$$

The plot of the coincidence probability against the time-delay τ between the arrival of the photons at input ports is shown in Fig.(A.4). This plot shows that the coincidence probability of having a bi-photon click at output port-1 and a single-photon click at the output port-1 and output port-2 simultaneously, for the case when we incident a bi-photon pulse at input port-1 and input port-2 such that there is a time delay τ is introduced between the arrival of the each photon at input port is minimum when there is no time delay between the arrival of the photons which is equal to the value of the permanent of the adjacent scattering matrix, The coincidence probability starts gradually increasing as the length of the time delay τ between the arrival of the photons at input ports of the balanced beam splitter increases and after a specific increase in the length of the time-delay τ it again starts decreasing. As we can see from Fig.(A.4)

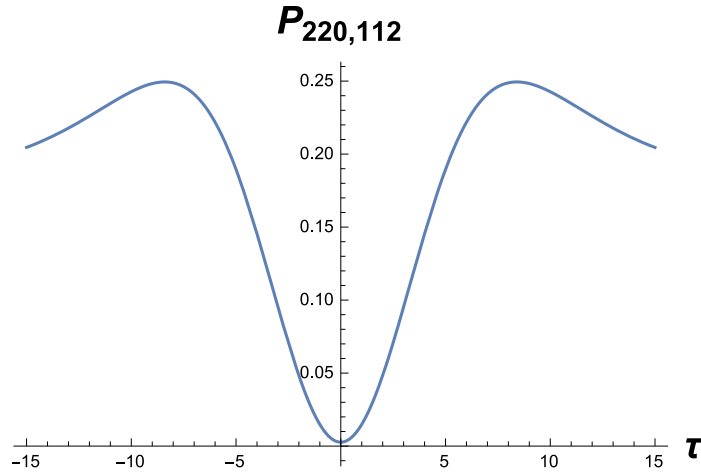


Figure A.4: (with $T(\tau_1, \tau_2, \tau_3, \tau_4) = T(-\tau, 0, \tau, 2\tau)$, $\sigma_o = 0.1$ and $\Omega(\alpha_1, \alpha_2, \alpha_3, \beta_1, \beta_2, \beta_3, \gamma_1, \gamma_2) = \Omega(0, 0, 0, \pi/2, \pi/2, \pi/2, 0, 0)$)

A.5 Tri-Photon Click on Output-1, Single-Photon Click on Output-3 and no click on Output-2

Now we shall discuss the coincidence probability for the output pattern, where we get a tri-photon click at output port-1 and a single-photon click on output port-3 for the same input state as defined in Eq.(3.5). For this case the output operators are defined as,

$$\Pi_1 = \int_{-\infty}^{\infty} \hat{a}_1^\dagger(\omega_5) \hat{a}_1^\dagger(\omega_8) \hat{a}_1^\dagger(\omega_{11}) |000\rangle \langle 000| \hat{a}_1^\dagger(\omega_5) \hat{a}_1^\dagger(\omega_8) \hat{a}_1^\dagger(\omega_{11}) d\omega_5 d\omega_8 d\omega_{11}, \quad (\text{A.17})$$

and

$$\Pi_3 = \int_{-\infty}^{\infty} \hat{a}_3^\dagger(\omega_7) |0\rangle \langle 0| \hat{a}_3(\omega_7) d\omega_7, \quad (\text{A.18})$$

the coincidence probability for this case can be written as

$$P_{220,301} = {}^s \langle 1111 | U^\dagger \Pi_1 \otimes \Pi_3 U | 1111 \rangle^s, \quad (\text{A.19})$$

so, the coincidence probability for this case is

$$\begin{aligned} P_{220,301} = & D_9 (D_{10})^* e^{-\sigma^2 \tau^2} + D_9 (D_{11})^* e^{-3\sigma^2 \tau^2} + D_9 (D_{12})^* e^{-6\sigma^2 \tau^2} + \\ & D_{10} (D_9)^* e^{-\sigma^2 \tau^2} + D_{10} (D_{11})^* e^{-\sigma^2 \tau^2} + D_{10} (D_{12})^* e^{-3\sigma^2 \tau^2} + \\ & D_{11} (D_9)^* e^{-3\sigma^2 \tau^2} + D_{11} (D_{10})^* e^{-\sigma^2 \tau^2} + D_{11} (D_{12})^* e^{-\sigma^2 \tau^2} + \\ & D_{12} (D_9)^* e^{-6\sigma^2 \tau^2} + D_{12} (D_{10})^* e^{-3\sigma^2 \tau^2} + D_{12} (D_{11})^* e^{-\sigma^2 \tau^2} + \\ & D_9 (D_9)^* + D_{10} (D_{10})^* + D_{11} (D_{11})^* + D_{12} (D_{12})^* \end{aligned} \quad (\text{A.20})$$

The plot of the coincidence probability for this specific output pattern against the time-delays τ between the arrival of the photons at input port of the balanced beam-splitter is shown in the Fig.(A.5). This plot in shows that the coincidence probability of having the desired output pattern, where we get a tri-photon click at output port-1 and a single-photon click at output port-3 is minimum but not zero, when the time-delay introduced between the arrival of the photons at the input ports of the balanced beam-splitter is zero and is equal to the value of the permanent of the adjacent scattering matrix. The coincidence probability starts gradually increasing as the length of the time-delay τ increases, as we see in Fig.(A.5).

A.6 Tri-Photon Click on Output-2, Single-Photon Click on Output-1 and no click on Output-3

Now we shall discuss the output state, when we get a tri-photon click at output port-2 and a single-photon click at output port-1 for the input state as defined in Eq.(3.5). For this case the output operators are defined as,

$$\Pi_1 = \int_{-\infty}^{\infty} \hat{a}_1^\dagger(\omega_5) |0\rangle \langle 0| \hat{a}_1^\dagger(\omega_5) d\omega_5, \quad (\text{A.21})$$

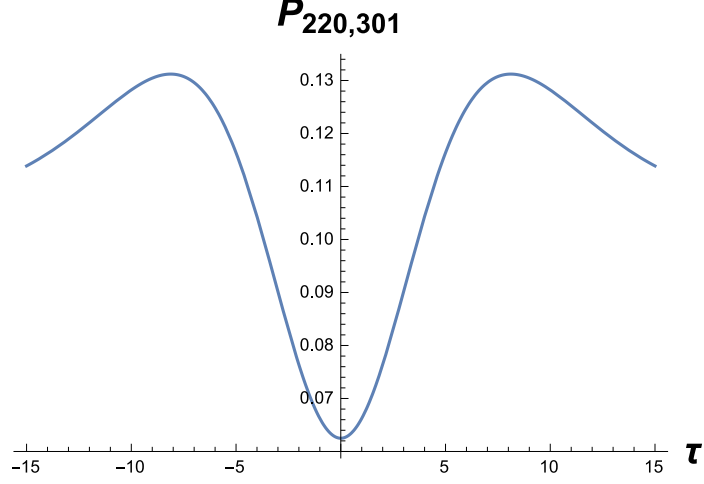


Figure A.5: (with $T(\tau_1, \tau_2, \tau_3, \tau_4) = T(-\tau, 0, \tau, 2\tau)$, $\sigma_o = 0.1$ and $\Omega(\alpha_1, \alpha_2, \alpha_3, \beta_1, \beta_2, \beta_3, \gamma_1, \gamma_2) = \Omega(0, 0, 0, \pi/2, \pi/2, \pi/2, 0, 0)$)

and

$$\Pi_2 = \int_{-\infty}^{\infty} \hat{a}_2^\dagger(\omega_6) \hat{a}_2^\dagger(\omega_9) \hat{a}_2^\dagger(\omega_{12}) |000\rangle \langle 000| \hat{a}_2(\omega_6) \hat{a}_2(\omega_9) \hat{a}_2(\omega_{12}) d\omega_6 d\omega_9 d\omega_{12}, \quad (\text{A.22})$$

the coincidence probability for this case can be written as

$$P_{220,130} = {}^s \langle 1111 | U^\dagger \Pi_1 \otimes \Pi_2 U | 1111 \rangle^s, \quad (\text{A.23})$$

so, the coincidence probability for this case is

$$\begin{aligned} P_{220,130} = & D_5 (D_6)^* e^{-\sigma^2 \tau^2} + D_5 (D_7)^* e^{-3\sigma^2 \tau^2} + D_5 (D_8)^* e^{-6\sigma^2 \tau^2} + D_6 (D_5)^* e^{-\sigma^2 \tau^2} + \\ & D_6 (D_7)^* e^{-\sigma^2 \tau^2} + D_6 (D_8)^* e^{-3\sigma^2 \tau^2} + D_7 (D_5)^* e^{-3\sigma^2 \tau^2} + D_7 (D_6)^* e^{-\sigma^2 \tau^2} + \\ & D_7 (D_8)^* e^{-\sigma^2 \tau^2} + D_8 (D_5)^* e^{-6\sigma^2 \tau^2} + D_8 (D_6)^* e^{-3\sigma^2 \tau^2} + D_8 (D_7)^* e^{-\sigma^2 \tau^2} + \\ & D_5 (D_5)^* + D_6 (D_6)^* + D_7 (D_7)^* + D_8 (D_8)^*. \end{aligned} \quad (\text{A.24})$$

The plot of the coincidence probability for this specific case against the time-delay introduced between the arrival of the photons at input port of the balanced beam-splitter is shown in the Fig.(A.6). This plot shows that the coincidence probability of having the desired output pattern, where we get a tri-photon click at output port-2 and a single-photon click at output port-1 is maximum when the length of the time delay introduced between the arrival of the photons at the input ports of the balanced beam-splitter is zero and is equal to the value of the permanent of adjacent scattering matrix. The coincidence probability starts gradually decreasing as the length of the time-delay τ increases.

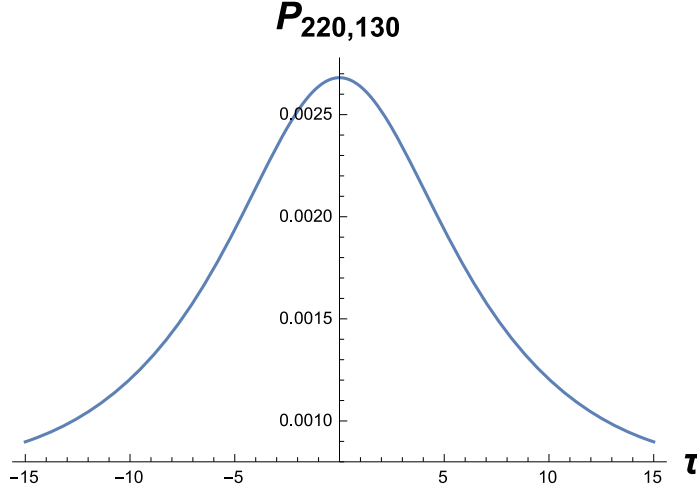


Figure A.6: (with $T(\tau_1, \tau_2, \tau_3, \tau_4) = T(-\tau, 0, \tau, 2\tau)$, $\sigma_o = 0.1$ and $\Omega(\alpha_1, \alpha_2, \alpha_3, \beta_1, \beta_2, \beta_3, \gamma_1, \gamma_2) = \Omega(0, 0, 0, \pi/2, \pi/2, \pi/2, 0, 0)$)

A.7 Tri-Photon Click on Output-2, Single-Photon Click on Output-3 and no click on Output-1

Now we shall discuss the coincidence probability for output pattern, where we get a tri-photon click at output port-2 and a single-photon click on output port-3 for the input state as defined in $W_q(3.5)$. For this case the output operators are defined as,

$$\Pi_2 = \int_{-\infty}^{\infty} \hat{a}_2^\dagger(\omega_6) \hat{a}_2^\dagger(\omega_9) \hat{a}_2^\dagger(\omega_{12}) |000\rangle \langle 000| \hat{a}_2(\omega_6) \hat{a}_2(\omega_9) \hat{a}_2(\omega_{12}) d\omega_6 d\omega_9 d\omega_{12}, \quad (\text{A.25})$$

and

$$\Pi_3 = \int_{-\infty}^{\infty} \hat{a}_3^\dagger(\omega_7) |0\rangle \langle 0| \hat{a}_3(\omega_7) d\omega_7, \quad (\text{A.26})$$

the coincidence probability for this case can be written as

$$P_{220,031} = {}^s \langle 1111 | U^\dagger \Pi_2 \otimes \Pi_3 U | 1111 \rangle^s, \quad (\text{A.27})$$

so, the coincidence probability for this case is

$$\begin{aligned} P_{220,031} = & D_{13} (D_{14})^* e^{-\sigma^2 \tau^2} + D_{13} (D_{15})^* e^{-3\sigma^2 \tau^2} + D_{13} (D_{16})^* e^{-6\sigma^2 \tau^2} + \\ & D_{14} (D_{13})^* e^{-\sigma^2 \tau^2} + D_{14} (D_{15})^* e^{-\sigma^2 \tau^2} + D_{14} (D_{16})^* e^{-3\sigma^2 \tau^2} + \\ & D_{15} (D_{13})^* e^{-3\sigma^2 \tau^2} + D_{15} (D_{14})^* e^{-\sigma^2 \tau^2} + D_{15} (D_{16})^* e^{-\sigma^2 \tau^2} + \end{aligned}$$

$$D_{16} (D_{13})^* e^{-6\sigma^2\tau^2} + D_{16} (D_{14})^* e^{-3\sigma^2\tau^2} + D_{16} (D_{15})^* e^{-\sigma^2\tau^2} + D_{13} (D_{13})^* + D_{14} (D_{14})^* + D_{15} (D_{15})^* + D_{16} (D_{16})^* \quad (\text{A.28})$$

The plot of the coincidence probability against the time delay τ between the arrival of the photons at input port of the balanced beam splitter is shown in the Fig.(A.7). This plot shows that the probability of having the desired output is greater when we introduce the time-delays between the arrival of the photon at input ports of the beam splitter and is equal to the value of the permanent of the adjacent scattering matrix. It slightly increases with the increase in the length of the time delay and then gradually decreases to zero with further increase in the length of the time-delay τ introduced.

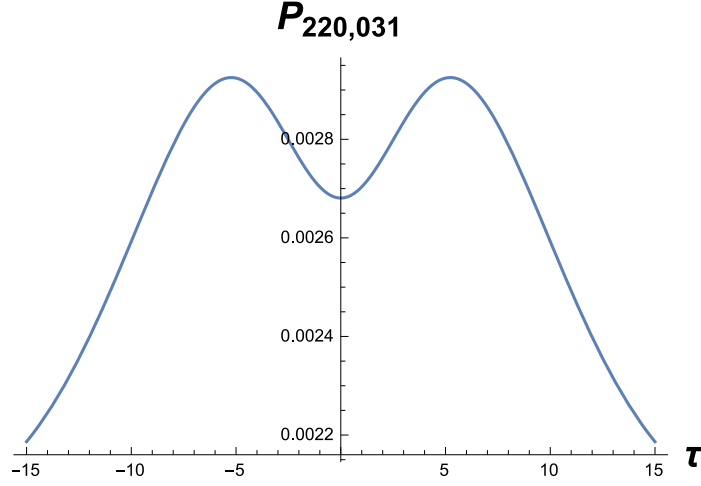


Figure A.7: (with $T(\tau_1, \tau_2, \tau_3, \tau_4) = T(-\tau, 0, \tau, 2\tau)$, $\sigma_o = 0.1$ and $\Omega(\alpha_1, \alpha_2, \alpha_3, \beta_1, \beta_2, \beta_3, \gamma_1, \gamma_2) = \Omega(0, 0, 0, \pi/2, \pi/2, \pi/2, 0, 0)$)

A.8 Tri-Photon Click on Output-3, Single-Photon Click on Output-1 and no click on Output-2

Now we shall discuss the coincidence probability of output pattern, where we get a tri-photon click at output port-3 and a single-photon click on output port-1, for the input state as defined in Eq.(3.5). For this case the output operators are defined as,

$$\Pi_1 = \int_{-\infty}^{\infty} \hat{a}_1^\dagger(\omega_5) |0\rangle \langle 0| \hat{a}_1^\dagger(\omega_5) d\omega_5, \quad (\text{A.29})$$

and

$$\Pi_3 = \int_{-\infty}^{\infty} \hat{a}_3^\dagger(\omega_7) \hat{a}_3^\dagger(\omega_{10}) \hat{a}_3^\dagger(\omega_{13}) |000\rangle \langle 000| \hat{a}_3(\omega_7) \hat{a}_3(\omega_{10}) \hat{a}_3(\omega_{13}) d\omega_7 d\omega_{10} d\omega_{13}, \quad (\text{A.30})$$

the coincidence probability for this case can be written as

$$P_{220,103} = {}^s \langle 1111 | U^\dagger \Pi_1 \otimes \Pi_3 U | 1111 \rangle^s, \quad (\text{A.31})$$

so, the coincidence probability for this case is

$$\begin{aligned} P_{220,103} = & D_{17} (D_{18})^* e^{-\sigma^2 \tau^2} + D_{17} (D_{19})^* e^{-3\sigma^2 \tau^2} + D_{17} (D_{20})^* e^{-6\sigma^2 \tau^2} + \\ & D_{18} (D_{17})^* e^{-\sigma^2 \tau^2} + D_{18} (D_{19})^* e^{-\sigma^2 \tau^2} + D_{18} (D_{20})^* e^{-3\sigma^2 \tau^2} + \\ & D_{19} (D_{17})^* e^{-3\sigma^2 \tau^2} + D_{19} (D_{18})^* e^{-\sigma^2 \tau^2} + D_{19} (D_{20})^* e^{-\sigma^2 \tau^2} + \\ & D_{20} (D_{17})^* e^{-6\sigma^2 \tau^2} + D_{20} (D_{18})^* e^{-3\sigma^2 \tau^2} + D_{20} (D_{19})^* e^{-\sigma^2 \tau^2} + \\ & D_{17} (D_{17})^* + D_{18} (D_{18})^* + D_{19} (D_{19})^* + D_{20} (D_{20})^* \end{aligned} \quad (\text{A.32})$$

The plot of the coincidence probability against the time-delays between the arrival of the photons at input port of the balanced beam-splitter is shown in the Fig.(A.8). This plot shows that the coincidence probability of having tri-photon click at output port-3 and a single-photon pulse at output port-1 is minimum, when the time-delays introduced between the arrival of the photons at the input ports of the balanced beam-splitter are zero and is equal to the value of the permanent of the adjacent scattering matrix. The coincidence probability starts gradually increasing as the length of time-delays τ increases and then again decreases when the length of the time-delays reaches a specific point.

A.9 Tri-Photon Click on Output-3, Single-Photon Click on Output-2 and no click on Output-1

Now we shall discuss the coincidence probability of output pattern, where we get a tri-photon click at output port-3 and a single-photon click on output port-2, for the input state as defined in Eq.(3.5). For this case the output operators are defined as,

$$\Pi_2 = \int_{-\infty}^{\infty} \hat{a}_2^\dagger(\omega_6) |0\rangle \langle 0| \hat{a}_2(\omega_6) d\omega_6, \quad (\text{A.33})$$

and

$$\Pi_3 = \int_{-\infty}^{\infty} \hat{a}_3^\dagger(\omega_7) \hat{a}_3^\dagger(\omega_{10}) \hat{a}_3^\dagger(\omega_{13}) |000\rangle \langle 000| \hat{a}_3(\omega_7) \hat{a}_3(\omega_{10}) \hat{a}_3(\omega_{13}) d\omega_7 d\omega_{10} d\omega_{13}, \quad (\text{A.34})$$

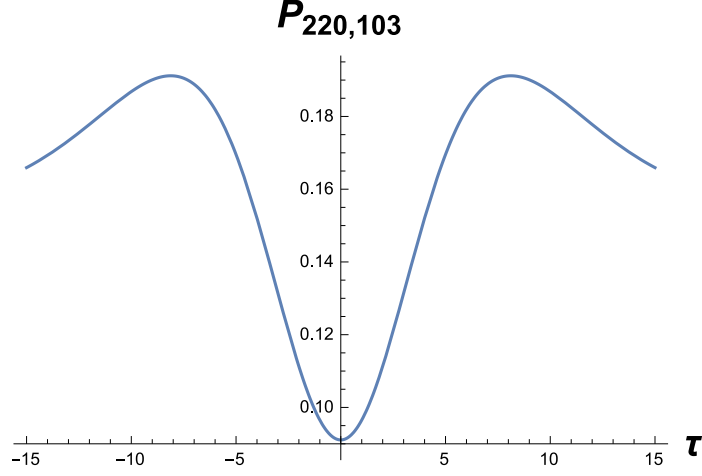


Figure A.8: (with $T(\tau_1, \tau_2, \tau_3, \tau_4) = T(-\tau, 0, \tau, 2\tau)$, $\sigma_o = 0.1$ and $\Omega(\alpha_1, \alpha_2, \alpha_3, \beta_1, \beta_2, \beta_3, \gamma_1, \gamma_2) = \Omega(0, 0, 0, \pi/2, \pi/2, \pi/2, 0, 0)$)

the coincidence probability for this case can be written as

$$P_{220,013} = {}^s \langle 1111 | U^\dagger \Pi_2 \otimes \Pi_3 U | 1111 \rangle^s, \quad (\text{A.35})$$

so, the coincidence probability for this case is

$$\begin{aligned} P_{220,013} = & D_{21} (D_{22})^* e^{-\sigma^2 \tau^2} + D_{21} (D_{23})^* e^{-3\sigma^2 \tau^2} + D_{21} (D_{24})^* e^{-6\sigma^2 \tau^2} + \\ & D_{22} (D_{21})^* e^{-\sigma^2 \tau^2} + D_{22} (D_{23})^* e^{-\sigma^2 \tau^2} + D_{22} (D_{24})^* e^{-3\sigma^2 \tau^2} + \\ & D_{23} (D_{21})^* e^{-3\sigma^2 \tau^2} + D_{23} (D_{22})^* e^{-\sigma^2 \tau^2} + D_{23} (D_{24})^* e^{-\sigma^2 \tau^2} + \\ & D_{24} (D_{21})^* e^{-6\sigma^2 \tau^2} + D_{24} (D_{22})^* e^{-3\sigma^2 \tau^2} + D_{24} (D_{23})^* e^{-\sigma^2 \tau^2} + \\ & D_{21} (D_{21})^* + D_{22} (D_{22})^* + D_{23} (D_{23})^* + D_{24} (D_{24})^* \end{aligned} \quad (\text{A.36})$$

The plot of the coincidence probability against the time delay τ between the arrival of the photons at input port of the balanced beam splitter is shown in the Fig.(A.9). This plot shows that the probability of having the desire output is greater when we introduce the time-delay between the arrival of the photon at input ports of the balanced beam splitter and is equal to the value of the permanent of the adjacent scattering matrix for this specific caes. The coincidence probability slightly increases with the increase in the length of the time delay τ and then gradually decreases to zero with further increase in the length of the time delay introduced.

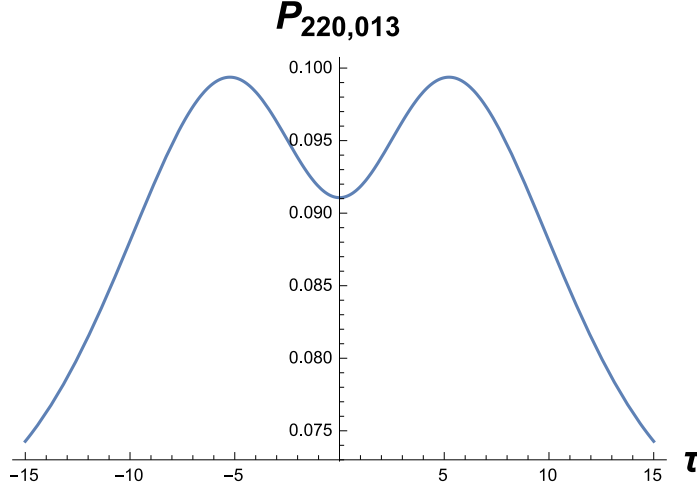


Figure A.9: (with $T(\tau_1, \tau_2, \tau_3, \tau_4) = T(-\tau, 0, \tau, 2\tau)$, $\sigma_o = 0.1$ and $\Omega(\alpha_1, \alpha_2, \alpha_3, \beta_1, \beta_2, \beta_3, \gamma_1, \gamma_2) = \Omega(0, 0, 0, \pi/2, \pi/2, \pi/2, 0, 0)$)

A.10 Tetra-Photon Click on Output-2 and no Click on Output-1 and Output-3

In this case, we shall discuss the coincidence probability for the case when we get a tetra-photon pulse at output port-2 and no click at output port-1 and output port-3. For this case the input state will same as defined in Eq.(3.5) and the output operators are defined as,

$$\begin{aligned} \Pi_2 = \int_{-\infty}^{\infty} \hat{a}_2^\dagger(\omega_6) \hat{a}_2^\dagger(\omega_9) \hat{a}_2^\dagger(\omega_{12}) \hat{a}_1^\dagger(\omega_{15}) |0000\rangle \langle 0000| \\ \hat{a}_2(\omega_6) \hat{a}_2(\omega_9) \hat{a}_2(\omega_{12}) \hat{a}_2(\omega_{15}) d\omega_6 d\omega_9 d\omega_{12} d\omega_{15}, \end{aligned} \quad (\text{A.37})$$

the coincidence probability for this case can be written as,

$$P_{220,040} = {}^s \langle 1111 | U^\dagger \Pi_2 U | 1111 \rangle^s, \quad (\text{A.38})$$

and the probability coefficient for this case are defined as,

$$V_2 = U_{21}^2 U_{22}^2; \quad (\text{A.39})$$

so, the coincidence probability for this case is

$$P_{220,040} = V_2 (V_2)^*. \quad (\text{A.40})$$

We can clearly see. the coincidence probability for this specific case does not depend on the time delay introduced between the arrival of the photons at input ports of a balanced beam splitter.

A.11 Tetra-Photon Click on Output-3 and no Click on Output-1 and Output-2

In this case, we shall discuss the coincidence probability for the case when we get a tetra-photon pulse at output port-3 and no click at output port-1 and output port-2. For this case the input state will same as defined in Eq.(3.5) and the output operators are defined as,

$$\begin{aligned} \Pi_3 = \int_{-\infty}^{\infty} \hat{a}_3^\dagger(\omega_7) \hat{a}_3^\dagger(\omega_{10}) \hat{a}_3^\dagger(\omega_{13}) \hat{a}_3^\dagger(\omega_{16}) |0000\rangle \langle 0000| \\ \hat{a}_3(\omega_7) \hat{a}_3(\omega_{10}) \hat{a}_3(\omega_{13}) \hat{a}_3(\omega_{16}) d\omega_7 d\omega_{10} d\omega_{13} d\omega_{16}, \end{aligned} \quad (\text{A.41})$$

the coincidence probability for this case can be written as,

$$P_{220,004} = {}^s \langle 1111 | U^\dagger \Pi_3 U | 1111 \rangle^s, \quad (\text{A.42})$$

and the probability coefficient for this case are defined as,

$$V_3 = U_{31}^2 U_{32}^2 \quad (\text{A.43})$$

so, the coincidence probability for this case is

$$P_{220,004} = V_3 (V_3)^*. \quad (\text{A.44})$$

We can clearly see. the coincidence probability for this specific case does not depend on the time delay introduced between the arrival of the photons at input ports of a balanced beam splitter.

B Rest of the Cases of Section 3.2

In this case, we have injected a bi-photon input pulse at input port 1, input port 3 and nothing input port 2 of a six port passive quantum optical interferometer and then calculate and plotted the coincidence probabilities of all output coincidence patterns as shown in Fig.3.8, Fig.3.10, Fig.3.12 and Fig.3.14.

B.1 Bi-Photon Click on Output-1 and Output-3 and no Click on Output-2

In this case, we shall discuss the coincidence probability for one of the possible output coincidence pattern such that we have a bi-photon click at output port-1 and at output port-3. For this kind of the output we have taken the same input pattern in which, we have injected a bi-photon pulse in input port-1 and in input

port-3 as shown in Fig.(3.8). The output operators for this specific case are the same as defined in Eq.(3.2) and Eq.(3.4), the input state is same as defined in Eq.(3.23) and the coincidence probability for this case can be written as,

$$P_{202,202} = {}^s \langle 1111 | U^\dagger \Pi_1 \otimes \Pi_3 U | 1111 \rangle^s, \quad (\text{B.1})$$

so, the coincidence probability is

$$\begin{aligned} P_{202,202} = & B_7 (B_8)^* e^{-\sigma^2 \tau^2} + B_7 (B_9)^* e^{-3\sigma^2 \tau^2} + B_7 (B_{10})^* e^{-3\sigma^2 \tau^2} + B_7 (B_{11})^* e^{-5\sigma^2 \tau^2} + \\ & B_7 (B_{12})^* e^{-8\sigma^2 \tau^2} + B_8 (B_7)^* e^{-\sigma^2 \tau^2} + B_8 (B_9)^* e^{-\sigma^2 \tau^2} + B_8 (B_{10})^* e^{-\sigma^2 \tau^2} + \\ & B_8 (B_{11})^* e^{-2\sigma^2 \tau^2} + B_8 (B_{12})^* e^{-5\sigma^2 \tau^2} + B_9 (B_7)^* e^{-3\sigma^2 \tau^2} + B_9 (B_8)^* e^{-\sigma^2 \tau^2} + \\ & B_9 (B_{10})^* e^{-2\sigma^2 \tau^2} + B_9 (B_{11})^* e^{-\sigma^2 \tau^2} + B_9 (B_{12})^* e^{-3\sigma^2 \tau^2} + B_{10} (B_7)^* e^{-3\sigma^2 \tau^2} + \\ & B_{10} (B_8)^* e^{-\sigma^2 \tau^2} + B_{10} (B_9)^* e^{-2\sigma^2 \tau^2} + B_{10} (B_{11})^* e^{-\sigma^2 \tau^2} + B_{10} (B_{12})^* e^{-3\sigma^2 \tau^2} + \\ & B_{11} (B_7)^* e^{-5\sigma^2 \tau^2} + B_{11} (B_8)^* e^{-2\sigma^2 \tau^2} + B_{11} (B_9)^* e^{-\sigma^2 \tau^2} + B_{11} (B_{10})^* e^{-\sigma^2 \tau^2} + \\ & B_{11} (B_{12})^* e^{-\sigma^2 \tau^2} + B_{12} (B_7)^* e^{-8\sigma^2 \tau^2} + B_{12} (B_8)^* e^{-5\sigma^2 \tau^2} + B_{12} (B_9)^* e^{-3\sigma^2 \tau^2} + \\ & B_{12} (B_{10})^* e^{-3\sigma^2 \tau^2} + B_{12} (B_{11})^* e^{-\sigma^2 \tau^2} + B_7 (B_7)^* + B_8 (B_8)^* + B_9 (B_9)^* + \\ & B_{10} (B_{10})^* + B_{11} (B_{11})^* + B_{12} (B_{12})^*. \end{aligned} \quad (\text{B.2})$$

Where B's are the probability coefficients and already been defined in the Eq.(3.25). The plot of the coincidence probability against the time-delay τ introduced between the arrival of the photons at input ports is shown in Fig.(B.1). The plot shows that the coincidence probability of having the output coincidence pattern such that we get a bi-photon click on output port-1 and output port-2 is maximum, when the time delay τ introduced between the arrival of the photon at input ports is maximum and equal to the value of the permanent of adjacent scattering matrix. This coincidence probability starts decreasing as the length of the time-delay introduced between the arrival of the photons at input ports increases and there is a point when the probability of having such output coincidence become zero.

B.2 Bi-Photon Click on Output-2 and Output-3 and no Click on Output-1

In this section, we shall discuss the output coincidence pattern where have a bi-photon click at output port-2 and at output port-3 and no click at output port-1, for the input state as define in Eq.(3.23). The output operators for this case are defined in Eq.(3.3) and Eq.(3.4) and the coincidence probability for this case can be written as,

$$P_{202,022} = {}^s \langle 1111 | U^\dagger \Pi_2 \otimes \Pi_3 U | 1111 \rangle^s, \quad (\text{B.3})$$

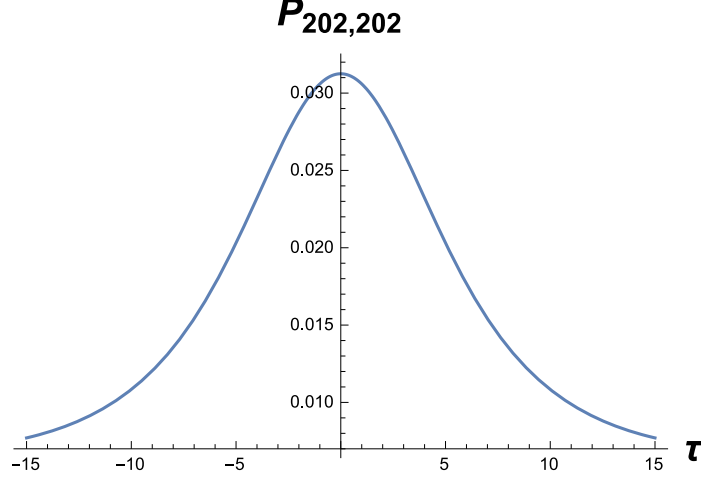


Figure B.1: (with $T(\tau_1, \tau_2, \tau_3, \tau_4) = T(-\tau, 0, \tau, 2\tau)$, $\sigma_o = 0.1$ and $\Omega(\alpha_1, \alpha_2, \alpha_3, \beta_1, \beta_2, \beta_3, \gamma_1, \gamma_2) = \Omega(0, 0, 0, \pi/2, \pi/2, \pi/2, 0, 0)$)

where B's are the probability coefficients and already been defined in the Eq.(3.25). The coincidence probability is

$$\begin{aligned}
P_{202,022} = & B_{13}(B_{14})^* e^{-\sigma^2 \tau^2} + B_{13}(B_{15})^* e^{-3\sigma^2 \tau^2} + B_{13}(B_{16})^* e^{-3\sigma^2 \tau^2} + B_{13}(B_{17})^* e^{-5\sigma^2 \tau^2} + \\
& B_{13}(B_{18})^* e^{-8\sigma^2 \tau^2} + B_{14}(B_{13})^* e^{-\sigma^2 \tau^2} + B_{14}(B_{15})^* e^{-\sigma^2 \tau^2} + B_{14}(B_{16})^* e^{-\sigma^2 \tau^2} + \\
& B_{14}(B_{17})^* e^{-2\sigma^2 \tau^2} + B_{14}(B_{18})^* e^{-5\sigma^2 \tau^2} + B_{15}(B_{13})^* e^{-3\sigma^2 \tau^2} + B_{15}(B_{14})^* e^{-\sigma^2 \tau^2} + \\
& B_{15}(B_{16})^* e^{-2\sigma^2 \tau^2} + B_{15}(B_{17})^* e^{-\sigma^2 \tau^2} + B_{15}(B_{18})^* e^{-3\sigma^2 \tau^2} + B_{16}(B_{13})^* e^{-3\sigma^2 \tau^2} + \\
& B_{16}(B_{14})^* e^{-\sigma^2 \tau^2} + B_{16}(B_{15})^* e^{-2\sigma^2 \tau^2} + B_{16}(B_{17})^* e^{-\sigma^2 \tau^2} + B_{16}(B_{18})^* e^{-3\sigma^2 \tau^2} + \\
& B_{17}(B_{13})^* e^{-5\sigma^2 \tau^2} + B_{17}(B_{14})^* e^{-2\sigma^2 \tau^2} + B_{17}(B_{15})^* e^{-\sigma^2 \tau^2} + B_{17}(B_{16})^* e^{-\sigma^2 \tau^2} + \\
& B_{17}(B_{18})^* e^{-\sigma^2 \tau^2} + B_{18}(B_{13})^* e^{-8\sigma^2 \tau^2} + B_{18}(B_{14})^* e^{-5\sigma^2 \tau^2} + B_{18}(B_{15})^* e^{-3\sigma^2 \tau^2} + \\
& B_{18}(B_{16})^* e^{-3\sigma^2 \tau^2} + B_{18}(B_{17})^* e^{-\sigma^2 \tau^2} + B_{13}(B_{13})^* + B_{14}(B_{14})^* + B_{15}(B_{15})^* + \\
& B_{16}(B_{16})^* + B_{17}(B_{17})^* + B_{18}(B_{18})^*. \tag{B.4}
\end{aligned}$$

The coincidence probability plot against the time-delays introduced between the arrival of the photons at input ports of the balanced beam-splitter is shown in Fig.(B.2). The plot shows that the coincidence probability of having a bi-photon click at output port-2 and output port-3, when we have injection a bi-photon click at input port-1 and input port-3 is minimum and equal to the value of the permanent of the adjacent scattering matrix when there are no time-delays τ introduced between the arrival of the photon at input ports of the balanced beam-splitter. The coincidence probability starts increasing when the length of

time-delays introduced between the arrival of the photons at input ports increases, first sharply the slowly and after a specific increase in the length of the time-delay the coincidence probability becomes constant.

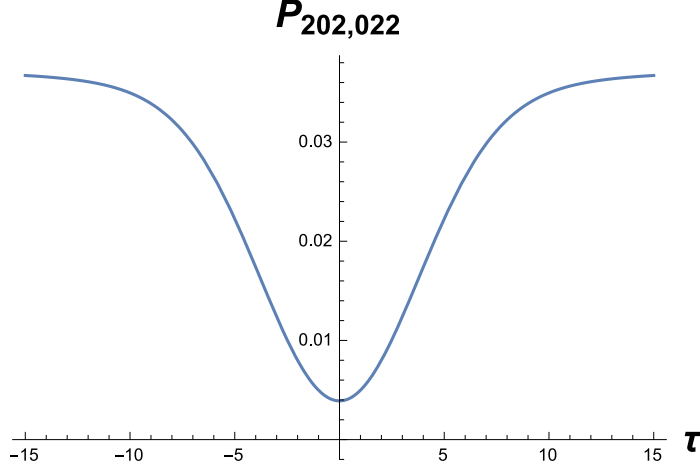


Figure B.2: (with $T(\tau_1, \tau_2, \tau_3, \tau_4) = T(-\tau, 0, \tau, 2\tau)$, $\sigma_o = 0.1$ and $\Omega(\alpha_1, \alpha_2, \alpha_3, \beta_1, \beta_2, \beta_3, \gamma_1, \gamma_2) = \Omega(0, 0, 0, \pi/2, \pi/2, \pi/2, 0, 0)$)

B.3 Bi-Photon Click on Output-2 and Single-Photon Click on Output-1 and Output-3

In the section, we shall discuss the coincidence probability for the second output pattern shown in Fig.(3.10). In this case we get a bi-photon click at output port-2 and single-photon clicks at output port-1 and output port-3. Input state has already been defined in Eq.(3.23) and output operators are defined as

$$\Pi_1 = \int_{-\infty}^{\infty} \hat{a}_1^\dagger(\omega_5) |0\rangle \langle 0| \hat{a}_1(\omega_5) d\omega_5, \quad (\text{B.5})$$

$$\Pi_2 = \int_{-\infty}^{\infty} \hat{a}_2^\dagger(\omega_6) \hat{a}_2^\dagger(\omega_9) |00\rangle \langle 00| \hat{a}_2(\omega_6) \hat{a}_2(\omega_9) d\omega_6 d\omega_9, \quad (\text{B.6})$$

and

$$\Pi_3 = \int_{-\infty}^{\infty} \hat{a}_3^\dagger(\omega_7) |0\rangle \langle 0| \hat{a}_3(\omega_7) d\omega_7, \quad (\text{B.7})$$

the coincidence probability for this case can be written as

$$P_{202,121} = \langle 1111|^s U^\dagger \Pi_1 \otimes \Pi_2 \otimes \Pi_3 U |1111\rangle^s, \quad (\text{B.8})$$

so the coincidence probability is,

$$\begin{aligned}
P_{202,121} = & (P_1) * P_1 + e^{-\sigma^2\tau^2} (P_2) * P_1 + e^{-\sigma^2\tau^2} (P_3) * P_1 + e^{-3\sigma^2\tau^2} (P_4) * P_1 + \\
& e^{-3\sigma^2\tau^2} (P_5) * P_1 + e^{-4\sigma^2\tau^2} (P_6) * P_1 + e^{-3\sigma^2\tau^2} (P_7) * P_1 + e^{-6\sigma^2\tau^2} (P_8) * P_1 + \\
& e^{-5\sigma^2\tau^2} (P_9) * P_1 + e^{-7\sigma^2\tau^2} (P_{10}) * P_1 + e^{-8\sigma^2\tau^2} (P_{11}) * P_1 + e^{-9\sigma^2\tau^2} (P_{12}) * P_1 + \\
& e^{-\sigma^2\tau^2} (P_1) * P_2 + (P_2) * P_2 + e^{-3\sigma^2\tau^2} (P_3) * P_2 + e^{-\sigma^2\tau^2} (P_4) * P_2 + \\
& e^{-4\sigma^2\tau^2} (P_5) * P_2 + e^{-3\sigma^2\tau^2} (P_6) * P_2 + e^{-6\sigma^2\tau^2} (P_7) * P_2 + e^{-3\sigma^2\tau^2} (P_8) * P_2 + \\
& e^{-7\sigma^2\tau^2} (P_9) * P_2 + e^{-5\sigma^2\tau^2} (P_{10}) * P_2 + e^{-9\sigma^2\tau^2} (P_{11}) * P_2 + e^{-8\sigma^2\tau^2} (P_{12}) * P_2 + \\
& e^{-\sigma^2\tau^2} (P_1) * P_3 + e^{-3\sigma^2\tau^2} (P_2) * P_3 + (P_3) * P_3 + e^{-4\sigma^2\tau^2} (P_4) * P_3 + \\
& e^{-\sigma^2\tau^2} (P_5) * P_3 + e^{-3\sigma^2\tau^2} (P_6) * P_3 + e^{-\sigma^2\tau^2} (P_7) * P_3 + e^{-7\sigma^2\tau^2} (P_8) * P_3 + \\
& e^{-2\sigma^2\tau^2} (P_9) * P_3 + e^{-6\sigma^2\tau^2} (P_{10}) * P_3 + e^{-5\sigma^2\tau^2} (P_{11}) * P_3 + e^{-7\sigma^2\tau^2} (P_{12}) * P_3 + \\
& e^{-3\sigma^2\tau^2} (P_1) * P_4 + e^{-\sigma^2\tau^2} (P_2) * P_4 + e^{-4\sigma^2\tau^2} (P_3) * P_4 + (P_4) * P_4 + \\
& e^{-3\sigma^2\tau^2} (P_5) * P_4 + e^{-\sigma^2\tau^2} (P_6) * P_4 + e^{-7\sigma^2\tau^2} (P_7) * P_4 + e^{-\sigma^2\tau^2} (P_8) * P_4 + \\
& e^{-6\sigma^2\tau^2} (P_9) * P_4 + e^{-2\sigma^2\tau^2} (P_{10}) * P_4 + e^{-7\sigma^2\tau^2} (P_{11}) * P_4 + e^{-5\sigma^2\tau^2} (P_{12}) * P_4 + \\
& e^{-3\sigma^2\tau^2} (P_1) * P_5 + e^{-4\sigma^2\tau^2} (P_2) * P_5 + e^{-\sigma^2\tau^2} (P_3) * P_5 + e^{-3\sigma^2\tau^2} (P_4) * P_5 + \\
& (P_5) * P_5 + e^{-\sigma^2\tau^2} (P_6) * P_5 + e^{-2\sigma^2\tau^2} (P_7) * P_5 + e^{-5\sigma^2\tau^2} (P_8) * P_5 + \\
& e^{-\sigma^2\tau^2} (P_9) * P_5 + e^{-3\sigma^2\tau^2} (P_{10}) * P_5 + e^{-3\sigma^2\tau^2} (P_{11}) * P_5 + e^{-4\sigma^2\tau^2} (P_{12}) * P_5 + \\
& e^{-4\sigma^2\tau^2} (P_1) * P_6 + e^{-3\sigma^2\tau^2} (P_2) * P_6 + e^{-3\sigma^2\tau^2} (P_3) * P_6 + e^{-\sigma^2\tau^2} (P_4) * P_6 + \\
& e^{-\sigma^2\tau^2} (P_5) * P_6 + (P_6) * P_6 + e^{-5\sigma^2\tau^2} (P_7) * P_6 + e^{-2\sigma^2\tau^2} (P_8) * P_6 + \\
& e^{-3\sigma^2\tau^2} (P_9) * P_6 + e^{-\sigma^2\tau^2} (P_{10}) * P_6 + e^{-4\sigma^2\tau^2} (P_{11}) * P_6 + e^{-3\sigma^2\tau^2} (P_{12}) * P_6 + \\
& e^{-3\sigma^2\tau^2} (P_1) * P_7 + e^{-6\sigma^2\tau^2} (P_2) * P_7 + e^{-\sigma^2\tau^2} (P_3) * P_7 + e^{-7\sigma^2\tau^2} (P_4) * P_7 + \\
& e^{-2\sigma^2\tau^2} (P_5) * P_7 + e^{-5\sigma^2\tau^2} (P_6) * P_7 + (P_7) * P_7 + e^{-9\sigma^2\tau^2} (P_8) * P_7 + \\
& e^{-\sigma^2\tau^2} (P_9) * P_7 + e^{-7\sigma^2\tau^2} (P_{10}) * P_7 + e^{-3\sigma^2\tau^2} (P_{11}) * P_7 + e^{-6\sigma^2\tau^2} (P_{12}) * P_7 + \\
& e^{-6\sigma^2\tau^2} (P_1) * P_8 + e^{-3\sigma^2\tau^2} (P_2) * P_8 + e^{-7\sigma^2\tau^2} (P_3) * P_8 + e^{-\sigma^2\tau^2} (P_4) * P_8 + \\
& e^{-5\sigma^2\tau^2} (P_5) * P_8 + e^{-2\sigma^2\tau^2} (P_6) * P_8 + e^{-9\sigma^2\tau^2} (P_7) * P_8 + (P_8) * P_8 + \\
& e^{-7\sigma^2\tau^2} (P_9) * P_8 + e^{-\sigma^2\tau^2} (P_{10}) * P_8 + e^{-6\sigma^2\tau^2} (P_{11}) * P_8 + e^{-3\sigma^2\tau^2} (P_{12}) * P_8 + \\
& e^{-5\sigma^2\tau^2} (P_1) * P_9 + e^{-7\sigma^2\tau^2} (P_2) * P_9 + e^{-2\sigma^2\tau^2} (P_3) * P_9 + e^{-6\sigma^2\tau^2} (P_4) * P_9 + \\
& e^{-\sigma^2\tau^2} (P_5) * P_9 + e^{-3\sigma^2\tau^2} (P_6) * P_9 + e^{-\sigma^2\tau^2} (P_7) * P_9 + e^{-7\sigma^2\tau^2} (P_8) * P_9 + \\
& (P_9) * P_9 + e^{-4\sigma^2\tau^2} (P_{10}) * P_9 + e^{-\sigma^2\tau^2} (P_{11}) * P_9 + e^{-3\sigma^2\tau^2} (P_{12}) * P_9 + \\
& e^{-7\sigma^2\tau^2} (P_1) * P_{10} + e^{-5\sigma^2\tau^2} (P_2) * P_{10} + e^{-6\sigma^2\tau^2} (P_3) * P_{10} + e^{-2\sigma^2\tau^2} (P_4) * P_{10} +
\end{aligned}$$

$$\begin{aligned}
& e^{-3\sigma^2\tau^2} (P_5) * P_{10} + e^{-\sigma^2\tau^2} (P_6) * P_{10} + e^{-7\sigma^2\tau^2} (P_7) * P_{10} + e^{-\sigma^2\tau^2} (P_8) * P_{10} + \\
& e^{-4\sigma^2\tau^2} (P_9) * P_{10} + (P_{10}) * P_{10} + e^{-3\sigma^2\tau^2} (P_{11}) * P_{10} + e^{-\sigma^2\tau^2} (P_{12}) * P_{10} + \\
& e^{-8\sigma^2\tau^2} (P_1) * P_{11} + e^{-9\sigma^2\tau^2} (P_2) * P_{11} + e^{-5\sigma^2\tau^2} (P_3) * P_{11} + e^{-7\sigma^2\tau^2} (P_4) * P_{11} + \\
& e^{-3\sigma^2\tau^2} (P_5) * P_{11} + e^{-4\sigma^2\tau^2} (P_6) * P_{11} + e^{-3\sigma^2\tau^2} (P_7) * P_{11} + e^{-6\sigma^2\tau^2} (P_8) * P_{11} + \\
& e^{-\sigma^2\tau^2} (P_9) * P_{11} + e^{-3\sigma^2\tau^2} (P_{10}) * P_{11} + (P_{11}) * P_{11} + e^{-\sigma^2\tau^2} (P_{12}) * P_{11} + \\
& e^{-9\sigma^2\tau^2} (P_1) * P_{12} + e^{-8\sigma^2\tau^2} (P_2) * P_{12} + e^{-7\sigma^2\tau^2} (P_3) * P_{12} + e^{-5\sigma^2\tau^2} (P_4) * P_{12} + \\
& e^{-4\sigma^2\tau^2} (P_5) * P_{12} + e^{-3\sigma^2\tau^2} (P_6) * P_{12} + e^{-6\sigma^2\tau^2} (P_7) * P_{12} + e^{-3\sigma^2\tau^2} (P_8) * P_{12} + \\
& e^{-3\sigma^2\tau^2} (P_9) * P_{12} + e^{-\sigma^2\tau^2} (P_{10}) * P_{12} + e^{-\sigma^2\tau^2} (P_{11}) * P_{12} + (P_{12}) * P_{12}.
\end{aligned} \tag{B.9}$$

Where P's are the probability coefficients and are given as

$$\begin{aligned}
P_1 &= U_{13}U_{21}^2U_{33}; & P_2 &= U_{13}U_{21}^2U_{33}; & P_3 &= U_{11}U_{21}U_{23}U_{33}; & P_4 &= U_{13}U_{21}U_{23}U_{31}; \\
P_5 &= U_{11}U_{21}U_{23}U_{33}; & P_6 &= U_{13}U_{21}U_{23}U_{31}; & P_7 &= U_{11}U_{21}U_{23}U_{33}; & P_8 &= U_{13}U_{21}U_{23}U_{31}; \\
P_9 &= U_{11}U_{21}U_{23}U_{33}; & P_{10} &= U_{13}U_{21}U_{23}U_{31}; & P_{11} &= U_{11}U_{23}^2U_{31}; & P_{12} &= U_{11}U_{23}^2U_{31}.
\end{aligned} \tag{B.10}$$

The coincidence probability plot against the time-delays introduced between the arrival of the photons at the input of the balanced beam-splitter is shown in Fig.(B.3). This Coincidence probability plot shows that the probability of having the above defined output coincidence patter is minimum when there is no time-delays introduced between the arrival of the photon at the input ports and is equal the value of the permanent of the adjacent scattering matrix. The value of the coincidence probability starts increases with the increase in the length of the time-delays introduced between the arrival of the photons till specific point and then again starts decreasing.

B.4 Bi-Photon Click on Output-3 and Single-Photon Click on Output-1 and Output-2

In the section, we shall discuss the coincidence probability of the third output coincidence pattern shown in Fig.(3.10). In this case we get a bi-photon click at output port-3 and single-photon clicks at output port-1 and output port-2. Input state has already been defined in Eq.(3.23) and output operators are defined as

$$\Pi_1 = \int_{-\infty}^{\infty} \hat{a}_1^\dagger(\omega_5) |0\rangle \langle 0| \hat{a}_1(\omega_5) d\omega_5, \tag{B.11}$$

$$\Pi_2 = \int_{-\infty}^{\infty} \hat{a}_2^\dagger(\omega_6) \hat{a}_2^\dagger(\omega_9) |00\rangle \langle 00| \hat{a}_2(\omega_6) \hat{a}_2(\omega_9) d\omega_6 d\omega_9, \tag{B.12}$$

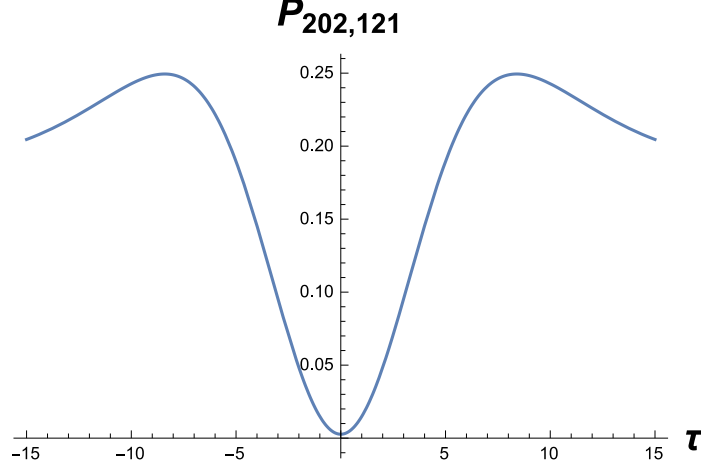


Figure B.3: (with $T(\tau_1, \tau_2, \tau_3, \tau_4) = T(-\tau, 0, \tau, 2\tau)$, $\sigma_o = 0.1$ and $\Omega(\alpha_1, \alpha_2, \alpha_3, \beta_1, \beta_2, \beta_3, \gamma_1, \gamma_2) = \Omega(0, 0, 0, \pi/2, \pi/2, \pi/2, 0, 0)$)

and

$$\Pi_3 = \int_{-\infty}^{\infty} \hat{a}_3^\dagger(\omega_7) \hat{a}_3^\dagger(\omega_{10}) |00\rangle \langle 00| \hat{a}_3(\omega_7) \hat{a}_3(\omega_{10}) d\omega_7 d\omega_{10}, \quad (\text{B.13})$$

the coincidence probability for this case can be written as

$$P_{202,112} = \langle 1111 |^s U^\dagger \Pi_1 \otimes \Pi_2 \otimes \Pi_3 U |1111\rangle^s, \quad (\text{B.14})$$

so the coincidence probability for this case is,

$$\begin{aligned} P_{202,112} = & (Q_1) * Q_1 + e^{-\sigma^2 \tau^2} (Q_2) * Q_1 + e^{-\sigma^2 \tau^2} (Q_3) * Q_1 + e^{-3\sigma^2 \tau^2} (Q_4) * Q_1 + \\ & e^{-3\sigma^2 \tau^2} (Q_5) * Q_1 + e^{-4\sigma^2 \tau^2} (Q_6) * Q_1 + e^{-3\sigma^2 \tau^2} (Q_7) * Q_1 + e^{-6\sigma^2 \tau^2} (Q_8) * Q_1 + \\ & e^{-5\sigma^2 \tau^2} (Q_9) * Q_1 + e^{-7\sigma^2 \tau^2} (Q_{10}) * Q_1 + e^{-8\sigma^2 \tau^2} (Q_{11}) * Q_1 + e^{-9\sigma^2 \tau^2} (Q_{12}) * Q_1 + \\ & e^{-\sigma^2 \tau^2} (Q_1) * Q_2 + (Q_2) * Q_2 + e^{-3\sigma^2 \tau^2} (Q_3) * Q_2 + e^{-\sigma^2 \tau^2} (Q_4) * Q_2 + \\ & e^{-4\sigma^2 \tau^2} (Q_5) * Q_2 + e^{-3\sigma^2 \tau^2} (Q_6) * Q_2 + e^{-6\sigma^2 \tau^2} (Q_7) * Q_2 + e^{-3\sigma^2 \tau^2} (Q_8) * Q_2 + \\ & e^{-7\sigma^2 \tau^2} (Q_9) * Q_2 + e^{-5\sigma^2 \tau^2} (Q_{10}) * Q_2 + e^{-9\sigma^2 \tau^2} (Q_{11}) * Q_2 + e^{-8\sigma^2 \tau^2} (Q_{12}) * Q_2 + \\ & e^{-\sigma^2 \tau^2} (Q_1) * Q_3 + e^{-3\sigma^2 \tau^2} (Q_2) * Q_3 + (Q_3) * Q_3 + e^{-4\sigma^2 \tau^2} (Q_4) * Q_3 + \\ & e^{-\sigma^2 \tau^2} (Q_5) * Q_3 + e^{-3\sigma^2 \tau^2} (Q_6) * Q_3 + e^{-\sigma^2 \tau^2} (Q_7) * Q_3 + e^{-7\sigma^2 \tau^2} (Q_8) * Q_3 + \\ & e^{-2\sigma^2 \tau^2} (Q_9) * Q_3 + e^{-6\sigma^2 \tau^2} (Q_{10}) * Q_3 + e^{-5\sigma^2 \tau^2} (Q_{11}) * Q_3 + e^{-7\sigma^2 \tau^2} (Q_{12}) * Q_3 + \\ & e^{-3\sigma^2 \tau^2} (Q_1) * Q_4 + e^{-\sigma^2 \tau^2} (Q_2) * Q_4 + e^{-4\sigma^2 \tau^2} (Q_3) * Q_4 + (Q_4) * Q_4 + \\ & e^{-3\sigma^2 \tau^2} (Q_5) * Q_4 + e^{-\sigma^2 \tau^2} (Q_6) * Q_4 + e^{-7\sigma^2 \tau^2} (Q_7) * Q_4 + e^{-\sigma^2 \tau^2} (Q_8) * Q_4 + \end{aligned}$$

$$\begin{aligned}
& e^{-6\sigma^2\tau^2} (Q_9) * Q_4 + e^{-2\sigma^2\tau^2} (Q_{10}) * Q_4 + e^{-7\sigma^2\tau^2} (Q_{11}) * Q_4 + e^{-5\sigma^2\tau^2} (Q_{12}) * Q_4 + \\
& e^{-3\sigma^2\tau^2} (Q_1) * Q_5 + e^{-4\sigma^2\tau^2} (Q_2) * Q_5 + e^{-\sigma^2\tau^2} (Q_3) * Q_5 + e^{-3\sigma^2\tau^2} (Q_4) * Q_5 + \\
& (Q_5) * Q_5 + e^{-\sigma^2\tau^2} (Q_6) * Q_5 + e^{-2\sigma^2\tau^2} (Q_7) * Q_5 + e^{-5\sigma^2\tau^2} (Q_8) * Q_5 + \\
& e^{-\sigma^2\tau^2} (Q_9) * Q_5 + e^{-3\sigma^2\tau^2} (Q_{10}) * Q_5 + e^{-3\sigma^2\tau^2} (Q_{11}) * Q_5 + e^{-4\sigma^2\tau^2} (Q_{12}) * Q_5 + \\
& e^{-4\sigma^2\tau^2} (Q_1) * Q_6 + e^{-3\sigma^2\tau^2} (Q_2) * Q_6 + e^{-3\sigma^2\tau^2} (Q_3) * Q_6 + e^{-\sigma^2\tau^2} (Q_4) * Q_6 + \\
& e^{-\sigma^2\tau^2} (Q_5) * Q_6 + (Q_6) * Q_6 + e^{-5\sigma^2\tau^2} (Q_7) * Q_6 + e^{-2\sigma^2\tau^2} (Q_8) * Q_6 + \\
& e^{-3\sigma^2\tau^2} (Q_9) * Q_6 + e^{-\sigma^2\tau^2} (Q_{10}) * Q_6 + e^{-4\sigma^2\tau^2} (Q_{11}) * Q_6 + e^{-3\sigma^2\tau^2} (Q_{12}) * Q_6 + \\
& e^{-3\sigma^2\tau^2} (Q_1) * Q_7 + e^{-6\sigma^2\tau^2} (Q_2) * Q_7 + e^{-\sigma^2\tau^2} (Q_3) * Q_7 + e^{-7\sigma^2\tau^2} (Q_4) * Q_7 + \\
& e^{-2\sigma^2\tau^2} (Q_5) * Q_7 + e^{-5\sigma^2\tau^2} (Q_6) * Q_7 + (Q_7) * Q_7 + e^{-9\sigma^2\tau^2} (Q_8) * Q_7 + \\
& e^{-\sigma^2\tau^2} (Q_9) * Q_7 + e^{-7\sigma^2\tau^2} (Q_{10}) * Q_7 + e^{-3\sigma^2\tau^2} (Q_{11}) * Q_7 + e^{-6\sigma^2\tau^2} (Q_{12}) * Q_7 + \\
& e^{-6\sigma^2\tau^2} (Q_1) * Q_8 + e^{-3\sigma^2\tau^2} (Q_2) * Q_8 + e^{-7\sigma^2\tau^2} (Q_3) * Q_8 + e^{-\sigma^2\tau^2} (Q_4) * Q_8 + \\
& e^{-5\sigma^2\tau^2} (Q_5) * Q_8 + e^{-2\sigma^2\tau^2} (Q_6) * Q_8 + e^{-9\sigma^2\tau^2} (Q_7) * Q_8 + (Q_8) * Q_8 + \\
& e^{-7\sigma^2\tau^2} (Q_9) * Q_8 + e^{-\sigma^2\tau^2} (Q_{10}) * Q_8 + e^{-6\sigma^2\tau^2} (Q_{11}) * Q_8 + e^{-3\sigma^2\tau^2} (Q_{12}) * Q_8 + \\
& e^{-5\sigma^2\tau^2} (Q_1) * Q_9 + e^{-7\sigma^2\tau^2} (Q_2) * Q_9 + e^{-2\sigma^2\tau^2} (Q_3) * Q_9 + e^{-6\sigma^2\tau^2} (Q_4) * Q_9 + \\
& e^{-\sigma^2\tau^2} (Q_5) * Q_9 + e^{-3\sigma^2\tau^2} (Q_6) * Q_9 + e^{-\sigma^2\tau^2} (Q_7) * Q_9 + e^{-7\sigma^2\tau^2} (Q_8) * Q_9 + \\
& (Q_9) * Q_9 + e^{-4\sigma^2\tau^2} (Q_{10}) * Q_9 + e^{-\sigma^2\tau^2} (Q_{11}) * Q_9 + e^{-3\sigma^2\tau^2} (Q_{12}) * Q_9 + \\
& e^{-7\sigma^2\tau^2} (Q_1) * Q_{10} + e^{-5\sigma^2\tau^2} (Q_2) * Q_{10} + e^{-6\sigma^2\tau^2} (Q_3) * Q_{10} + e^{-2\sigma^2\tau^2} (Q_4) * Q_{10} + \\
& e^{-3\sigma^2\tau^2} (Q_5) * Q_{10} + e^{-\sigma^2\tau^2} (Q_6) * Q_{10} + e^{-7\sigma^2\tau^2} (Q_7) * Q_{10} + e^{-\sigma^2\tau^2} (Q_8) * Q_{10} + \\
& e^{-4\sigma^2\tau^2} (Q_9) * Q_{10} + (Q_{10}) * Q_{10} + e^{-3\sigma^2\tau^2} (Q_{11}) * Q_{10} + e^{-\sigma^2\tau^2} (Q_{12}) * Q_{10} + \\
& e^{-8\sigma^2\tau^2} (Q_1) * Q_{11} + e^{-9\sigma^2\tau^2} (Q_2) * Q_{11} + e^{-5\sigma^2\tau^2} (Q_3) * Q_{11} + e^{-7\sigma^2\tau^2} (Q_4) * Q_{11} + \\
& e^{-3\sigma^2\tau^2} (Q_5) * Q_{11} + e^{-4\sigma^2\tau^2} (Q_6) * Q_{11} + e^{-3\sigma^2\tau^2} (Q_7) * Q_{11} + e^{-6\sigma^2\tau^2} (Q_8) * Q_{11} + \\
& e^{-\sigma^2\tau^2} (Q_9) * Q_{11} + e^{-3\sigma^2\tau^2} (Q_{10}) * Q_{11} + (Q_{11}) * Q_{11} + e^{-\sigma^2\tau^2} (Q_{12}) * Q_{11} + \\
& e^{-9\sigma^2\tau^2} (Q_1) * Q_{12} + e^{-8\sigma^2\tau^2} (Q_2) * Q_{12} + e^{-7\sigma^2\tau^2} (Q_3) * Q_{12} + e^{-5\sigma^2\tau^2} (Q_4) * Q_{12} + \\
& e^{-4\sigma^2\tau^2} (Q_5) * Q_{12} + e^{-3\sigma^2\tau^2} (Q_6) * Q_{12} + e^{-6\sigma^2\tau^2} (Q_7) * Q_{12} + e^{-3\sigma^2\tau^2} (Q_8) * Q_{12} + \\
& e^{-3\sigma^2\tau^2} (Q_9) * Q_{12} + e^{-\sigma^2\tau^2} (Q_{10}) * Q_{12} + e^{-\sigma^2\tau^2} (Q_{11}) * Q_{12} + (Q_{12}) * Q_{12}.
\end{aligned} \tag{B.15}$$

Where Q 's are the probability coefficients and are given as

$$\begin{aligned}
Q_1 &= U_{13}U_{23}U_{31}^2; & Q_2 &= U_{13}U_{23}U_{31}^2; & Q_3 &= U_{11}U_{23}U_{31}U_{33}; & Q_4 &= U_{13}U_{21}U_{31}U_{33}; \\
Q_5 &= U_{11}U_{23}U_{31}U_{33}; & Q_6 &= U_{13}U_{21}U_{31}U_{33}; & Q_7 &= U_{11}U_{23}U_{31}U_{33}; & Q_8 &= U_{13}U_{21}U_{31}U_{33};
\end{aligned}$$

$$Q_9 = U_{11}U_{23}U_{31}U_{33}; \quad Q_{10} = U_{13}U_{21}U_{31}U_{33}; \quad Q_{11} = U_{11}U_{21}U_{33}^2; \quad Q_{12} = U_{11}U_{21}U_{33}^2. \quad (\text{B.16})$$

The coincidence probability plot against the time-delays introduced between the arrival of the photons at the input of the balanced beam-splitter is shown in Fig.(B.4). The coincidence probability plot shows that the coincidence probability of getting a bi-photon click at output port-3 and single-photon clicks at output port-1 and output port-2 is maximum and equal the value of the permanent of adjacent scattering matrix, when the time-delays introduced between the arrival of the photons at input ports of the balanced beam-splitter. The coincidence probability starts decreasing as the length of the time-delay increases and gradually drops to zero when length reaches a specific point.

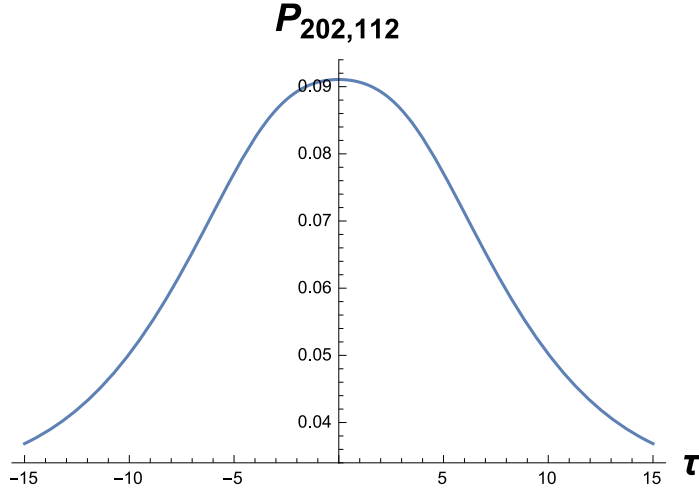


Figure B.4: (with $T(\tau_1, \tau_2, \tau_3, \tau_4) = T(-\tau, 0, \tau, 2\tau)$, $\sigma_o = 0.1$ and $\Omega(\alpha_1, \alpha_2, \alpha_3, \beta_1, \beta_2, \beta_3, \gamma_1, \gamma_2) = \Omega(0, 0, 0, \pi/2, \pi/2, \pi/2, 0, 0)$)

B.5 Tri-Photon Click on Output-1, Single-Photon Click on Output-3 and no click on Output-2

In this case, we shall discuss second output in Fig.(3.12, in which we get a tri-photon click at output port-1, a single-photon click at output port-3 and no click at output detector-2. The Input state has already been defined in Eq.(3.23) and the output operators for this case are defined as,

$$\Pi_1 = \int_{-\infty}^{\infty} \hat{a}_1^\dagger(\omega_5) \hat{a}_1^\dagger(\omega_8) \hat{a}_1^\dagger(\omega_{11}) |000\rangle \langle 000| \hat{a}_1(\omega_5) \hat{a}_1(\omega_8) \hat{a}_1(\omega_{11}) d\omega_5 d\omega_8 d\omega_{11}, \quad (\text{B.17})$$

and

$$\Pi_3 = \int_{-\infty}^{\infty} \hat{a}_3^\dagger(\omega_7) |0\rangle \langle 0| \hat{a}_3^\dagger(\omega_7) d\omega_7, \quad (\text{B.18})$$

the coincidence probability for this case can be written as

$$P_{202,301} = {}^s \langle 1111 | U^\dagger \Pi_1 \otimes \Pi_3 U | 1111 \rangle^s, \quad (\text{B.19})$$

the probability coefficients (F's) have already been defined in Eq.(3.37). The coincidence probability is

$$\begin{aligned} P_{202,301} = & F_1(F_2)^* e^{-\sigma^2 \tau^2} + F_1(F_3)^* e^{-3\sigma^2 \tau^2} + F_1(F_4)^* e^{-6\sigma^2 \tau^2} + F_2(F_1)^* e^{-\sigma^2 \tau^2} + \\ & F_2(F_3)^* e^{-\sigma^2 \tau^2} + F_2(F_4)^* e^{-3\sigma^2 \tau^2} + F_3(F_1)^* e^{-3\sigma^2 \tau^2} + F_3(F_2)^* e^{-\sigma^2 \tau^2} + \\ & F_3(F_4)^* e^{-\sigma^2 \tau^2} + F_4(F_1)^* e^{-6\sigma^2 \tau^2} + F_4(F_2)^* e^{-3\sigma^2 \tau^2} + F_4(F_3)^* e^{-\sigma^2 \tau^2} + \\ & F_1(F_1)^* + F_2(F_2)^* + F_3(F_3)^* + F_4(F_4)^*. \end{aligned} \quad (\text{B.20})$$

The coincidence probability plot against the time-delays introduced between the arrival of the photons at input ports of the balanced beam-splitter is shown in Fig.(B.5). The coincidence probability plot against the time-delays introduced between the arrival of the photons at the input ports of the balanced beam-splitter shows that the probability of having the above defined output coincidence pattern is maximum and is equal to the value of the permanent of the adjacent scattering matrix, when there is no time-delays introduced between the arrival of the photons. The coincidence probability starts decreasing with the increase in the length of the time-delays introduced between the arrival of the photons at input ports of the balanced beam-splitter and gradually become zero when the length of the time-delays increases to a specific point.

B.6 Tri-Photon Click on Output-2, Single-Photon Click on Output-1 and no click on Output-3

In this case, we shall discuss the coincidence probability of having a tri-photon click at output port-2 and a single-photon click at output port-1 as shown in Fig.(3.12). The input state for this specific case is same as defined in Eq3.23 and the output operators are defined as,

$$\Pi_1 = \int_{-\infty}^{\infty} \hat{a}_1^\dagger(\omega_5) |0\rangle \langle 0| \hat{a}_1(\omega_5) d\omega_5, \quad (\text{B.21})$$

and

$$\Pi_2 = \int_{-\infty}^{\infty} \hat{a}_2^\dagger(\omega_6) \hat{a}_2^\dagger(\omega_9) \hat{a}_2^\dagger(\omega_{12}) |000\rangle \langle 000| \hat{a}_2(\omega_6) \hat{a}_2(\omega_9) \hat{a}_2(\omega_{12}) d\omega_6 d\omega_9 d\omega_{12}, \quad (\text{B.22})$$

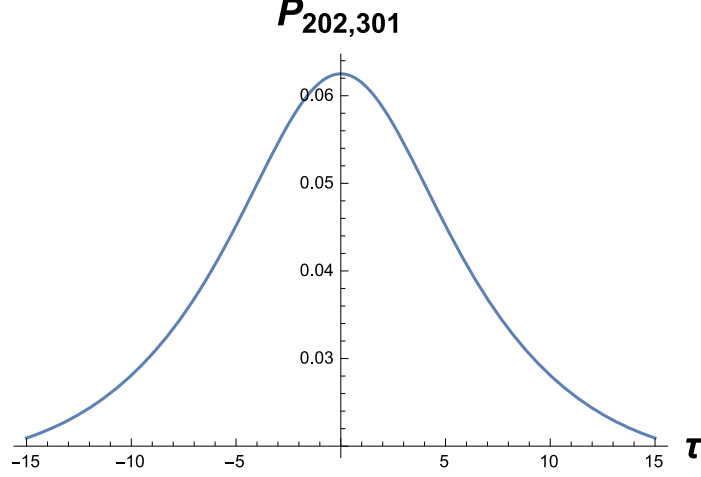


Figure B.5: (with $T(\tau_1, \tau_2, \tau_3, \tau_4) = T(-\tau, 0, \tau, 2\tau)$, $\sigma_o = 0.1$ and $\Omega(\alpha_1, \alpha_2, \alpha_3, \beta_1, \beta_2, \beta_3, \gamma_1, \gamma_2) = \Omega(0, 0, 0, \pi/2, \pi/2, \pi/2, 0, 0)$)

the coincidence probability for this case can be written as,

$$P_{202,130} = {}^s \langle 1111 | U^\dagger \Pi_1 \otimes \Pi_2 U | 1111 \rangle^s, \quad (\text{B.23})$$

the probability coefficients (F's) have already been defined in Eq.(3.37). The coincidence probability is

$$\begin{aligned} P_{202,130} = & F_{13}(F_{14})^* e^{-\sigma^2 \tau^2} + F_{13}(F_{15})^* e^{-3\sigma^2 \tau^2} + F_{13}(F_{16})^* e^{-6\sigma^2 \tau^2} + \\ & F_{14}(F_{13})^* e^{-\sigma^2 \tau^2} + F_{14}(F_{15})^* e^{-\sigma^2 \tau^2} + F_{14}(F_{16})^* e^{-3\sigma^2 \tau^2} + \\ & F_{15}(F_{13})^* e^{-3\sigma^2 \tau^2} + F_{15}(F_{14})^* e^{-\sigma^2 \tau^2} + F_{15}(F_{16})^* e^{-\sigma^2 \tau^2} + \\ & F_{16}(F_{13})^* e^{-6\sigma^2 \tau^2} + F_{16}(F_{14})^* e^{-3\sigma^2 \tau^2} + F_{16}(F_{15})^* e^{-\sigma^2 \tau^2} + \\ & F_{13}(F_{13})^* + F_{14}(F_{14})^* + F_{15}(F_{15})^* + F_{16}(F_{16})^*. \end{aligned} \quad (\text{B.24})$$

The plot of the coincidence probability for this case against the time-delays introduced between the arrival of the photon at input ports is shown in Fig.(B.6). This plot of coincidence probability of having a tri-photon click at output port-2 and single-photon click at output port-2 shows that the coincidence probability is minimum and equal to the value of the permanent of the adjacent scattering matrix, when the time-delays τ introduced between the arrival of the photons at input ports of the balanced beam-splitter is zero. This coincidence probability of having the above-mentioned output coincidence pattern increases with the increase in the length of the time-delays τ till a specific value of the time-delays and then again decreases with any further increase in the length of the time-delays.

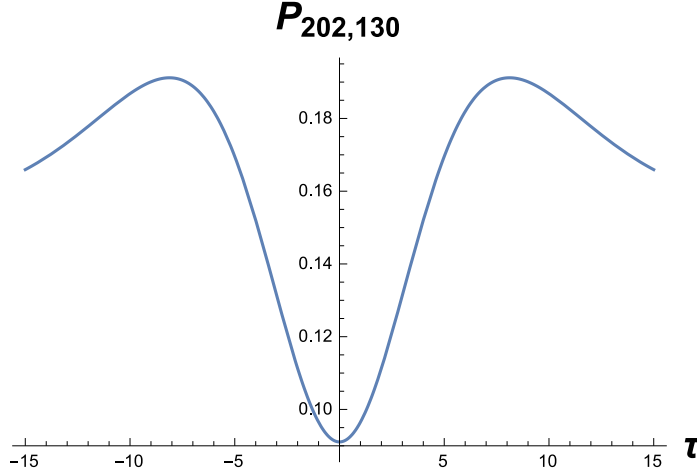


Figure B.6: (with $T(\tau_1, \tau_2, \tau_3, \tau_4) = T(-\tau, 0, \tau, 2\tau)$, $\sigma_o = 0.1$ and $\Omega(\alpha_1, \alpha_2, \alpha_3, \beta_1, \beta_2, \beta_3, \gamma_1, \gamma_2) = \Omega(0, 0, 0, \pi/2, \pi/2, \pi/2, 0, 0)$)

B.7 Tri-Photon Click on Output-2, Single-Photon Click on Output-3 and no click on Output-1

In this case, we shall discuss the coincidence probability of having a tri-photon click at output port-2 and a single-photon click at output port-3 as shown in Fig.(3.12). The input state for this case is the same as defined in Eq.(3.23) and the output operators are defined as,

$$\Pi_3 = \int_{-\infty}^{\infty} \hat{a}_3^\dagger(\omega_7) |0\rangle \langle 0| \hat{a}_3(\omega_7) d\omega_7, \quad (\text{B.25})$$

and

$$\Pi_2 = \int_{-\infty}^{\infty} \hat{a}_2^\dagger(\omega_6) \hat{a}_2^\dagger(\omega_9) \hat{a}_2^\dagger(\omega_{12}) |000\rangle \langle 000| \hat{a}_2(\omega_6) \hat{a}_2(\omega_9) \hat{a}_2(\omega_{12}) d\omega_6 d\omega_9 d\omega_{12}, \quad (\text{B.26})$$

the coincidence probability for this case can be written as,

$$P_{202,031} = {}^s \langle 1111 | U^\dagger \Pi_2 \otimes \Pi_3 U | 1111 \rangle^s, \quad (\text{B.27})$$

the probability coefficients (F's) have already been defined in Eq.(3.37). The coincidence probability is

$$P_{202,031} = F_{17}(F_{18})^* e^{-\sigma^2 \tau^2} + F_{17}(F_{19})^* e^{-3\sigma^2 \tau^2} + F_{17}(F_{20})^* e^{-6\sigma^2 \tau^2} + \\ F_{18}(F_{17})^* e^{-\sigma^2 \tau^2} + F_{18}(F_{19})^* e^{-\sigma^2 \tau^2} + F_{18}(F_{20})^* e^{-3\sigma^2 \tau^2} +$$

$$\begin{aligned}
& F_{19} (F_{17})^* e^{-3\sigma^2\tau^2} + F_{19} (F_{18})^* e^{-\sigma^2\tau^2} + F_{19} (F_{20})^* e^{-\sigma^2\tau^2} + \\
& F_{20} (F_{17})^* e^{-6\sigma^2\tau^2} + F_{20} (F_{18})^* e^{-3\sigma^2\tau^2} + F_{20} (F_{19})^* e^{-\sigma^2\tau^2} + \\
& F_{17} (F_{17})^* + F_{18} (F_{18})^* + F_{19} (F_{19})^* + F_{20} (F_{20})^* \quad (\text{B.28})
\end{aligned}$$

The coincidence probability plot of having a tri-photon click at output port-2 and single-photon click at output port-3 against the time-delays τ introduced between the arrival of the photons at input ports is shown in Fig.(B.7). The plot shows that the coincidence probability of having the above defined output coincidence pattern is relatively high and equal to the value of the permanent of the adjacent scattering matrix, when time-delays τ introduced between the arrival of the incident photons at input ports is zero. The coincidence probability slightly increases as we increase the length of the time-delays τ then after a specific increase in the length of the time-delay, coincidence probability starts to decrease and become zero when the time-delays increases to a specific value.

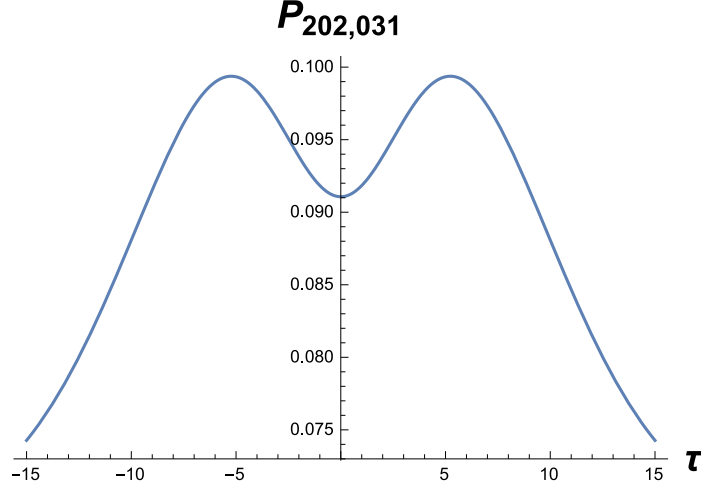


Figure B.7: (with $T(\tau_1, \tau_2, \tau_3, \tau_4) = T(-\tau, 0, \tau, 2\tau)$, $\sigma_o = 0.1$ and $\Omega(\alpha_1, \alpha_2, \alpha_3, \beta_1, \beta_2, \beta_3, \gamma_1, \gamma_2) = \Omega(0, 0, 0, \pi/2, \pi/2, \pi/2, 0, 0)$)

B.8 Tri-Photon Click on Output-3, Single-Photon Click on Output-1 and no click on Output-2

In this case, we shall discuss the coincidence probability of the output coincidence pattern shown in Fig.(3.12), in which we get a tri-photon click at output port-3 and a single-photon click at output port-1. The input state is same as defined in Eq.(3.23) and the output operator for this case are defined as

$$\Pi_1 = \int_{-\infty}^{\infty} \hat{a}_1^\dagger(\omega_5) |0\rangle \langle 0| \hat{a}_1(\omega_5) d\omega_5, \quad (\text{B.29})$$

and

$$\Pi_3 = \int_{-\infty}^{\infty} \hat{a}_3^\dagger(\omega_7) \hat{a}_3^\dagger(\omega_{10}) \hat{a}_3^\dagger(\omega_{13}) |000\rangle \langle 000| \hat{a}_3(\omega_7) \hat{a}_3(\omega_{10}) \hat{a}_3(\omega_{13}) d\omega_7 d\omega_{10} d\omega_{13}, \quad (\text{B.30})$$

the coincidence probability for this case can be written as

$$P_{202,103} = {}^s \langle 1111 | U^\dagger \Pi_1 \otimes \Pi_3 U | 1111 \rangle^s, \quad (\text{B.31})$$

the probability coefficients (F's) have already been defined in Eq.(3.37). The coincidence probability is

$$\begin{aligned} P_{202,103} = & F_5 (F_6)^* e^{-\sigma^2 \tau^2} + F_5 (F_7)^* e^{-3\sigma^2 \tau^2} + F_5 (F_8)^* e^{-6\sigma^2 \tau^2} + F_6 (F_5)^* e^{-\sigma^2 \tau^2} + \\ & F_6 (F_7)^* e^{-\sigma^2 \tau^2} + F_6 (F_8)^* e^{-3\sigma^2 \tau^2} + F_7 (F_5)^* e^{-3\sigma^2 \tau^2} + F_7 (F_6)^* e^{-\sigma^2 \tau^2} + \\ & F_7 (F_8)^* e^{-\sigma^2 \tau^2} + F_8 (F_5)^* e^{-6\sigma^2 \tau^2} + F_8 (F_6)^* e^{-3\sigma^2 \tau^2} + F_8 (F_7)^* e^{-\sigma^2 \tau^2} + \\ & F_5 (F_5)^* + F_6 (F_6)^* + F_7 (F_7)^* + F_8 (F_8)^*. \end{aligned} \quad (\text{B.32})$$

The coincidence probability plot against the time-delays introduced between the arrival of the photons at input ports of the balanced beam-splitter is shown in Fig.(B.8). The coincidence probability plot shows that the probability of having the above defined output coincidence pattern is maximum and is equal to the value of the permanent of the adjacent matrix, when there is no time-delays introduced between the arrival of the photons at input ports. The probability coincidence starts decreasing with the increase in the length of the time-delays τ introduced between the arrival of the photons at input ports of the balanced beam-splitter and gradually become zero when the length of the time-delays increases to a specific point.

B.9 Tri-Photon Click on Output-3, Single-Photon Click on Output-2 and no click on Output-1

In this case, we shall discuss the coincidence probability of the output coincidence pattern shown in Fig.(3.12) in which we get a tri-photon click at output port-3 and a single-photon click at output port-2. The input state will same as defined in Eq.(3.23) and the output operator for the case are defined as

$$\Pi_2 = \int_{-\infty}^{\infty} \hat{a}_2^\dagger(\omega_6) |0\rangle \langle 0| \hat{a}_2(\omega_6) d\omega_6, \quad (\text{B.33})$$

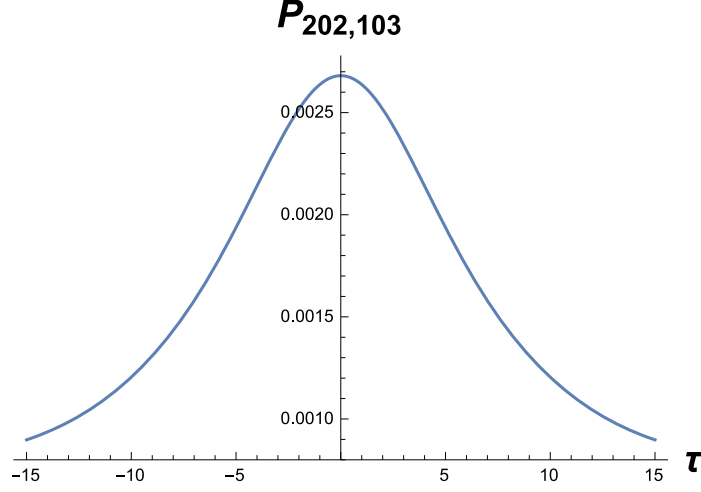


Figure B.8: (with $T(\tau_1, \tau_2, \tau_3, \tau_4) = T(-\tau, 0, \tau, 2\tau)$, $\sigma_o = 0.1$ and $\Omega(\alpha_1, \alpha_2, \alpha_3, \beta_1, \beta_2, \beta_3, \gamma_1, \gamma_2) = \Omega(0, 0, 0, \pi/2, \pi/2, \pi/2, 0, 0)$)

and

$$\Pi_3 = \int_{-\infty}^{\infty} \hat{a}_3^\dagger(\omega_7) \hat{a}_3^\dagger(\omega_{10}) \hat{a}_3^\dagger(\omega_{13}) |000\rangle \langle 000| \hat{a}_3^\dagger(\omega_7) \hat{a}_3(\omega_{10}) \hat{a}_3(\omega_{13}) d\omega_7 d\omega_{10} d\omega_{13}, \quad (\text{B.34})$$

the coincidence probability for this case can be written as

$$P_{202,013} = {}^s \langle 1111 | U^\dagger \Pi_2 \otimes \Pi_3 U | 1111 \rangle^s, \quad (\text{B.35})$$

the probability coefficients for this case have already been defined in Eq.(3.37). The coincidence probability is

$$\begin{aligned} P_{202,013} = & F_{21}(F_{22})^* e^{-\sigma^2 \tau^2} + F_{21}(F_{23})^* e^{-3\sigma^2 \tau^2} + F_{21}(F_{24})^* e^{-6\sigma^2 \tau^2} + \\ & F_{22}(F_{21})^* e^{-\sigma^2 \tau^2} + F_{22}(F_{23})^* e^{-\sigma^2 \tau^2} + F_{22}(F_{24})^* e^{-3\sigma^2 \tau^2} + \\ & F_{23}(F_{21})^* e^{-3\sigma^2 \tau^2} + F_{23}(F_{22})^* e^{-\sigma^2 \tau^2} + F_{23}(F_{24})^* e^{-\sigma^2 \tau^2} + \\ & F_{24}(F_{21})^* e^{-6\sigma^2 \tau^2} + F_{24}(F_{22})^* e^{-3\sigma^2 \tau^2} + F_{24}(F_{23})^* e^{-\sigma^2 \tau^2} + \\ & F_{21}(F_{21})^* + F_{22}(F_{22})^* + F_{23}(F_{23})^* + F_{24}(F_{24})^*. \end{aligned} \quad (\text{B.36})$$

The coincidence probability plot against the time-delays introduced between the arrival of the photons at input ports of the balanced beam-splitter is shown in Fig.(B.9). The plot shows that the coincidence probability of having the above defined output coincidence pattern is relatively high and equal to the value of the permanent of the adjacent matrix, when time-delays τ introduced between the

arrival of the incident photons is zero. The coincidence probability slightly increases as we increase the length of the time-delays τ than after a specific increase in the length of the time-delay, coincidence probability starts to decrease and become zero when the time-delays τ increases to a specific value.

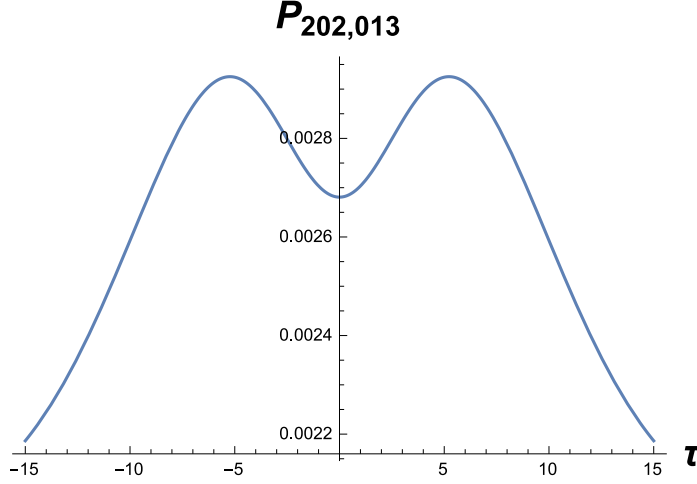


Figure B.9: (with $T(\tau_1, \tau_2, \tau_3, \tau_4) = T(-\tau, 0, \tau, 2\tau)$, $\sigma_o = 0.1$ and $\Omega(\alpha_1, \alpha_2, \alpha_3, \beta_1, \beta_2, \beta_3, \gamma_1, \gamma_2) = \Omega(0, 0, 0, \pi/2, \pi/2, \pi/2, 0, 0)$)

B.10 Tetra-Photon Click on Output-2 and no Click on Output-1 and Output-3

In this case, we shall discuss the coincidence probability for the case when we get a tetra-photon click at output port-2 and no click at output port-1 and output port-3, as shown in Fig.(3.14). For this case the input state will same as defined in Eq.(3.23) and the output operators are defined as,

$$\begin{aligned} \Pi_2 = \int_{-\infty}^{\infty} \hat{a}_2^\dagger(\omega_6) \hat{a}_2^\dagger(\omega_9) \hat{a}_2^\dagger(\omega_{12}) \hat{a}_1^\dagger(\omega_{15}) |0000\rangle \langle 0000| \\ \hat{a}_2(\omega_6) \hat{a}_2(\omega_9) \hat{a}_2(\omega_{12}) \hat{a}_2(\omega_{15}) d\omega_6 d\omega_9 d\omega_{12} d\omega_{15}, \end{aligned} \quad (\text{B.37})$$

the coincidence probability for this case can be written as,

$$P_{202,040} = {}^s \langle 1111 | U^\dagger \Pi_2 U | 1111 \rangle^s, \quad (\text{B.38})$$

and the probability coefficient for this case are defined as,

$$V_5 = U_{21}^2 U_{23}^2; \quad (\text{B.39})$$

so, the coincidence probability for this case is

$$P_{202,040} = V_5 (V_5)^*. \quad (\text{B.40})$$

We can clearly see that, the coincidence probability for this case do not depend on the time-delays τ introduced between the arrival of the photon at the input ports of the balanced beam-splitter.

B.11 Tetra-Photon Click on Output-3 and no Click on Output-1 and Output-2

In this case, we shall discuss the coincidence probability for the case when we get a tetra-photon pulse at output port-3 and no click at output port-1 and output port-2, as shown in Fig.(3.14). For this case the input state will same as defined in Eq.(3.23) and the output operators are defined as,

$$\begin{aligned} \Pi_3 = \int_{-\infty}^{\infty} & \hat{a}_3^\dagger(\omega_7) \hat{a}_3^\dagger(\omega_{10}) \hat{a}_3^\dagger(\omega_{13}) \hat{a}_3^\dagger(\omega_{16}) |0000\rangle \langle 0000| \\ & \hat{a}_3(\omega_7) \hat{a}_3(\omega_{10}) \hat{a}_3(\omega_{13}) \hat{a}_3(\omega_{16}) d\omega_7 d\omega_{10} d\omega_{13} d\omega_{16}, \end{aligned} \quad (\text{B.41})$$

the coincidence probability for this case can be written as,

$$P_{202,004} = {}^s \langle 1111 | U^\dagger \Pi_3 U | 1111 \rangle^s, \quad (\text{B.42})$$

and the probability coefficient for this case are defined as,

$$V_6 = U_{31}^2 U_{33}^2; \quad (\text{B.43})$$

so, the coincidence probability for this case is

$$P_{202,004} = V_6 (V_6)^*. \quad (\text{B.44})$$

We can clearly see that, the coincidence probability for this case do not depend on the time-delays τ introduced between the arrival of the photon at the input ports of the balanced beam-splitter.

C Rest of the Cases of Section 3.3

In this case, we have injected a bi-photon input pulse at input port 2, input port 3 and nothing input port 1 of a six port passive quantum optical interferometer and then calculate and plotted the coincidence probabilities of all output coincidence patterns as shown in Fig.3.15, Fig.3.17, Fig.3.19 and Fig.3.21.

C.1 Bi-Photon Click on Output-1 and Output-3 and no Click on Output-2

In this case, we shall discuss second output coincidence pattern in which we get a bi-photon click at output port-1 and output port-3 for the case where we have injected a bi-photon pulse in input port-2 and port-3 as shown in Fig.(3.15). The output operators for this specific case are the same as defined in Eq.(3.2) and Eq.(3.4), the input state is same as defined in Eq.(3.42) and the coincidence probability is

$$P_{022,202} = {}^s \langle 1111 | U^\dagger \Pi_1 \otimes \Pi_3 U | 1111 \rangle^s, \quad (\text{C.1})$$

the probability coefficients have already been defined in Eq.(3.44) and the coincidence probability is

$$\begin{aligned} P_{022,202} = & C_7 (C_8)^* e^{-\sigma^2 \tau^2} + C_7 (C_9)^* e^{-3\sigma^2 \tau^2} + C_7 (C_{10})^* e^{-3\sigma^2 \tau^2} + C_7 (C_{11})^* e^{-5\sigma^2 \tau^2} + \\ & C_7 (C_{12})^* e^{-8\sigma^2 \tau^2} + C_8 (C_7)^* e^{-\sigma^2 \tau^2} + C_8 (C_9)^* e^{-\sigma^2 \tau^2} + C_8 (C_{10})^* e^{-\sigma^2 \tau^2} + \\ & C_8 (C_{11})^* e^{-2\sigma^2 \tau^2} + C_8 (C_{12})^* e^{-5\sigma^2 \tau^2} + C_9 (C_7)^* e^{-3\sigma^2 \tau^2} + C_9 (C_8)^* e^{-\sigma^2 \tau^2} + \\ & C_9 (C_{10})^* e^{-2\sigma^2 \tau^2} + C_9 (C_{11})^* e^{-\sigma^2 \tau^2} + C_9 (C_{12})^* e^{-3\sigma^2 \tau^2} + C_{10} (C_7)^* e^{-3\sigma^2 \tau^2} + \\ & C_{10} (C_8)^* e^{-\sigma^2 \tau^2} + C_{10} (C_9)^* e^{-2\sigma^2 \tau^2} + C_{10} (C_{11})^* e^{-\sigma^2 \tau^2} + C_{10} (C_{12})^* e^{-3\sigma^2 \tau^2} + \\ & C_{11} (C_7)^* e^{-5\sigma^2 \tau^2} + C_{11} (C_8)^* e^{-2\sigma^2 \tau^2} + C_{11} (C_9)^* e^{-\sigma^2 \tau^2} + C_{11} (C_{10})^* e^{-\sigma^2 \tau^2} + \\ & C_{11} (C_{12})^* e^{-\sigma^2 \tau^2} + C_{12} (C_7)^* e^{-8\sigma^2 \tau^2} + C_{12} (C_8)^* e^{-5\sigma^2 \tau^2} + C_{12} (C_9)^* e^{-3\sigma^2 \tau^2} + \\ & C_{12} (C_{10})^* e^{-3\sigma^2 \tau^2} + C_{12} (C_{11})^* e^{-\sigma^2 \tau^2} + C_7 (C_7)^* + C_8 (C_8)^* + C_9 (C_9)^* + \\ & C_{10} (C_{10})^* + C_{11} (C_{11})^* + C_{12} (C_{12})^*. \end{aligned} \quad (\text{C.2})$$

The plot of the coincidence probability against the time-delay τ introduced between the arrival of the photons at input ports is shown in Fig.(C.1). This plot shows that the coincidence probability of getting a bi-photon click at output port-1 and output port-2 is minimum and is equal to the value of the permanent of the adjacent scattering matrix but not zero when there is no time-delay introduced between the arrival of the photons at input ports. The coincidence probability of having this output increases with the increase in length of the time-delay τ but at specific point it gradually becomes constant.

C.2 Bi-Photon Click on Output-2 and Output-3 and no Click on Output-1

In this case, we shall discuss the third output coincidence pattern in which we get a bi-photon click at output port-2 and output port-3 and no click at output port-1. The input state is the same as define in Eq.(3.42). The output operators for this

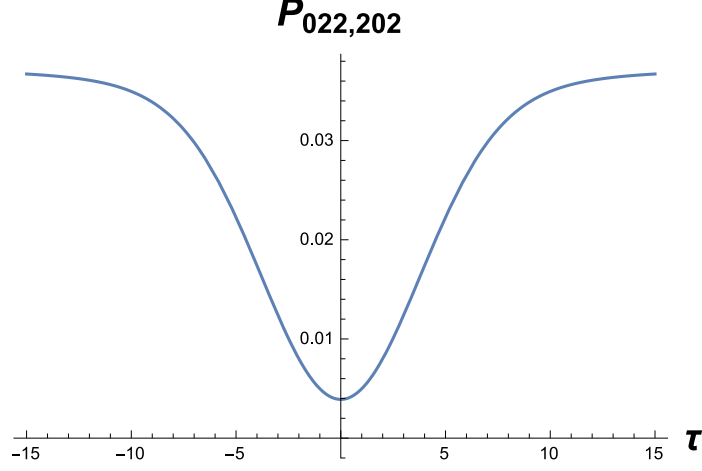


Figure C.1: (with $T(\tau_1, \tau_2, \tau_3, \tau_4) = T(-\tau, 0, \tau, 2\tau)$, $\sigma_o = 0.1$ and $\Omega(\alpha_1, \alpha_2, \alpha_3, \beta_1, \beta_2, \beta_3, \gamma_1, \gamma_2) = \Omega(0, 0, 0, \pi/2, \pi/2, \pi/2, 0, 0)$)

case are defined in Eq.(3.3) and Eq.(3.4) and the coincidence probability for this case can be written as

$$P_{022,022} = {}^s \langle 1111 | U^\dagger \Pi_2 \otimes \Pi_3 U | 1111 \rangle^s, \quad (\text{C.3})$$

where C's are the probability coefficients and are already been defined in Eq.(3.44) and the coincidence probability is

$$\begin{aligned} P_{022,022} = & C_{13} (C_{14})^* e^{-\sigma^2 \tau^2} + C_{13} (C_{15})^* e^{-3\sigma^2 \tau^2} + C_{13} (C_{16})^* e^{-3\sigma^2 \tau^2} + C_{13} (C_{17})^* e^{-5\sigma^2 \tau^2} + \\ & C_{13} (C_{18})^* e^{-8\sigma^2 \tau^2} + C_{14} (C_{13})^* e^{-\sigma^2 \tau^2} + C_{14} (C_{15})^* e^{-\sigma^2 \tau^2} + C_{14} (C_{16})^* e^{-\sigma^2 \tau^2} + \\ & C_{14} (C_{17})^* e^{-2\sigma^2 \tau^2} + C_{14} (C_{18})^* e^{-5\sigma^2 \tau^2} + C_{15} (C_{13})^* e^{-3\sigma^2 \tau^2} + C_{15} (C_{14})^* e^{-\sigma^2 \tau^2} + \\ & C_{15} (C_{16})^* e^{-2\sigma^2 \tau^2} + C_{15} (C_{17})^* e^{-\sigma^2 \tau^2} + C_{15} (C_{18})^* e^{-3\sigma^2 \tau^2} + C_{16} (C_{13})^* e^{-3\sigma^2 \tau^2} + \\ & C_{16} (C_{14})^* e^{-\sigma^2 \tau^2} + C_{16} (C_{15})^* e^{-2\sigma^2 \tau^2} + C_{16} (C_{17})^* e^{-\sigma^2 \tau^2} + C_{16} (C_{18})^* e^{-3\sigma^2 \tau^2} + \\ & C_{17} (C_{13})^* e^{-5\sigma^2 \tau^2} + C_{17} (C_{14})^* e^{-2\sigma^2 \tau^2} + C_{17} (C_{15})^* e^{-\sigma^2 \tau^2} + C_{17} (C_{16})^* e^{-\sigma^2 \tau^2} + \\ & C_{17} (C_{18})^* e^{-\sigma^2 \tau^2} + C_{18} (C_{13})^* e^{-8\sigma^2 \tau^2} + C_{18} (C_{14})^* e^{-5\sigma^2 \tau^2} + C_{18} (C_{15})^* e^{-3\sigma^2 \tau^2} + \\ & C_{18} (C_{16})^* e^{-3\sigma^2 \tau^2} + C_{18} (C_{17})^* e^{-\sigma^2 \tau^2} + C_{13} (C_{13})^* + C_{14} (C_{14})^* + C_{15} (C_{15})^* + \\ & C_{16} (C_{16})^* + C_{17} (C_{17})^* + C_{18} (C_{18})^*. \end{aligned} \quad (\text{C.4})$$

The plot of coincidence probability against the time-delays τ introduced between the arrival of the photons at input ports of the balanced beam-splitter is shown in Fig.(C.2). The plot shows that the coincidence probability of having a bi-photon click at output port-2 and output port-3, when we have injection a bi-photon

pulse in input port-2 and input port-3 is maximum and is equal to the value of the permanent of the adjacent scattering matrix when there are no time-delays τ introduced between the arrival of the photons at input ports of the balanced beam-splitter. The coincidence probability starts decreasing when the length of time-delays introduced between the arrival of the photons at input ports increases, first sharply then slowly and after a specific increase in the length of the time-delay the coincidence probability becomes zero.

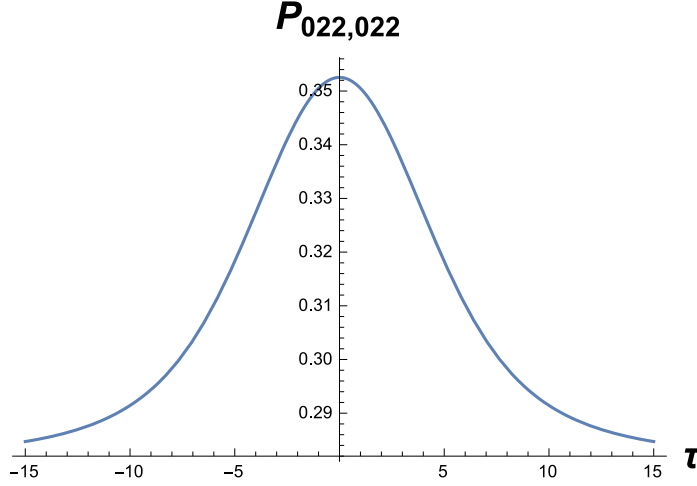


Figure C.2: (with $T(\tau_1, \tau_2, \tau_3, \tau_4) = T(-\tau, 0, \tau, 2\tau)$, $\sigma_o = 0.1$ and $\Omega(\alpha_1, \alpha_2, \alpha_3, \beta_1, \beta_2, \beta_3, \gamma_1, \gamma_2) = \Omega(0, 0, 0, \pi/2, \pi/2, \pi/2, 0, 0)$)

C.3 Bi-Photon Click on Output-2 and Single-Photon Click on Output-1 and Output-3

In the case, we shall discuss the coincidence probability of the second output coincidence pattern as shown in Fig.(3.17). In this case we get a bi-photon click at output port-2 and single-photon clicks at output port-1 and port-3 and the input state has already been defined in Eq.(3.42) and output operators are defined as

$$\Pi_1 = \int_{-\infty}^{\infty} \hat{a}_1^\dagger(\omega_5) |0\rangle \langle 0| \hat{a}_1(\omega_5) d\omega_5, \quad (\text{C.5})$$

$$\Pi_2 = \int_{-\infty}^{\infty} \hat{a}_2^\dagger(\omega_6) \hat{a}_2^\dagger(\omega_9) |00\rangle \langle 00| \hat{a}_2(\omega_6) \hat{a}_2(\omega_9) d\omega_6 d\omega_9, \quad (\text{C.6})$$

and

$$\Pi_3 = \int_{-\infty}^{\infty} \hat{a}_3^\dagger(\omega_7) |0\rangle \langle 0| \hat{a}_3(\omega_7) d\omega_7, \quad (\text{C.7})$$

the coincidence probability for this case can be written as

$$P_{022,121} = \langle 1111 | {}^s U^\dagger \Pi_1 \otimes \Pi_2 \otimes \Pi_3 U | 1111 \rangle^s, \quad (\text{C.8})$$

so the coincidence probability for this case is,

$$\begin{aligned} P_{022,121} = & (S_1)^* S_1 + e^{-\sigma^2 \tau^2} (S_2)^* S_1 + e^{-\sigma^2 \tau^2} (S_3)^* S_1 + e^{-3\sigma^2 \tau^2} (S_4)^* S_1 + \\ & e^{-3\sigma^2 \tau^2} (S_5)^* S_1 + e^{-4\sigma^2 \tau^2} (S_6)^* S_1 + e^{-3\sigma^2 \tau^2} (S_7)^* S_1 + e^{-6\sigma^2 \tau^2} (S_8)^* S_1 + \\ & e^{-5\sigma^2 \tau^2} (S_9)^* S_1 + e^{-7\sigma^2 \tau^2} (S_{10})^* S_1 + e^{-8\sigma^2 \tau^2} (S_{11})^* S_1 + e^{-9\sigma^2 \tau^2} (S_{12})^* S_1 + \\ & e^{-\sigma^2 \tau^2} (S_1)^* S_2 + (S_2)^* S_2 + e^{-3\sigma^2 \tau^2} (S_3)^* S_2 + e^{-\sigma^2 \tau^2} (S_4)^* S_2 + \\ & e^{-4\sigma^2 \tau^2} (S_5)^* S_2 + e^{-3\sigma^2 \tau^2} (S_6)^* S_2 + e^{-6\sigma^2 \tau^2} (S_7)^* S_2 + e^{-3\sigma^2 \tau^2} (S_8)^* S_2 + \\ & e^{-7\sigma^2 \tau^2} (S_9)^* S_2 + e^{-5\sigma^2 \tau^2} (S_{10})^* S_2 + e^{-9\sigma^2 \tau^2} (S_{11})^* S_2 + e^{-8\sigma^2 \tau^2} (S_{12})^* S_2 + \\ & e^{-\sigma^2 \tau^2} (S_1)^* S_3 + e^{-3\sigma^2 \tau^2} (S_2)^* S_3 + (S_3)^* S_3 + e^{-4\sigma^2 \tau^2} (S_4)^* S_3 + \\ & e^{-\sigma^2 \tau^2} (S_5)^* S_3 + e^{-3\sigma^2 \tau^2} (S_6)^* S_3 + e^{-\sigma^2 \tau^2} (S_7)^* S_3 + e^{-7\sigma^2 \tau^2} (S_8)^* S_3 + \\ & e^{-2\sigma^2 \tau^2} (S_9)^* S_3 + e^{-6\sigma^2 \tau^2} (S_{10})^* S_3 + e^{-5\sigma^2 \tau^2} (S_{11})^* S_3 + e^{-7\sigma^2 \tau^2} (S_{12})^* S_3 + \\ & e^{-3\sigma^2 \tau^2} (S_1)^* S_4 + e^{-\sigma^2 \tau^2} (S_2)^* S_4 + e^{-4\sigma^2 \tau^2} (S_3)^* S_4 + (S_4)^* S_4 + \\ & e^{-3\sigma^2 \tau^2} (S_5)^* S_4 + e^{-\sigma^2 \tau^2} (S_6)^* S_4 + e^{-7\sigma^2 \tau^2} (S_7)^* S_4 + e^{-\sigma^2 \tau^2} (S_8)^* S_4 + \\ & e^{-6\sigma^2 \tau^2} (S_9)^* S_4 + e^{-2\sigma^2 \tau^2} (S_{10})^* S_4 + e^{-7\sigma^2 \tau^2} (S_{11})^* S_4 + e^{-5\sigma^2 \tau^2} (S_{12})^* S_4 + \\ & e^{-3\sigma^2 \tau^2} (S_1)^* S_5 + e^{-4\sigma^2 \tau^2} (S_2)^* S_5 + e^{-\sigma^2 \tau^2} (S_3)^* S_5 + e^{-3\sigma^2 \tau^2} (S_4)^* S_5 + \\ & (S_5)^* S_5 + e^{-\sigma^2 \tau^2} (S_6)^* S_5 + e^{-2\sigma^2 \tau^2} (S_7)^* S_5 + e^{-5\sigma^2 \tau^2} (S_8)^* S_5 + \\ & e^{-\sigma^2 \tau^2} (S_9)^* S_5 + e^{-3\sigma^2 \tau^2} (S_{10})^* S_5 + e^{-3\sigma^2 \tau^2} (S_{11})^* S_5 + e^{-4\sigma^2 \tau^2} (S_{12})^* S_5 + \\ & e^{-4\sigma^2 \tau^2} (S_1)^* S_6 + e^{-3\sigma^2 \tau^2} (S_2)^* S_6 + e^{-3\sigma^2 \tau^2} (S_3)^* S_6 + e^{-\sigma^2 \tau^2} (S_4)^* S_6 + \\ & e^{-\sigma^2 \tau^2} (S_5)^* S_6 + (S_6)^* S_6 + e^{-5\sigma^2 \tau^2} (S_7)^* S_6 + e^{-2\sigma^2 \tau^2} (S_8)^* S_6 + \\ & e^{-3\sigma^2 \tau^2} (S_9)^* S_6 + e^{-\sigma^2 \tau^2} (S_{10})^* S_6 + e^{-4\sigma^2 \tau^2} (S_{11})^* S_6 + e^{-3\sigma^2 \tau^2} (S_{12})^* S_6 + \\ & e^{-3\sigma^2 \tau^2} (S_1)^* S_7 + e^{-6\sigma^2 \tau^2} (S_2)^* S_7 + e^{-\sigma^2 \tau^2} (S_3)^* S_7 + e^{-7\sigma^2 \tau^2} (S_4)^* S_7 + \\ & e^{-2\sigma^2 \tau^2} (S_5)^* S_7 + e^{-5\sigma^2 \tau^2} (S_6)^* S_7 + (S_7)^* S_7 + e^{-9\sigma^2 \tau^2} (S_8)^* S_7 + \\ & e^{-\sigma^2 \tau^2} (S_9)^* S_7 + e^{-7\sigma^2 \tau^2} (S_{10})^* S_7 + e^{-3\sigma^2 \tau^2} (S_{11})^* S_7 + e^{-6\sigma^2 \tau^2} (S_{12})^* S_7 + \\ & e^{-6\sigma^2 \tau^2} (S_1)^* S_8 + e^{-3\sigma^2 \tau^2} (S_2)^* S_8 + e^{-7\sigma^2 \tau^2} (S_3)^* S_8 + e^{-\sigma^2 \tau^2} (S_4)^* S_8 + \\ & e^{-5\sigma^2 \tau^2} (S_5)^* S_8 + e^{-2\sigma^2 \tau^2} (S_6)^* S_8 + e^{-9\sigma^2 \tau^2} (S_7)^* S_8 + (S_8)^* S_8 + \\ & e^{-7\sigma^2 \tau^2} (S_9)^* S_8 + e^{-\sigma^2 \tau^2} (S_{10})^* S_8 + e^{-6\sigma^2 \tau^2} (S_{11})^* S_8 + e^{-3\sigma^2 \tau^2} (S_{12})^* S_8 + \\ & e^{-5\sigma^2 \tau^2} (S_1)^* S_9 + e^{-7\sigma^2 \tau^2} (S_2)^* S_9 + e^{-2\sigma^2 \tau^2} (S_3)^* S_9 + e^{-6\sigma^2 \tau^2} (S_4)^* S_9 + \\ & e^{-\sigma^2 \tau^2} (S_5)^* S_9 + e^{-3\sigma^2 \tau^2} (S_6)^* S_9 + e^{-\sigma^2 \tau^2} (S_7)^* S_9 + e^{-7\sigma^2 \tau^2} (S_8)^* S_9 + \end{aligned}$$

$$\begin{aligned}
& (S_9)^* S_9 + e^{-4\sigma^2\tau^2} (S_{10})^* S_9 + e^{-\sigma^2\tau^2} (S_{11})^* S_9 + e^{-3\sigma^2\tau^2} (S_{12})^* S_9 + \\
& e^{-7\sigma^2\tau^2} (S_1)^* S_{10} + e^{-5\sigma^2\tau^2} (S_2)^* S_{10} + e^{-6\sigma^2\tau^2} (S_3)^* S_{10} + e^{-2\sigma^2\tau^2} (S_4)^* S_{10} + \\
& e^{-3\sigma^2\tau^2} (S_5)^* S_{10} + e^{-\sigma^2\tau^2} (S_6)^* S_{10} + e^{-7\sigma^2\tau^2} (S_7)^* S_{10} + e^{-\sigma^2\tau^2} (S_8)^* S_{10} + \\
& e^{-4\sigma^2\tau^2} (S_9)^* S_{10} + (S_{10})^* S_{10} + e^{-3\sigma^2\tau^2} (S_{11})^* S_{10} + e^{-\sigma^2\tau^2} (S_{12})^* S_{10} + \\
& e^{-8\sigma^2\tau^2} (S_1)^* S_{11} + e^{-9\sigma^2\tau^2} (S_2)^* S_{11} + e^{-5\sigma^2\tau^2} (S_3)^* S_{11} + e^{-7\sigma^2\tau^2} (S_4)^* S_{11} + \\
& e^{-3\sigma^2\tau^2} (S_5)^* S_{11} + e^{-4\sigma^2\tau^2} (S_6)^* S_{11} + e^{-3\sigma^2\tau^2} (S_7)^* S_{11} + e^{-6\sigma^2\tau^2} (S_8)^* S_{11} + \\
& e^{-\sigma^2\tau^2} (S_9)^* S_{11} + e^{-3\sigma^2\tau^2} (S_{10})^* S_{11} + (S_{11})^* S_{11} + e^{-\sigma^2\tau^2} (S_{12})^* S_{11} + \\
& e^{-9\sigma^2\tau^2} (S_1)^* S_{12} + e^{-8\sigma^2\tau^2} (S_2)^* S_{12} + e^{-7\sigma^2\tau^2} (S_3)^* S_{12} + e^{-5\sigma^2\tau^2} (S_4)^* S_{12} + \\
& e^{-4\sigma^2\tau^2} (S_5)^* S_{12} + e^{-3\sigma^2\tau^2} (S_6)^* S_{12} + e^{-6\sigma^2\tau^2} (S_7)^* S_{12} + e^{-3\sigma^2\tau^2} (S_8)^* S_{12} + \\
& e^{-3\sigma^2\tau^2} (S_9)^* S_{12} + e^{-\sigma^2\tau^2} (S_{10})^* S_{12} + e^{-\sigma^2\tau^2} (S_{11})^* S_{12} + (S_{12})^* S_{12}.
\end{aligned} \tag{C.9}$$

Where S's are the probability coefficients and are defined as

$$\begin{aligned}
S_1 &= U_{13}U_{22}^2U_{33}; & S_2 &= U_{13}U_{22}^2U_{33}; & S_3 &= U_{12}U_{22}U_{23}U_{33}; & S_4 &= U_{13}U_{22}U_{23}U_{32}; \\
S_5 &= U_{12}U_{22}U_{23}U_{33}; & S_6 &= U_{13}U_{22}U_{23}U_{32}; & S_7 &= U_{12}U_{22}U_{23}U_{33}; & S_8 &= U_{13}U_{22}U_{23}U_{32}; \\
S_9 &= U_{12}U_{22}U_{23}U_{33}; & S_{10} &= U_{13}U_{22}U_{23}U_{32}; & S_{11} &= U_{12}U_{23}^2U_{32}; & S_{12} &= U_{12}U_{23}^2U_{32}; .
\end{aligned} \tag{C.10}$$

The plot of coincidence probability against the time-delays introduced between the arrival of the photons at input ports of the balanced beam-splitter is shown in Fig.(C.3). This Coincidence probability plot shows that the probability of having the above defined output coincidence pattern is minimum and is equal to the value of the permanent of the adjacent scattering matrix but not zero when there is no time-delays τ introduced between the arrival of the photon at the input ports. The coincidence probability increases with the increase in the length of the time-delays introduced between the arrival of the photons till specific point and then again starts decreasing.

C.4 Bi-Photon Click on Output-3 and Single-Photon Click on Output-1 and Output-2

In the case, we shall discuss the coincidence probability of the third output coincidence pattern shown in Fig.(3.17). In this case we get a bi-photon click at output port-3 and single-photon clicks at output port-1 and output port-2. Input state has already been defined in Eq.(3.23) and output operators are defined as

$$\Pi_1 = \int_{-\infty}^{\infty} \hat{a}_1^\dagger(\omega_5) |0\rangle \langle 0| \hat{a}_1(\omega_5) d\omega_5, \tag{C.11}$$

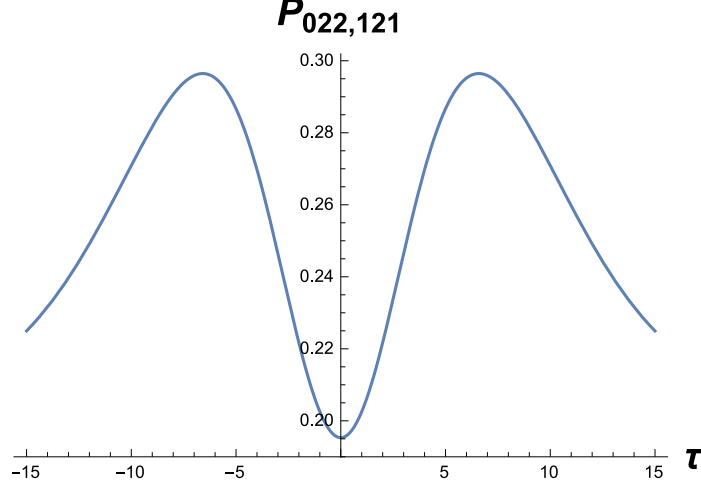


Figure C.3: (with $T(\tau_1, \tau_2, \tau_3, \tau_4) = T(-\tau, 0, \tau, 2\tau)$, $\sigma_o = 0.1$ and $\Omega(\alpha_1, \alpha_2, \alpha_3, \beta_1, \beta_2, \beta_3, \gamma_1, \gamma_2) = \Omega(0, 0, 0, \pi/2, \pi/2, \pi/2, 0, 0)$)

$$\Pi_2 = \int_{-\infty}^{\infty} \hat{a}_2^\dagger(\omega_6) \hat{a}_2^\dagger(\omega_9) |00\rangle \langle 00| \hat{a}_2(\omega_6) \hat{a}_2(\omega_9) d\omega_6 d\omega_9, \quad (\text{C.12})$$

and

$$\Pi_3 = \int_{-\infty}^{\infty} \hat{a}_3^\dagger(\omega_7) \hat{a}_3^\dagger(\omega_{10}) |00\rangle \langle 00| \hat{a}_3(\omega_7) \hat{a}_3(\omega_{10}) d\omega_7 d\omega_{10}, \quad (\text{C.13})$$

the coincidence probability for this case can be written as

$$P_{022,112} = \langle 1111 |^s U^\dagger \Pi_1 \otimes \Pi_2 \otimes \Pi_3 U | 1111 \rangle^s, \quad (\text{C.14})$$

so the coincidence probability for this case is,

$$\begin{aligned} P_{022,112} = & (T_1)^* T_1 + e^{-\sigma^2 \tau^2} (T_2)^* T_1 + e^{-\sigma^2 \tau^2} (T_3)^* T_1 + e^{-3\sigma^2 \tau^2} (T_4)^* T_1 + \\ & e^{-3\sigma^2 \tau^2} (T_5)^* T_1 + e^{-4\sigma^2 \tau^2} (T_6)^* T_1 + e^{-3\sigma^2 \tau^2} (T_7)^* T_1 + e^{-6\sigma^2 \tau^2} (T_8)^* T_1 + \\ & e^{-5\sigma^2 \tau^2} (T_9)^* T_1 + e^{-7\sigma^2 \tau^2} (T_{10})^* T_1 + e^{-8\sigma^2 \tau^2} (T_{11})^* T_1 + e^{-9\sigma^2 \tau^2} (T_{12})^* T_1 + \\ & e^{-\sigma^2 \tau^2} (T_1)^* T_2 + (T_2)^* T_2 + e^{-3\sigma^2 \tau^2} (T_3)^* T_2 + e^{-\sigma^2 \tau^2} (T_4)^* T_2 + \\ & e^{-4\sigma^2 \tau^2} (T_5)^* T_2 + e^{-3\sigma^2 \tau^2} (T_6)^* T_2 + e^{-6\sigma^2 \tau^2} (T_7)^* T_2 + e^{-3\sigma^2 \tau^2} (T_8)^* T_2 + \\ & e^{-7\sigma^2 \tau^2} (T_9)^* T_2 + e^{-5\sigma^2 \tau^2} (T_{10})^* T_2 + e^{-9\sigma^2 \tau^2} (T_{11})^* T_2 + e^{-8\sigma^2 \tau^2} (T_{12})^* T_2 + \\ & e^{-\sigma^2 \tau^2} (T_1)^* T_3 + e^{-3\sigma^2 \tau^2} (T_2)^* T_3 + (T_3)^* T_3 + e^{-4\sigma^2 \tau^2} (T_4)^* T_3 + \\ & e^{-\sigma^2 \tau^2} (T_5)^* T_3 + e^{-3\sigma^2 \tau^2} (T_6)^* T_3 + e^{-\sigma^2 \tau^2} (T_7)^* T_3 + e^{-7\sigma^2 \tau^2} (T_8)^* T_3 + \\ & e^{-2\sigma^2 \tau^2} (T_9)^* T_3 + e^{-6\sigma^2 \tau^2} (T_{10})^* T_3 + e^{-5\sigma^2 \tau^2} (T_{11})^* T_3 + e^{-7\sigma^2 \tau^2} (T_{12})^* T_3 + \end{aligned}$$

$$\begin{aligned}
& e^{-3\sigma^2\tau^2} (T_1) * T_4 + e^{-\sigma^2\tau^2} (T_2) * T_4 + e^{-4\sigma^2\tau^2} (T_3) * T_4 + (T_4) * T_4 + \\
& e^{-3\sigma^2\tau^2} (T_5) * T_4 + e^{-\sigma^2\tau^2} (T_6) * T_4 + e^{-7\sigma^2\tau^2} (T_7) * T_4 + e^{-\sigma^2\tau^2} (T_8) * T_4 + \\
& e^{-6\sigma^2\tau^2} (T_9) * T_4 + e^{-2\sigma^2\tau^2} (T_{10}) * T_4 + e^{-7\sigma^2\tau^2} (T_{11}) * T_4 + e^{-5\sigma^2\tau^2} (T_{12}) * T_4 + \\
& e^{-3\sigma^2\tau^2} (T_1) * T_5 + e^{-4\sigma^2\tau^2} (T_2) * T_5 + e^{-\sigma^2\tau^2} (T_3) * T_5 + e^{-3\sigma^2\tau^2} (T_4) * T_5 + \\
& (T_5) * T_5 + e^{-\sigma^2\tau^2} (T_6) * T_5 + e^{-2\sigma^2\tau^2} (T_7) * T_5 + e^{-5\sigma^2\tau^2} (T_8) * T_5 + \\
& e^{-\sigma^2\tau^2} (T_9) * T_5 + e^{-3\sigma^2\tau^2} (T_{10}) * T_5 + e^{-3\sigma^2\tau^2} (T_{11}) * T_5 + e^{-4\sigma^2\tau^2} (T_{12}) * T_5 + \\
& e^{-4\sigma^2\tau^2} (T_1) * T_6 + e^{-3\sigma^2\tau^2} (T_2) * T_6 + e^{-3\sigma^2\tau^2} (T_3) * T_6 + e^{-\sigma^2\tau^2} (T_4) * T_6 + \\
& e^{-\sigma^2\tau^2} (T_5) * T_6 + (T_6) * T_6 + e^{-5\sigma^2\tau^2} (T_7) * T_6 + e^{-2\sigma^2\tau^2} (T_8) * T_6 + \\
& e^{-3\sigma^2\tau^2} (T_9) * T_6 + e^{-\sigma^2\tau^2} (T_{10}) * T_6 + e^{-4\sigma^2\tau^2} (T_{11}) * T_6 + e^{-3\sigma^2\tau^2} (T_{12}) * T_6 + \\
& e^{-3\sigma^2\tau^2} (T_1) * T_7 + e^{-6\sigma^2\tau^2} (T_2) * T_7 + e^{-\sigma^2\tau^2} (T_3) * T_7 + e^{-7\sigma^2\tau^2} (T_4) * T_7 + \\
& e^{-2\sigma^2\tau^2} (T_5) * T_7 + e^{-5\sigma^2\tau^2} (T_6) * T_7 + (T_7) * T_7 + e^{-9\sigma^2\tau^2} (T_8) * T_7 + \\
& e^{-\sigma^2\tau^2} (T_9) * T_7 + e^{-7\sigma^2\tau^2} (T_{10}) * T_7 + e^{-3\sigma^2\tau^2} (T_{11}) * T_7 + e^{-6\sigma^2\tau^2} (T_{12}) * T_7 + \\
& e^{-6\sigma^2\tau^2} (T_1) * T_8 + e^{-3\sigma^2\tau^2} (T_2) * T_8 + e^{-7\sigma^2\tau^2} (T_3) * T_8 + e^{-\sigma^2\tau^2} (T_4) * T_8 + \\
& e^{-5\sigma^2\tau^2} (T_5) * T_8 + e^{-2\sigma^2\tau^2} (T_6) * T_8 + e^{-9\sigma^2\tau^2} (T_7) * T_8 + (T_8) * T_8 + \\
& e^{-7\sigma^2\tau^2} (T_9) * T_8 + e^{-\sigma^2\tau^2} (T_{10}) * T_8 + e^{-6\sigma^2\tau^2} (T_{11}) * T_8 + e^{-3\sigma^2\tau^2} (T_{12}) * T_8 + \\
& e^{-5\sigma^2\tau^2} (T_1) * T_9 + e^{-7\sigma^2\tau^2} (T_2) * T_9 + e^{-2\sigma^2\tau^2} (T_3) * T_9 + e^{-6\sigma^2\tau^2} (T_4) * T_9 + \\
& e^{-\sigma^2\tau^2} (T_5) * T_9 + e^{-3\sigma^2\tau^2} (T_6) * T_9 + e^{-\sigma^2\tau^2} (T_7) * T_9 + e^{-7\sigma^2\tau^2} (T_8) * T_9 + \\
& (T_9) * T_9 + e^{-4\sigma^2\tau^2} (T_{10}) * T_9 + e^{-\sigma^2\tau^2} (T_{11}) * T_9 + e^{-3\sigma^2\tau^2} (T_{12}) * T_9 + \\
& e^{-7\sigma^2\tau^2} (T_1) * T_{10} + e^{-5\sigma^2\tau^2} (T_2) * T_{10} + e^{-6\sigma^2\tau^2} (T_3) * T_{10} + e^{-2\sigma^2\tau^2} (T_4) * T_{10} + \\
& e^{-3\sigma^2\tau^2} (T_5) * T_{10} + e^{-\sigma^2\tau^2} (T_6) * T_{10} + e^{-7\sigma^2\tau^2} (T_7) * T_{10} + e^{-\sigma^2\tau^2} (T_8) * T_{10} + \\
& e^{-4\sigma^2\tau^2} (T_9) * T_{10} + (T_{10}) * T_{10} + e^{-3\sigma^2\tau^2} (T_{11}) * T_{10} + e^{-\sigma^2\tau^2} (T_{12}) * T_{10} + \\
& e^{-8\sigma^2\tau^2} (T_1) * T_{11} + e^{-9\sigma^2\tau^2} (T_2) * T_{11} + e^{-5\sigma^2\tau^2} (T_3) * T_{11} + e^{-7\sigma^2\tau^2} (T_4) * T_{11} + \\
& e^{-3\sigma^2\tau^2} (T_5) * T_{11} + e^{-4\sigma^2\tau^2} (T_6) * T_{11} + e^{-3\sigma^2\tau^2} (T_7) * T_{11} + e^{-6\sigma^2\tau^2} (T_8) * T_{11} + \\
& e^{-\sigma^2\tau^2} (T_9) * T_{11} + e^{-3\sigma^2\tau^2} (T_{10}) * T_{11} + (T_{11}) * T_{11} + e^{-\sigma^2\tau^2} (T_{12}) * T_{11} + \\
& e^{-9\sigma^2\tau^2} (T_1) * T_{12} + e^{-8\sigma^2\tau^2} (T_2) * T_{12} + e^{-7\sigma^2\tau^2} (T_3) * T_{12} + e^{-5\sigma^2\tau^2} (T_4) * T_{12} + \\
& e^{-4\sigma^2\tau^2} (T_5) * T_{12} + e^{-3\sigma^2\tau^2} (T_6) * T_{12} + e^{-6\sigma^2\tau^2} (T_7) * T_{12} + e^{-3\sigma^2\tau^2} (T_8) * T_{12} + \\
& e^{-3\sigma^2\tau^2} (T_9) * T_{12} + e^{-\sigma^2\tau^2} (T_{10}) * T_{12} + e^{-\sigma^2\tau^2} (T_{11}) * T_{12} + (T_{12}) * T_{12}.
\end{aligned} \tag{C.15}$$

Where T 's are the probability coefficients and are defined as

$$T_1 = U_{13}U_{23}U_{32}^2; \quad T_2 = U_{13}U_{23}U_{32}^2; \quad T_3 = U_{12}U_{23}U_{32}U_{33}; \quad T_4 = U_{13}U_{22}U_{32}U_{33};$$

$$\begin{aligned}
T_5 &= U_{12}U_{23}U_{32}U_{33}; & T_6 &= U_{13}U_{22}U_{32}U_{33}; & T_7 &= U_{12}U_{23}U_{32}U_{33}; & T_8 &= U_{13}U_{22}U_{32}U_{33}; \\
T_9 &= U_{12}U_{23}U_{32}U_{33}; & T_{10} &= U_{13}U_{22}U_{32}U_{33}; & T_{11} &= U_{12}U_{22}U_{33}^2; & T_{12} &= U_{12}U_{22}U_{33}^2.
\end{aligned}
\tag{C.16}$$

The plot of coincidence probability against the time-delays introduced between the arrival of the photons at the input port of the balanced beam-splitter is shown in Fig.(C.4). This Coincidence probability plot shows that the probability of having the above defined output coincidence pattern is minimum and is equal to the value of the permanent of the adjacent scattering matrix but not zero when there is no time-delays τ introduced between the arrival of the photon at the input ports. The coincidence probability increases with the increase in the length of the time-delays introduced between the arrival of the photons till specific point and then again starts decreasing.

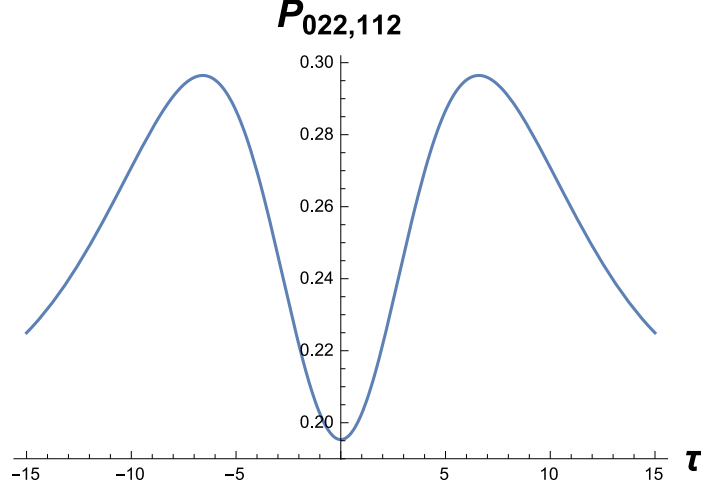


Figure C.4: (with $T(\tau_1, \tau_2, \tau_3, \tau_4) = T(-\tau, 0, \tau, 2\tau)$, $\sigma_o = 0.1$ and $\Omega(\alpha_1, \alpha_2, \alpha_3, \beta_1, \beta_2, \beta_3, \gamma_1, \gamma_2) = \Omega(0, 0, 0, \pi/2, \pi/2, \pi/2, 0, 0)$)

C.5 Tri-Photon Click on Output-1, Single-Photon Click on Output-3 and no click on Output-2

In this case, we shall discuss second output coincidence pattern as shown in Fig.(3.19), in which we get a tri-photon click at output port-1, a single-photon click at output port-3 and no click at output port-2. The Input state will be the same as defined

in Eq.(3.42) and the output operators for this case are defined as,

$$\Pi_1 = \int_{-\infty}^{\infty} \hat{a}_1^\dagger(\omega_5) \hat{a}_1^\dagger(\omega_8) \hat{a}_1^\dagger(\omega_{11}) |000\rangle \langle 000| \hat{a}_1(\omega_5) \hat{a}_1(\omega_8) \hat{a}_1(\omega_{11}) d\omega_5 d\omega_8 d\omega_{11}, \quad (\text{C.17})$$

and

$$\Pi_3 = \int_{-\infty}^{\infty} \hat{a}_3^\dagger(\omega_7) |0\rangle \langle 0| \hat{a}_3^\dagger(\omega_7) d\omega_7, \quad (\text{C.18})$$

the coincidence probability for this case can be written as

$$P_{202,301} = {}^s \langle 1111 | U^\dagger \Pi_1 \otimes \Pi_3 U | 1111 \rangle^s, \quad (\text{C.19})$$

Where G 's are the probability coefficient and are defined in Eq.(3.52). So the coincidence probability is

$$\begin{aligned} P_{202,301} = & G_{13} (G_{14})^* e^{-\sigma^2 \tau^2} + G_{13} (G_{15})^* e^{-3\sigma^2 \tau^2} + G_{13} (G_{16})^* e^{-6\sigma^2 \tau^2} + \\ & G_{14} (G_{13})^* e^{-\sigma^2 \tau^2} + G_{14} (G_{15})^* e^{-\sigma^2 \tau^2} + G_{14} (G_{16})^* e^{-3\sigma^2 \tau^2} + \\ & G_{15} (G_{13})^* e^{-3\sigma^2 \tau^2} + G_{15} (G_{14})^* e^{-\sigma^2 \tau^2} + G_{15} (G_{16})^* e^{-\sigma^2 \tau^2} + \\ & G_{16} (G_{13})^* e^{-6\sigma^2 \tau^2} + G_{16} (G_{14})^* e^{-3\sigma^2 \tau^2} + G_{16} (G_{15})^* e^{-\sigma^2 \tau^2} + \\ & G_{13} (G_{13})^* + G_{14} (G_{14})^* + G_{15} (G_{15})^* + G_{16} (G_{16})^*. \end{aligned} \quad (\text{C.20})$$

The plot of coincidence probability against the time-delays introduced between the arrival of the photons at input ports of the balanced beam-splitter is shown in Fig.(C.5). This plot shows that the probability of having the desired output is relatively high and is equal to the value of the permanent of the adjacent scattering matrix when the time-delays τ introduced between the arrival of the photon at inputs of the beam-splitter is zero. The coincidence probability slightly increases with the increase in the length of the time-delays τ and then gradually decreases to zero with further increase in the length of the time-delays τ .

C.6 Tri-Photon Click on Output-2, Single-Photon Click on Output-1 and no click on Output-3

In this case, we shall discuss third output coincidence pattern as shown in Fig.(3.19, in which we get a tri-photon click at output port-2, a single-photon click at output port-1 and no click at output port-3. The Input state will be the same as defined in Eq.(3.42) and the output operators for this case are defined as,

$$\Pi_2 = \int_{-\infty}^{\infty} \hat{a}_2^\dagger(\omega_6) \hat{a}_2^\dagger(\omega_9) \hat{a}_2^\dagger(\omega_{12}) |000\rangle \langle 000| \hat{a}_2(\omega_6) \hat{a}_2(\omega_9) \hat{a}_2(\omega_{12}) d\omega_6 d\omega_9 d\omega_{12}, \quad (\text{C.21})$$

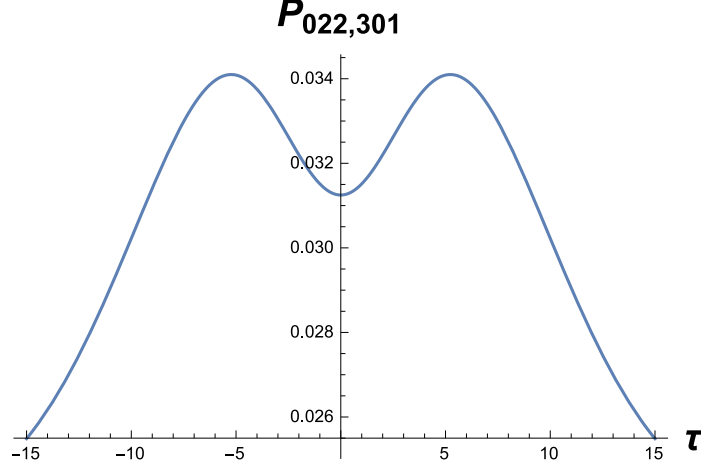


Figure C.5: (with $T(\tau_1, \tau_2, \tau_3, \tau_4) = T(-\tau, 0, \tau, 2\tau)$, $\sigma_o = 0.1$ and $\Omega(\alpha_1, \alpha_2, \alpha_3, \beta_1, \beta_2, \beta_3, \gamma_1, \gamma_2) = \Omega(0, 0, 0, \pi/2, \pi/2, \pi/2, 0, 0)$)

and

$$\Pi_1 = \int_{-\infty}^{\infty} \hat{a}_1^\dagger(\omega_5) |0\rangle \langle 0| \hat{a}_1^\dagger(\omega_5) d\omega_5, \quad (\text{C.22})$$

the coincidence probability for this case can be written as

$$P_{022,130} = {}^s \langle 1111 | U^\dagger \Pi_2 \otimes \Pi_3 U | 1111 \rangle^s, \quad (\text{C.23})$$

Where G 's are the probability coefficients and are defined in Eq.(3.52). So the coincidence probability is

$$\begin{aligned} P_{022,130} = & G_{17} (G_{18})^* e^{-\sigma^2 \tau^2} + G_{17} (G_{19})^* e^{-3\sigma^2 \tau^2} + G_{17} (G_{20})^* e^{-6\sigma^2 \tau^2} + \\ & G_{18} (G_{17})^* e^{-\sigma^2 \tau^2} + G_{18} (G_{19})^* e^{-\sigma^2 \tau^2} + G_{18} (G_{20})^* e^{-3\sigma^2 \tau^2} + \\ & G_{19} (G_{17})^* e^{-3\sigma^2 \tau^2} + G_{19} (G_{18})^* e^{-\sigma^2 \tau^2} + G_{19} (G_{20})^* e^{-\sigma^2 \tau^2} + \\ & G_{20} (G_{17})^* e^{-6\sigma^2 \tau^2} + G_{20} (G_{18})^* e^{-3\sigma^2 \tau^2} + G_{20} (G_{19})^* e^{-\sigma^2 \tau^2} + \\ & G_{17} (G_{17})^* + G_{18} (G_{18})^* + G_{19} (G_{19})^* + G_{20} (G_{20})^* \end{aligned} \quad (\text{C.24})$$

The plot of coincidence probability against the time-delays introduced between the arrival of the photons at input ports of the balanced beam-splitter is shown in Fig.(C.6). This plot shows that the probability of having the desired output is relatively high and is equal to the value of the permanent of the adjacent scattering matrix when the time-delays τ introduced between the arrival of the photon at inputs of the beam-splitter is zero. The coincidence probability slightly increases with the increase in the length of the time-delays τ and then gradually decreases to zero with further increase in the length of the time-delays τ .

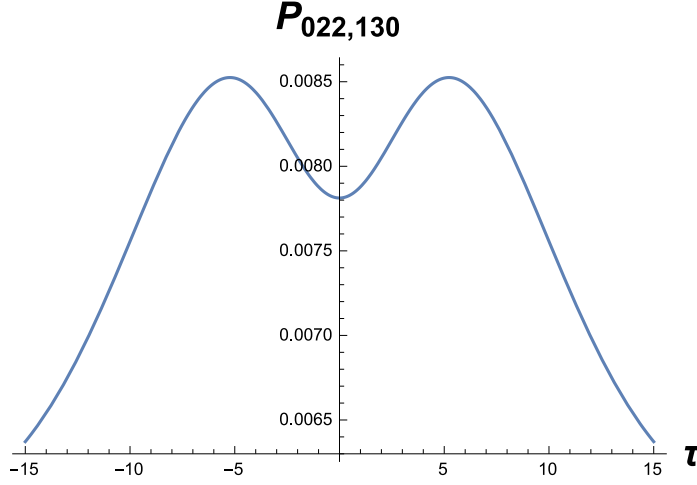


Figure C.6: (with $T(\tau_1, \tau_2, \tau_3, \tau_4) = T(-\tau, 0, \tau, 2\tau)$, $\sigma_o = 0.1$ and $\Omega(\alpha_1, \alpha_2, \alpha_3, \beta_1, \beta_2, \beta_3, \gamma_1, \gamma_2) = \Omega(0, 0, 0, \pi/2, \pi/2, \pi/2, 0, 0)$)

C.7 Tri-Photon Click on Output-2, Single-Photon Click on Output-3 and no click on Output-1

In this case, we shall discuss forth output coincidence pattern as shown in Fig.(3.19), in which we get a tri-photon click at output port-2, a single-photon click at output port-3 and no click at output port-1. The Input state will be the same as defined in Eq.(3.42) and the output operators for this case are defined as,

$$\Pi_2 = \int_{-\infty}^{\infty} \hat{a}_2^\dagger(\omega_6) \hat{a}_2^\dagger(\omega_9) \hat{a}_2^\dagger(\omega_{12}) |000\rangle \langle 000| \hat{a}_2(\omega_6) \hat{a}_2(\omega_9) \hat{a}_2(\omega_{12}) d\omega_6 d\omega_9 d\omega_{12}, \quad (\text{C.25})$$

and

$$\Pi_3 = \int_{-\infty}^{\infty} \hat{a}_3^\dagger(\omega_7) |0\rangle \langle 0| \hat{a}_3^\dagger(\omega_7) d\omega_7, \quad (\text{C.26})$$

the coincidence probability for this case ca be written as

$$P_{022,031} = {}^s \langle 1111 | U^\dagger \Pi_2 \otimes \Pi_3 U | 1111 \rangle^s, \quad (\text{C.27})$$

Where G's are the probability coefficients and are defined in Eq.(3.52). So the coincidence probability is

$$\begin{aligned} P_{202,031} = & G_1 (G_2)^* e^{-\sigma^2 \tau^2} + G_1 (G_3)^* e^{-3\sigma^2 \tau^2} + G_1 (G_4)^* e^{-6\sigma^2 \tau^2} + G_2 (G_1)^* e^{-\sigma^2 \tau^2} + \\ & G_2 (G_3)^* e^{-\sigma^2 \tau^2} + G_2 (G_4)^* e^{-3\sigma^2 \tau^2} + G_3 (G_1)^* e^{-3\sigma^2 \tau^2} + G_3 (G_2)^* e^{-\sigma^2 \tau^2} + \\ & G_3 (G_4)^* e^{-\sigma^2 \tau^2} + G_4 (G_1)^* e^{-6\sigma^2 \tau^2} + G_4 (G_2)^* e^{-3\sigma^2 \tau^2} + G_4 (G_3)^* e^{-\sigma^2 \tau^2} + \end{aligned}$$

$$G_1(G_1)^* + G_2(G_2)^* + G_3(G_3)^* + G_4(G_4)^*. \quad (\text{C.28})$$

The plot of coincidence probability against the time-delays introduced between the arrival of the photons at input ports of the balanced beam-splitter is shown in Fig.(C.7). The plot shows that the coincidence probability of having the above-mentioned output coincidence patten is maximum and is equal to the value of the permanent of the adjacent scattering matrix when time-delays τ introduced between the arrival of the incident photons is zero. The coincidence probability decreases with the increase in the length of the time-delays τ introduced between the arrival of the photons at input ports of the balanced beam-splitter increases and eventually becomes zero at a specific value of the time-delay τ .

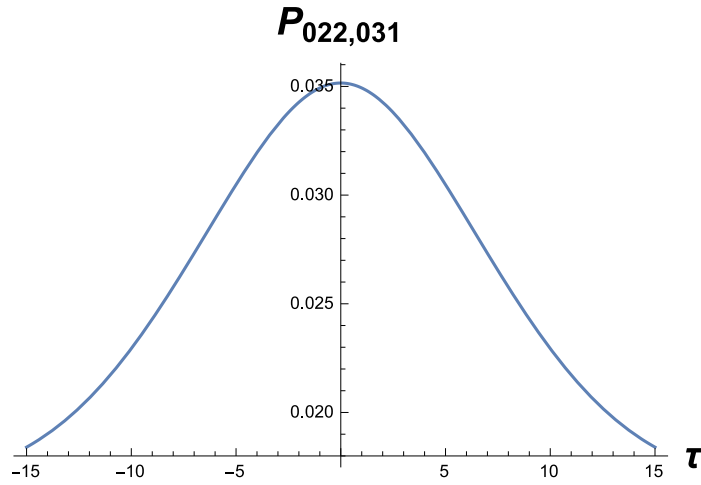


Figure C.7: (with $T(\tau_1, \tau_2, \tau_3, \tau_4) = T(-\tau, 0, \tau, 2\tau)$, $\sigma_o = 0.1$ and $\Omega(\alpha_1, \alpha_2, \alpha_3, \beta_1, \beta_2, \beta_3, \gamma_1, \gamma_2) = \Omega(0, 0, 0, \pi/2, \pi/2, \pi/2, 0, 0)$)

C.8 Tri-Photon Click on Output-3, Single-Photon Click on Output-1 and no click on Output-2

In this case, we shall discuss fifth output coincidence pattern as shown in Fig.(3.19, in which we get a tri-photon click at output port-3, a single-photon click at output port-1 and no click at output port-2. The Input state will be the same as defined in Eq.(3.42) and the output operators for this case are defined as,

$$\Pi_1 = \int_{-\infty}^{\infty} \hat{a}_1^\dagger(\omega_5) |0\rangle \langle 0| \hat{a}_1(\omega_5) d\omega_5, \quad (\text{C.29})$$

and

$$\Pi_3 = \int_{-\infty}^{\infty} \hat{a}_3^\dagger(\omega_7) \hat{a}_3^\dagger(\omega_{10}) \hat{a}_3^\dagger(\omega_{13}) |000\rangle \langle 000| \hat{a}_3^\dagger(\omega_7) \hat{a}_3(\omega_{10}) \hat{a}_3(\omega_{13}) d\omega_7 d\omega_{10} d\omega_{13}, \quad (\text{C.30})$$

the coincidence probability for this case can be written as

$$P_{022,103} = {}^s \langle 1111 | U^\dagger \Pi_1 \otimes \Pi_3 U | 1111 \rangle^s, \quad (\text{C.31})$$

where G's are the probability coefficients and are defined in Eq.(3.52). So the coincidence probability is

$$\begin{aligned} P_{202,103} = & G_{21} (G_{22})^* e^{-\sigma^2 \tau^2} + G_{21} (G_{23})^* e^{-3\sigma^2 \tau^2} + G_{21} (G_{24})^* e^{-6\sigma^2 \tau^2} + \\ & G_{22} (G_{21})^* e^{-\sigma^2 \tau^2} + G_{22} (G_{23})^* e^{-\sigma^2 \tau^2} + G_{22} (G_{24})^* e^{-3\sigma^2 \tau^2} + \\ & G_{23} (G_{21})^* e^{-3\sigma^2 \tau^2} + G_{23} (G_{22})^* e^{-\sigma^2 \tau^2} + G_{23} (G_{24})^* e^{-\sigma^2 \tau^2} + \\ & G_{24} (G_{21})^* e^{-6\sigma^2 \tau^2} + G_{24} (G_{22})^* e^{-3\sigma^2 \tau^2} + G_{24} (G_{23})^* e^{-\sigma^2 \tau^2} + \\ & G_{21} (G_{21})^* + G_{22} (G_{22})^* + G_{23} (G_{23})^* + G_{24} (G_{24})^* \end{aligned} \quad (\text{C.32})$$

The plot of coincidence probability against the time-delays introduced between the arrival of the photons at input ports of the balanced beam-splitter is shown in Fig.(C.8). This plot shows that the probability of having the desired output is relatively high and is equal to the value of the permanent of the adjacent scattering matrix when the time-delays τ introduced between the arrival of the photon at inputs of the beam-splitter is zero. The coincidence probability slightly increases with the increase in the length of the time-delays τ and then gradually decreases to zero with further increase in the length of the time-delays τ .

C.9 Tri-Photon Click on Output-3, Single-Photon Click on Output-2 and no click on Output-1

In this case, we shall discuss last output coincidence pattern as shown in Fig.(3.19), in which we get a tri-photon click at output port-3, a single-photon click at output port-2 and no click at output port-1. The Input state will be the same as defined in Eq.(3.42) and the output operators for this case are defined as,

$$\Pi_2 = \int_{-\infty}^{\infty} \hat{a}_2^\dagger(\omega_6) |0\rangle \langle 0| \hat{a}_2(\omega_6) d\omega_6, \quad (\text{C.33})$$

and

$$\Pi_3 = \int_{-\infty}^{\infty} \hat{a}_3^\dagger(\omega_7) \hat{a}_3^\dagger(\omega_{10}) \hat{a}_3^\dagger(\omega_{13}) |000\rangle \langle 000| \hat{a}_3^\dagger(\omega_7) \hat{a}_3(\omega_{10}) \hat{a}_3(\omega_{13}) d\omega_7 d\omega_{10} d\omega_{13}, \quad (\text{C.34})$$

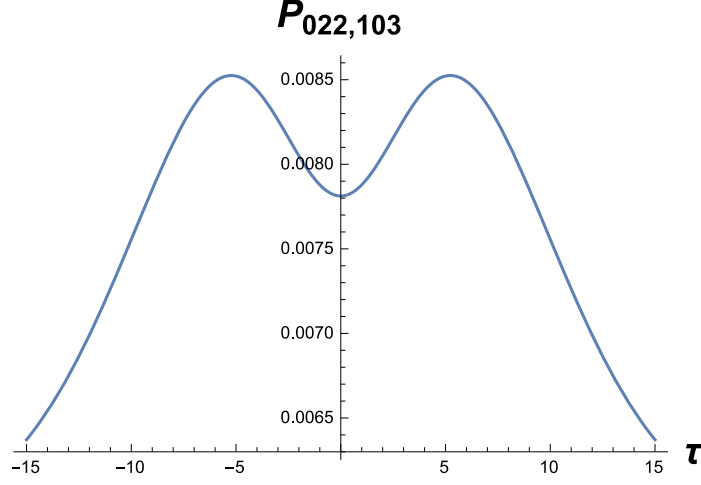


Figure C.8: (with $T(\tau_1, \tau_2, \tau_3, \tau_4) = T(-\tau, 0, \tau, 2\tau)$, $\sigma_o = 0.1$ and $\Omega(\alpha_1, \alpha_2, \alpha_3, \beta_1, \beta_2, \beta_3, \gamma_1, \gamma_2) = \Omega(0, 0, 0, \pi/2, \pi/2, \pi/2, 0, 0)$)

the coincidence probability for this case can be written as

$$P_{022,013} = {}^s \langle 1111 | U^\dagger \Pi_2 \otimes \Pi_3 U | 1111 \rangle^s, \quad (\text{C.35})$$

where G 's are the probability coefficients and are defined in Eq.(3.52). So the coincidence probability is

$$\begin{aligned} P_{202,013} = & G_5 (G_6)^* e^{-\sigma^2 \tau^2} + G_5 (G_7)^* e^{-3\sigma^2 \tau^2} + G_5 (G_8)^* e^{-6\sigma^2 \tau^2} + G_6 (G_5)^* e^{-\sigma^2 \tau^2} + \\ & G_6 (G_7)^* e^{-\sigma^2 \tau^2} + G_6 (G_8)^* e^{-3\sigma^2 \tau^2} + G_7 (G_5)^* e^{-3\sigma^2 \tau^2} + G_7 (G_6)^* e^{-\sigma^2 \tau^2} + \\ & G_7 (G_8)^* e^{-\sigma^2 \tau^2} + G_8 (G_5)^* e^{-6\sigma^2 \tau^2} + G_8 (G_6)^* e^{-3\sigma^2 \tau^2} + G_8 (G_7)^* e^{-\sigma^2 \tau^2} + \\ & G_5 (G_5)^* + G_6 (G_6)^* + G_7 (G_7)^* + G_8 (G_8)^*. \end{aligned} \quad (\text{C.36})$$

The plot of coincidence probability against the time-delays introduced between the arrival of the photons at input ports of the balanced beam-splitter is shown in Fig.(C.9). The plot shows that the coincidence probability of having the above-mentioned output coincidence patten is maximum and is equal to the value of the permanent of the adjacent scattering matrix when time-delays τ introduced between the arrival of the incident photons is zero. The coincidence probability decreases with the increase in the length of the time-delays τ introduced between the arrival of the photons at input ports of the balanced beam-splitter increases and eventually becomes zero at a specific value of the time-delay τ .

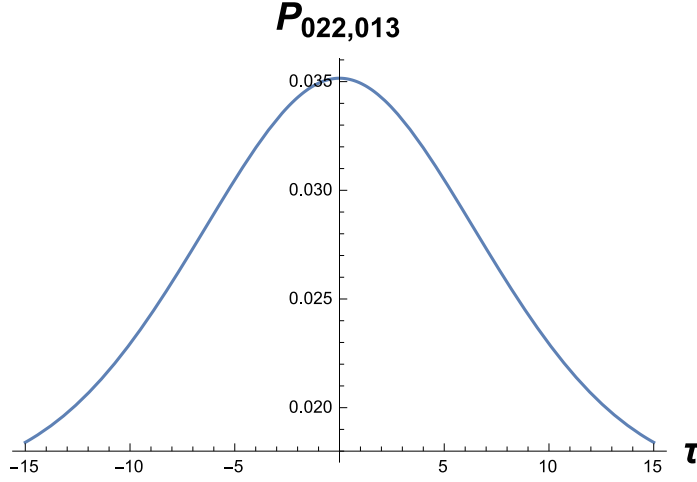


Figure C.9: (with $T(\tau_1, \tau_2, \tau_3, \tau_4) = T(-\tau, 0, \tau, 2\tau)$, $\sigma_o = 0.1$ and $\Omega(\alpha_1, \alpha_2, \alpha_3, \beta_1, \beta_2, \beta_3, \gamma_1, \gamma_2) = \Omega(0, 0, 0, \pi/2, \pi/2, \pi/2, 0, 0)$)

C.10 Tetra-Photon Click on Output-2 and no Click on Output-1 and Output-3

In this case, we shall discuss the coincidence probability of the second output coincidence pattern as shown Fig.(3.21) which shows that we get a tetra-photon pulse at output port-2 and no clicks at output-1 and at output-3. The input state for this case is same as defined in Eq.(3.42) and the output operator is define as,

$$\begin{aligned} \Pi_2 = \int_{-\infty}^{\infty} \hat{a}_2^\dagger(\omega_6) \hat{a}_2^\dagger(\omega_9) \hat{a}_2^\dagger(\omega_{12}) \hat{a}_1^\dagger(\omega_{15}) |0000\rangle \langle 0000| \\ \hat{a}_2(\omega_6) \hat{a}_2(\omega_9) \hat{a}_2(\omega_{12}) \hat{a}_2(\omega_{15}) d\omega_6 d\omega_9 d\omega_{12} d\omega_{15}, \end{aligned} \quad (\text{C.37})$$

the coincidence probability for this case can be written as,

$$P_{022,040} = {}^s \langle 1111 | U^\dagger \Pi_2 U | 1111 \rangle^s, \quad (\text{C.38})$$

and the probability coefficient for this case are defined as,

$$V_8 = U_{22}^2 U_{23}^2; \quad (\text{C.39})$$

so, the coincidence probability for this case is

$$P_{202,040} = V_8 (V_8)^*. \quad (\text{C.40})$$

We can clearly see that, the coincidence probability for this case do not depend on the time-delays introduced between the arrival of the photon at the input ports of the balanced beam-splitter.

C.11 Tetra-Photon Click on Output-3 and no Click on Output-1 and Output-2

In this case, we shall discuss the coincidence probability of the third output coincidence pattern as shown Fig.(3.21) which shows that we get a tetra-photon pulse at output port-3 and no clicks at output-1 and at output-2. The input state for this case is same as defined in Eq.(3.42) and the output operator is define as,

$$\begin{aligned} \Pi_3 = \int_{-\infty}^{\infty} \hat{a}_3^\dagger(\omega_7) \hat{a}_3^\dagger(\omega_{10}) \hat{a}_3^\dagger(\omega_{13}) \hat{a}_3^\dagger(\omega_{16}) |0000\rangle \langle 0000| \\ \hat{a}_3(\omega_7) \hat{a}_3(\omega_{10}) \hat{a}_3(\omega_{13}) \hat{a}_3(\omega_{16}) d\omega_7 d\omega_{10} d\omega_{13} d\omega_{16}, \end{aligned} \quad (\text{C.41})$$

the coincidence probability for this case can be written as,

$$P_{022,004} = {}^s \langle 1111 | U^\dagger \Pi_3 U | 1111 \rangle^s, \quad (\text{C.42})$$

and the probability coefficient for this case are defined as,

$$V_9 = U_{32}^2 U_{33}^2; \quad (\text{C.43})$$

so, the coincidence probability for this case is

$$P_{022,004} = V_9 (V_9)^*. \quad (\text{C.44})$$

We can clearly see that, the coincidence probability for this case do not depend on the time-delays introduced between the arrival of the photon at the input ports of the balanced beam-splitter.

Bibliography

- [1] Werner Heisenberg. *Physics and philosophy*. 1958.
- [2] Nouredine Zettili. *Quantum mechanics: concepts and applications*. John Wiley & Sons, 2009.
- [3] Christopher Gerry and Peter Knight. *Introductory quantum optics*. Cambridge university press, 2005.
- [4] Hubert de Guise, Si-Hui Tan, Isaac P Poulin, and Barry C Sanders. Coincidence landscapes for three-channel linear optical networks. *Physical Review A*, 89(6):063819, 2014.
- [5] Si-Hui Tan, Yvonne Y Gao, Hubert de Guise, and Barry C Sanders. Su (3) quantum interferometry with single-photon input pulses. *Physical review letters*, 110(11):113603, 2013.
- [6] Richard A Campos. Three-photon hong-ou-mandel interference at a multiport mixer. *Physical Review A*, 62(1):013809, 2000.
- [7] C. K. Hong, Z. Y. Ou, and L. Mandel. Measurement of subpicosecond time intervals between two photons by interference. *Phys. Rev. Lett.*, 59:2044–2046, Nov 1987.
- [8] Emanuel Knill, Raymond Laflamme, and Gerald J Milburn. A scheme for efficient quantum computation with linear optics. *nature*, 409(6816):46, 2001.
- [9] Bryan T Gard, Keith R Motes, Jonathan P Olson, Peter P Rohde, and Jonathan P Dowling. An introduction to boson-sampling. In *From atomic to mesoscale: The role of quantum coherence in systems of various complexities*, pages 167–192. World Scientific, 2015.
- [10] S Aaronson and A Arkhipov. Proceedings of the 43rd annual acm symposium on theory of computing. 2011.

- [11] Benjamin J Metcalf, Nicholas Thomas-Peter, Justin B Spring, Dmytro Kundys, Matthew A Broome, Peter C Humphreys, Xian-Min Jin, Marco Barbieri, W Steven Kolthammer, James C Gates, et al. Multiphoton quantum interference in a multiport integrated photonic device. *Nature communications*, 4:1356, 2013.
- [12] Matthew A Broome, Alessandro Fedrizzi, Saleh Rahimi-Keshari, Justin Dove, Scott Aaronson, Timothy C Ralph, and Andrew G White. Photonic boson sampling in a tunable circuit. *Science*, 339(6121):794–798, 2013.
- [13] Justin B Spring, Benjamin J Metcalf, Peter C Humphreys, W Steven Kolthammer, Xian-Min Jin, Marco Barbieri, Animesh Datta, Nicholas Thomas-Peter, Nathan K Langford, Dmytro Kundys, et al. Boson sampling on a photonic chip. *Science*, 339(6121):798–801, 2013.
- [14] Max Tillmann, Borivoje Dakić, René Heilmann, Stefan Nolte, Alexander Szameit, and Philip Walther. Experimental boson sampling. *Nature Photonics*, 7(7):540, 2013.
- [15] Andrea Crespi, Roberto Osellame, Roberta Ramponi, Daniel J Brod, Ernesto F Galvao, Nicolo Spagnolo, Chiara Vitelli, Enrico Maiorino, Paolo Mataloni, and Fabio Sciarrino. Integrated multimode interferometers with arbitrary designs for photonic boson sampling. *Nature Photonics*, 7(7):545, 2013.
- [16] Keith R Motes, Jonathan P Dowling, Alexei Gilchrist, and Peter P Rohde. Implementing bosonsampling with time-bin encoding: analysis of loss, mode mismatch, and time jitter. *Physical Review A*, 92(5):052319, 2015.
- [17] N Spagnolo, C Vitelli, M Bentivegna, DJ Brod, A Crespi, F Flamini, S Giacomo, G Milani, R Ramponi, P Mataloni, et al. Efficient experimental validation of photonic boson sampling against the uniform distribution. *arXiv preprint arXiv:1311.1622*, 2013.
- [18] Jacques Carolan, Jasmin DA Meinecke, Peter J Shadbolt, Nicholas J Russell, Nur Ismail, Kerstin Wörhoff, Terry Rudolph, Mark G Thompson, Jeremy L O’Brien, Jonathan CF Matthews, et al. On the experimental verification of quantum complexity in linear optics. *Nature Photonics*, 8(8):621, 2014.
- [19] Avinash Wasuedo Joshi. *Elements of group theory for physicists*. New Age International, 1997.
- [20] Abdullah Khalid, Dylan Spivak, Barry C Sanders, and Hubert de Guise. Permutational symmetries for coincidence rates in multimode multiphotonic interferometry. *Physical Review A*, 97(6):063802, 2018.

- [21] Marvin Marcus and Henryk Minc. Permanents. *The American Mathematical Monthly*, 72(6):577–591, 1965.
- [22] Jagdish K Patel and Campbell B Read. *Handbook of the normal distribution*, volume 150. CRC Press, 1996.